Quantification of affinity mediated cell/surface interactions

Usman, Jauhr

Award date:
1997

Awarding institution:
University of Bath

QUANTIFICATION OF AFFINITY MEDIATED CELL/SURFACE INTERACTIONS

submitted by **JAUHR USMAN**

for the degree of Ph.D.

of the University of Bath

1997

ProQuest LLC
789 East Eisenhower Parkway
P.O. Box 1346
Ann Arbor, MI 48106-1346

ABSTRACT

The physiological function of many cells is dependent on their ability to adhere via receptors to ligand-coated surfaces under fluid flow conditions. The aim of this project was to investigate the effects of ligand and receptor densities as well as hydrodynamic shear on the detachment of prototype cells from a lectin based affinity support in a parallel-plate chamber. A parallel-plate flow chamber was used to allow direct observation of the detachment process under specified conditions of applied force. Results are reported for the detachment of ovalbumin-coated polystyrene beads from a cellulose membrane covalently derivatized with Concanavalin A. It was found that both the ligand and receptor densities did not effect the detachment process over the range studied. The lowest Con A density of 41.5μg/cm^2 was found to cover the dialysis membrane to the equivalent of at least a monolayer. At this concentration the number of Con A molecules found in the contact region between bead and surface were greater by a factor of 100 than the number of ovalbumin molecules at the highest concentration used (13.90 x 10^6 molecules/bead). Thus it is the ovalbumin receptors in the contact region that limit the number of bonds formed in this study. Lower concentration ranges for both the ovalbumin and Con A were attempted but due to insufficient and sensitive protein determination methods for immobilised proteins these smaller amounts could not be detected accurately.

Detachment with increase in shear stress was found to show a time-dependent effect. Although no systematic trend was observed. Competitive elution of attached beads with glucose showed a marked increase in the fraction of beads detached indicating an specific affinity based interaction. The experimental data were analyzed with a mathematical multivalent model based on the theoretical framework of Yon (1988). The detachment profiles obtained from the experimental data showed a variety of curves, where only one type of curve was found to fit the model. This variation was attributed to the presence of clustered receptor populations and to the difference of the ratio of un-clustered and clustered receptor populations found in a sample.

Acknowledgments

I would like to thank my supervisors John and Bill for their patience and continued support throughout my three years at Bath. Fang Ming was of immense help during my time in Bath and always found the time to help me out. The arrival of Suzanne in the lab was an uplifting event, and she was of great moral support. Also my fellow colleagues Mikey Boy, Rimmer, Yang and Ping Wu for fun in the lab. Not forgetting the fiery Mr. Acosta whose immense knowledge of the engineering aspects was an invaluable aid to me and Richard Bull for his helpful hints on many areas. And, of course, Andrew for his understanding and the loan of his shoulders throughout the most daunting task of the actual thesis writing. Lastly, the whole of the Department of Chemical Engineering for making my three years at Bath something to remember.

I should also like to acknowledge E.P.S.R.C for providing financial support.

Abbreviations

Ach	Acetylcholine
BCA	Bicinchonic Acid
BCA-WR	Bicinchonic Acid Working Reagent
CAMs	Cell Adhesion Molecules
Con A	Concanavalin A
EMEM	Eagle's minimum essential medium
Ig	Immunoglobulins
IMACS	Immunomagnetic-Affinity Cell Sorting
MHC H2-D	Major Histocompatibility Complex
MHSM	Microvilli Hard Sphere Model
NAD	Nicotinic Acetyl Dehydrogenase
NMR	Nuclear Magnetic Resonance
PAM	Point Attachment Model
PBS	Phosphate Buffered Saline
PMA	Phorbol 12-myristate-13-acetate
PTFE	Poly(tetrafluorethane)
RFDA	Radial-Flow Detachment Assay
SSEA-1	Stage Specific Embryonic Antigen-1
WGA	Wheat Germ Agglutinin

Glossary

a	contact area radius
b	mean distance between receptors on a bead
Bc	number of bonds in the contact region
Btot	total number of bonds formed
C	suspended cell concentration
C_b	bound Con A to the membrane
Cb	bound cells removed by a given force
Cbtot	total bound cells
Cm	number of moles/cm^2 or per bead
Cmol	number of molecules/cm^2 or per bead
C_o	initial protein incubation concentration
Cs	solution concentration after binding
d	half channel depth
D	pipe diameter
F	fraction of beads attached
fb	force to break single bond
Feq	fraction of attached cells at steady state
h_s	separation distance between plate and bead
H	maximum plate and bead separation distance

k_{-1}	on constant
k_1	off constant
K	dimensionless dissociation constant
k_f	rate constant for bond formation
k_r	rate constant for bond dissociation
K_d	dissociation constant
K_p	surface association constant
L	free ligand concentration
L_c	ligand molecules in the contact region
L_i	immobilised ligand concentration
N_a	number of attached beads at any given time
N_b	bond density
N_{co}	initial receptor density on cell
N_d	number of detached beads
N_o	initial number of attached beads
Q	volumetric flow rate
R	unoccupied receptor surface concentration
R_c	receptor number in contact region
R_T	total receptor number per bead
Re	Reynolds number
S	surface shear stress
S_c	critical shear stress
S_W	wall shear rate
μ	fluid viscosity
u	linear velocity

ρ	fluid density

Contents Page

CHAPTER 1

Introduction

This review will consider the range of techniques for cell separation with an assessment of their potential for the use in cell fractionation. As any quantitative assessment of fractionation will be dependent on the availability of defined cell samples a brief account of animal culture techniques is provided as background for future methodological development.

1.1. Cell Culture and Biotechnology

The ability to isolate cells from their natural environment allowed scientists to observe cells as entities in their own right. This led to characterization of many membrane bound proteins and their subsequent application in biotechnology.

Cell culture was first used in the beginning of this century by Harrison 1907 and Carrel 1912. Harrison allowed dissected nerve tissue from frog embryos in the lymph fluid to clot on the underside of a microscope slide, and followed the growth of the nerve cells for a few weeks. These initial findings enabled scientists to study animal and plant cells without the variations associated with the extracellular environment of cells *in vivo*.

Technology involving tissue culture has been used extensively in fields such as medicine and industry, e.g. the amniocentesis test allows doctors to detect genetic defects in the unborn child (Nrgaard-Pedersen *et al.*, 1990) and pharmaceutical assessment of the effects of potential drugs on animal cells. Cell cultures are also used for the production of vaccines. The polio virus was the first virus to be vaccinated against in 1949. The ability of the poliomyelitis virus to grow in cultured

human embryonic cells allowed for the development of the large scale production of the vaccine, the polio vaccine being one of the first major commercial products of cultured animal cells (Ecihner *et al.,* 1996).

1.1.1. Animal Cell Culture

Animal cells *in vivo* are supplied with nutrients, growth factors and metabolic substrates by the vascular system allowing them to grow in a controlled environment. Therefore to grow cells *in vitro* conditions similar to those *in vivo* must be provided. Chemically defined media developed in the 1950's by Eagle and Earle, (Eagle's minimum essential medium -EMEM) is now widely used, replacing the poorly defined biological extracts used previously. Growth media usually includes a mixture of carbohydrates, amino acids, salts, growth factors, vitamins and hormones, dependent on the type of cell line being cultured. Blood serum containing unidentified growth factors and hormones is added to most culture medium to maintain cell growth but the addition of serum can have disadvantages as it is a chemically undefined mixture (Belford *et al.,* 1995). The salt concentration is maintained at isotonic levels for all cell lines, and the pH is maintained at the optimum pH for growth of 7.4. Often phenol red is added as an indication of the pH of the medium: a change in colour from red to yellow indicates acidity which is usually an indication of contamination by bacteria (O'Conner *et al.,* 1990). To ensure that cells are grown without bacterial moulds or yeast contamination of the cultures, techniques must be carried out under sterile conditions. The introduction of antibiotics in the 1940's allowed easier handling of culture media and reduced the chances of bacterial contamination (Castel *et al.,* 1990).

1.1.2 Characteristics of Animal Cells in Culture

a) Primary Cell Culture

Animal cells can be obtained from four different types of tissue explants: epithelial, connective, muscle or nerve tissue. Cells taken directly from animal or human tissue are inoculated into growth medium establishing a primary cell culture. Initially the tissue is fragmented, then a proteolytic enzyme such as trypsin, is used to dissaggregate the tissue into individual cells. Often cells are placed at a glass-liquid interface where following attachment, migration is promoted in the plane of the solid substrate. Cells can often be recognized morphologically by observation under an inverted light microscope e.g. fibroblasts are spherical on treatment with trypsin and elongate into a spindle shape on attachment to the substratum whereas epithelial cells appear to be cobble stoned.

Cells in culture can be divided into anchorage dependent and non-anchorage dependent. Anchorage dependent cells have a requirement for a substratum for growth and form a monolayer. All normal mammalian cells which are not derived from the blood or the lymph fluids fall into this category, e.g. fibroblasts (Dalton *et al.,* 1992). Non-anchorage dependent cells grow in suspension e.g. blood cells, of which lymphocytes are used most commonly in culture.

b) Secondary Cell Culture

Sub-culturing of the primary culture gives rise to the secondary cell culture and allows the expansion of the culture. For sub-culturing of non-anchorage dependent cells, the primary culture is diluted with medium only when the cells have grown to a high density; anchorage dependent cells, at confluence, are trypsinized, removed from the substratum and re-inoculated into fresh medium. Therefore both types of cells are dispersed into a cell suspension.

Repeated culture through cycles of growth, trypsinization and sub-culturing leads to the establishment of a cell line. In general cell lines have a limited life span,

although embryonically derived cells grow for a longer period of time than those derived from adult tissue. This is because cell lines derived from the embryo may contain more stem cells and precursor cells, therefore having a greater capacity for self-renewal than cultures from adults.

1.1.3 Transformed Animal Cells

Some cell lines have the ability to undergo transformation which allows them to become immortal. Such cell lines are able to lose their anchorage dependence and can continue exponential growth indefinitely. Human fibroblasts remain predominately euploid throughout their cell culture life and never give rise to continuous cell lines, unlike transformed diploid cells which often become aneuploid. Cells with finite growth capacity, over several months, show three distinct phases of growth. Phase 1 shows initial slow growth, known also as the lag phase, phase 2 exhibits exponential growth and phase 3 the cells enter a senescent phase and the number of viable cells decreases.

Transformed cells show good growth characteristics and are easily established in culture (Kimata *et al.,* 1990). Transformation *in vivo* is usually malignant and is not necessarily identical to *in vitro* transformation. Determination of malignant cell lines is obtained by injection of the cells into experimental animals and observing the formation of a tumor. The most commonly used human cell line, HeLa was established in 1952 from a cancer patient, Henrietta Lacks.

1.1.4 Cell Separation

For clinical applications cell depletion techniques have been adequate for large scale removal of unwanted cell subtypes, whilst cell enrichment and expansion culture technologies still require further development (Zavazava *et al.,* 1991). Cell affinity separations are based on the selective adsorption of cell phenotype using antibodies, lectins or other moieties specific for binding cell surface markers (Norden *et al.,* 1994).

Cells exhibiting different functions and at different stages of differentiation can be separated from one another. Fractionation and characterization of different kinds of cells allows the study of molecular mechanisms involved in cell recognition and interaction, and malignancy (Smith *et al.,* 1994).

Affinity methods offer the selectivity of monoclonal antibody based separations and are required for large-scale clinical applications. Large scale affinity separation techniques (> 10^9 cells) have played an important role in the development of bone marrow transplant and adsorptive cellular immunotherapy (Foa *et al.,* 1996).

The application of lectins, a class of carbohydrate-binding and cell-agglutinating proteins, to the isolation and characterization of soluble glycoproteins and for probing cell surface sugars is well established (Rottman *et al.,* 1973). In principal, any population of single cells may be sorted into sub-populations with the aid of lectins, provided there are differences in their surface sugars. Therefore affinity interactions can be employed to separate cell lines which express different surface glyco-proteins (Norden *et al.,* 1994).

1.2 Affinity Interactions

The acrchetypical specific interaction is the bond formed between an antibody and an antigen, but many other biospecific interactions are found including: neurotransmitters and their receptors, lectins and carbohydrates, hormonal receptors and their hormones and enzymes and their substrates.

1.2.1 Ligand-Receptor Affinity Interactions

Neurotransmitters interact with their specific receptors on the surface of the cell membrane for example acetylcholine (Ach) which is responsible for muscle contraction, is found at the neuromuscular junction and on release from the pre-synaptic neuron it

specifically binds to the ACh-Receptor present on the post-synaptic neuron (Voet & Voet 1990).

1.2.2 Enzyme Substrate and Enzyme Inhibitor Interactions

The lock and key hypothesis as described by Emil Fischer in 1894 likens the specificity of an enzyme for its substrate to that of a key for its lock. This specificity is due to the complementary geometrical shapes of each molecule involved (Voet & Voet 1990). However conformational changes can also occur in the enzyme to allow for complementary binding to the substrate. Geometric constraints as well as stereospecificity are required for the binding of the enzyme to its substrate. The forces involved in this interaction are non-covalent and include Van der Waals, electrostatic, hydrogen-bonding and hydrophobic interactions. Although the biological role of an enzyme is to promote a reaction whereby the metastable complex formed between enzyme and substrate/ligand is broken down, it is possible to adjust conditions such that the enzyme can be used solely as a binding protein e.g. separation of cofactors using immobilised dehydrogenases (Lilly *et al.*, 1994).

1.2.3 Antigen-Antibody Interactions

Protein interactions *in vivo* are observed in the immune system of all higher animals. The interactions are analogous to those between an enzyme and its substrate in many respects in that both interactions are based on the recognition of specific protein motifs (Roit *et al.*, 1985). Antibodies or immunoglobulins (Ig) are glycoproteins that specifically bind to and recognize cell surface proteins present on the cell membrane (antigens). Antibodies are a product of a sub-set of lymphocytes (white blood cells) which have the potential to produce a range of antibodies which is dependent upon previous exposure of the organism to specific antigens.

There are five classes of immunoglobulins; A, G, M, D and E of which IgG is the most abundant and well understood. IgG has a molecular weight of 150 kDa and is composed of four polypeptides of which two are heavy chains and the other two the light chains held together by disulphide bridges. The variable region found at the N-termini of the

antibody is responsible for the specific binding to the antigen and is referred to as an idiotype. The specificity of the binding of antibodies can be determined by the 3-dimensional structure of the idiotype, which complements the region on the antigen and is known as the epitope of the antibody.

The nature of antibody-antigen binding is analogous to that of enzyme-substrate binding, since the interactions are non-covalent and depend upon electrostatic, H-bonding and non-polar interactions. These forces maintain a strong and specific binding with a dissociation constant of up to 10^{-12}M (Turner 1994).

A study by Swann *et al.,* (1992) reported the potential for selection of different sub-populations of cell lines on the basis of the density of surface antigens. Embryonic cells were used from the two carcinoma cell lines F9 and PSMB. Changes in levels of expression of the surface antigens Stage Specific Embryonic Antigen-1 (SSEA-1), and Major Histocompatibility Complex (MHC H2-D) were followed in the F9 cell line after treatment with retinoic acid, which induces differentiation leading to either increased or decreased levels of expression of surface antigens.

The changes in levels of expression were demonstrated using flow cytometry and differential binding of magnetic particles (Dynabeads) conjugated with monoclonal antibodies for SSEA-1 and MHC-H2-D (Swann *et al.,* 1992). Therefore the number of beads bound to the cells reflects the number of antigens expressed on the surface of the cells, and will separate cell populations dependent on the expression of the two antigens, SSEA-1 and MHC H2-D. The cell line PSMB was used to illustrate that cell growth is unaffected in the presence of a constant magnetic field of 0.05T, and that the presence of magnetic beads has no effect on cell proliferation showing the biologically inert nature of these beads. Once loaded with beads the differing magnetic susceptibilities of cells can be employed to assist the sub-fractionation of immunopositive cell populations.

1.2.4 Lectin-Carbohydrate Interactions

Lectins are proteins that recognize and bind to specific carbohydrate sequences. Carbohydrates in the form of glycoproteins and glycolipid are present on the surface of cells, where the glyco-moieties are exposed. Therefore cells which express different carbohydrates on their surfaces can be separated by being passed through a column of adsorbent to which a lectin specific for a certain carbohydrate is immobilised (Resiner *et al.,* 1980). Affinity separation employing lectins is of interest only when particular cell type shows a specific affinity interaction with a particular lectin (Boldt *et al.,* 1979). Also the importance of lectin-carbohydrate interactions has been demonstrated by the observation that oligosaccharide recognition by selectins is an important first step in the adhesion of leukocytes to the endothelium during inflammation (Puri *et al.,* 1997; Symon *et al.,* 1996).

The use of lectins to separate viable cells bearing different surface carbohydrates is a recent development (Davies *et al.,* 1996). Most of this work has been done with mammalian cells, particularly lymphocytes. In practice any population of cells, whether from animals, plants, or microorganisms, may be sorted into subpopulations by interaction with lectins, provided the cells differ in their cell-surface sugars (Resiner *et al.,* 1980: Norden *et al.,* 1994).

Since the binding of lectins to cells can be reversed by the addition of an appropriate sugar, without damage to the cells, both the lectin-reactive and non-reactive cells are readily recovered (Sharma *et al.,* 1980). In this respect lectins, which have a significantly higher dissociation constant, offer a distinct advantage over antibodies to cell-surface constituents, which can often be difficult to dissociate. This factor becomes even more significant when multivalent interactions are considered and may explain the role of lectin like molecules in mammalian cell interactions (Parekh *et al.,* 1994).

For cell separation by affinity chromatography, lectins immobilised on a solid support, either by covalent or noncovalent attachment, are commonly employed (Norden *et al.,* 1994). The same affinity adsorbent can be used repeatedly, giving

economical and reproducible separations. Cell viability is not impaired and the total yields are high. Generally separations are performed on columns of immobilsed lectin (Rosenburg *et al.,* 1986), but can also be performed in tubes or dishes to which the lectin is attached (Boldt *et al.,* 1979).

Cell separation techniques are discussed in the following section with regard to the use of affinity interactions to allow different cell populations to be separated.

1.3 The Composition and Properties of Affinity Supports

1.3.1 Examples of Affinity Supports

a) Cellulose

The primary structure of cellulose has been determined through methylation analysis (Doran 1995). Cellulose is a polymer of up to 15000 D-Glucose residues linked by β(1→4) glycosidic bonds (figure 1.1). It's structure is dominated by hydrogen bonding which causes chain aggregation into linear sheets which also bond one another by Van der Waals interaction to form three dimensional elementary fibrils. Cellulose fibrils are composed of bunches of such fibrils which aggregate randomly, but with their axes running along the fiber axis. Due to the degree of hydrogen bonding on accessible fibrilar surfaces cellulose is highly resistant to chemical attack, with the exception of strong acids and reducing agents.

Membrane formats are popular cellulose matrices as used in these investigations. There has been a recent increase in the use of hydrophilic affinity microporous membranes composed of reinforced reactive cellulosic polymers. This affinity membrane provides reactive aldehyde sites for covalent coupling to the amino groups of proteins and other ligands. Cellulose as a "surface-only" matrix might be

advantageous for certain detection applications in which washing away non-target molecules is important, since this is not easily done on porous supports.

The primary hydroxyl groups of the cellulose membrane were derivatized as described in Section 4.2.1.

Figure 1.1 The Structure of Cellulose.

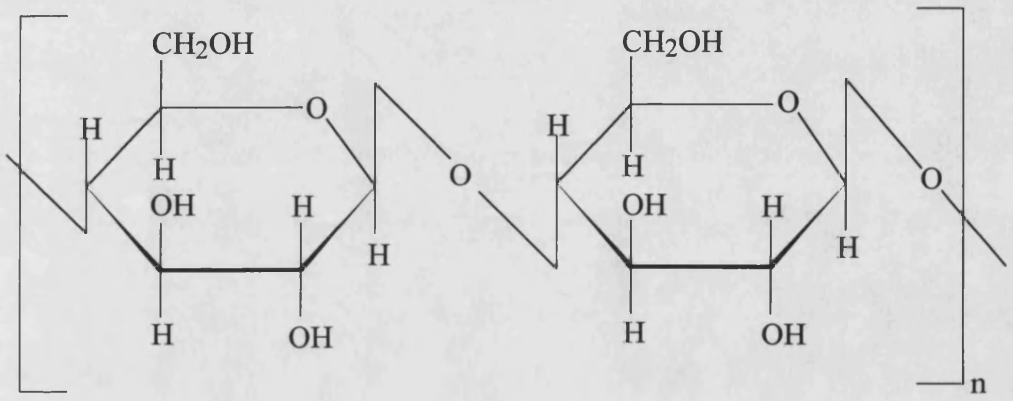

n = number of glucose residues

b) Agarose

Agarose is an alternating linear polymer of 1,3 linked β-D-galactosepyranose and 2,4 linked 3-6-anhydro-α-L-galactopyranose. It is a natural product extracted from certain seaweed's and marine algae. The sugar building blocks of processed agarose provide an uncharged hydrophilic matrix. It is readily formed into uniform spherical particles of desired size (Hjerten, 1964) which show excellent porosity and very low non-specific adsorption. Due to it's more open structure it is more reactive than cellulose for derivatisation although this can be complicated by its incompatibility with many organic solvents. It's disadvantages lie in its sensitivity to organic solvents which break down the hydrogen bonds holding the triple helix agarose strands together in a three dimensional network. This effect can be reduced by

covalent cross linking, which yields a much more rigid but highly permeable gel, such as Sepharose.

c) Dextran

Dextran is an α-1,6-D-glucopyranose polymer, with occasional α-1,3 linked branches, produced by fermentation of *Leuconostoc mesenteroides* and other related species with sucrose used as the carbon source. About 5% of the total residues appear as branches, and 85%, of which many are short, consist of only one or two residues. The remaining 15% have an average length of 33 with a maximum of about 50 (Sidebotham, 1974). Crude dextran has a molecular weight of about $50x10^6$ Da. Lower molecular weight fractions are produced by partial acid, base, or enzyme hydrolysis, or various physical methods. Due to the flexibility of the α-1,6 bond, soluble dextran forms random coil structures in solution.

Cross-linked dextran gels would be good candidates for an affinity support as they possess most of the required characteristics and are more hydrophilic with enhanced chemical stability than agarose. Unfortunately rigidity can only be obtained by sacrificing porosity due to the high degree of cross-linking required. This makes the porous gels hydrodynamically weak and inferior to agarose gels for affinity applications.

1.3.2 The Choice of the Ligand

The choice of the ligand is primarily decided by the need for a molecule that shows a high degree of affinity for the protein or molecule to be isolated. This ligand may be specific for the target molecule, but usually ligands with a wider range of binding specificity are used as they are more versatile in their use and do not require the need for a new matrix to be synthesized for the purification of each protein. These include lectins, for particular groups of glycoproteins, and synthetic ligands such as the dye-ligands e.g. cibacron blue sepharose, for binding NAD requiring enzymes.

The orientation of the ligand on coupling to a spacer arm or directly to the support is extremely important to the success of the extent of the purification. The groups on the ligand involved in the binding to the target protein should be unchanged in the coupling procedure and available for binding.

1.4 Cell Separation Techniques

Cell separation techniques fall into two distinct categories: the first includes techniques based on gross differences in size and density, typically used for primary recovery. The second category are based on more subtle distinctions including differences in surface properties which may be exploited using biospecific interactions.

1.4.1 Centrifugation and Sedimentation.

Centrifugation and sedimentation are effective methods of separating cells and are based on the use of gravitational effects. Sedimentation is the separation of cells on the basis of cell size and density in the gravitational field.

Centrifugation is used to separate materials of different density when a force greater than gravity is required and which involves rotation about a fixed axis to produce a centrifugal (g) force. The force applied on the cells enables them to travel through the liquid medium and the rate of this movement is dependent on the size and density of the cells and the viscosity of the liquid. In bioprocessing, centrifugation is used to remove cells from fermentation broths, to eliminate cell debris, to collect precipitates and to prepare fermentation media.

Differential pelleting and density gradient centrifugation are the two basic types of centrifugation for cell separation (Heuff *et al.,* 1995). In differential pelleting, the medium is homogenous and cells are separated on the basis of size. The medium used is a low density medium which is usually an isotonic buffer or growth medium which allows the cells to remain in favorable conditions during separation. The cells are spun

at a low speed and the rates at which the cells separate increases with increasing gravitational force. One of the disadvantages of differential pelleting is that the force required to separate large particles is also enough to pellet smaller particles, therefore it is only possible to obtain a pure sample of the smallest particles.

An example of the use of differential pelleting is the separation of the amoebae of the cellular slime mould *Dictyostelieum discoideum* from *E.coli* on which the amoebae feed. In order to obtain a pure population of the amoebae, the contaminating bacteria must be removed. In order to achieve this separation, the growth medium containing the amoebae, *E. coli* and the soluble constituents are centrifuged and the supernatant containing most of the *E. coli* is discarded. The pellet containing the amoebae is re-centrifuged leading to a purer sample of the amoebae, but the yield of the amoebae obtained in each pellet is reduced during each wash (Sharpe 1988).

Where fractionation is required from a mixture of more than two cell types; density gradient centrifugation offers a more practical alternative to a sequence of centrifugation steps at different g forces. This technique differs from differential pelleting in that the medium increases in density down the tube. The use of a heterogeneous medium means that the migration of each cell type will cease when it reaches a point where its density matches that of the surrounding medium. This means that a number of cell types having different densities can be separated using a single centrifugation run.

The two types of density gradient centrifugation used for cell separation are rate zonal and isopynic centrifugation. The former is similar to differential pelleting except in that the cells are separated through a density gradient. Isopynic centrifugation or buoyant density sedimentation involves the sedimentation of cells in continuous gradients with sufficient force and for a sufficient period of time to allow the cells to settle at their respective densities in the gradient. Therefore the cells are separated according to their densities.

1.4.2 Affinity Cell Separations

a) Affinity chromatography

Chromatography is a separation procedure for resolving mixtures and isolating components. The basis of chromatography is differential migration; i.e the selective retardation of solute molecules during passage through a bed of resin particles (Sharma *et al.,* 1980: Doran 1995). As solvent flows through the column, the solutes travel at different speeds depending on their relative affinities for the resin particles. As a result they will be separated and appear at the end of the column at different times for collection. Chromatography is a high-resolution technique and suitable for recovery of high-purity therapeutics and pharmaceuticals. Chromatography methods available for the purification of proteins, peptides, amino acids, nucleic acids, vitamins and many other biological materials include adsorption, ion-exchange, gel filtration and affinity chromatography (Doran 1995).

Affinity chromatography separation technique exploits the binding specificity of biomolecules. Enzymes, hormones, receptors, antibodies, antigens, binding proteins, lectins, whole cells and other components capable of specific and reversible binding are amenable to highly selective affinity purification (Sharma *et al.,* 1980).

The theory behind affinity chromatography of cells is similar to that behind affinity chromatography of soluble molecules such as proteins. Both are dependent on the specific and reversible interaction between an immobilised ligand and the protein or cell to be separated.

The general method used in affinity chromatography is a column of beads to which a ligand is covalently attached. The insoluble support is usually agarose in the form of sepharose beads since -OH groups on the agarose can be derivatized for covalent attachment (Hermanson *et al.,* 1992). The ligand must possess groups that can easily be modified to allow attachment to the matrix and the ligand must be attached to the support in a such a manner that its binding properties are not seriously affected.

Molecules known as spacer arms are often used to set the ligand away from the support and make it more accessible to the solute.

The passage of a mixture of cell lines through a column containing an immobilised ligand specific for a particular cell type allows the cells with an affinity for the ligand to bind to the beads and remain in the column, whereas those lacking this affinity pass through. Conditions for elution depend on the specific binding complexes formed. Elution usually involves a change in pH, ionic strength or buffer composition. The gentlest method of recovering bound cells is via competitive elution. One way to optimize the elution conditions is to continuously monitor the number of cells, bound and unbound, recovered from the column as a percentage of the total added. Conditions are then chosen which give the highest possible recovery of bound cells in as short a time as possible (Sharpe 1988).

However problems arise when affinity chromatography techniques developed for molecular systems are applied to cell separations. These include, entrapment of cells within the bed voids, leading to blockage, the inability to generate sufficiently high superficial fluid velocities to remove bound cells, and the difficulty of eluting cells bound through multivalent interactions and to non-specific binding of cells to the column material (Sharma *et al.,* 1980: Hermanson *et al.,* 1992).

These problems have severely limited the use of column based systems for affinity cell separations and have resulted in the development of a radically new approach based on the use of magnetic beads.

b) Immuno-Affinity Separations

The specific affinity interaction between antigen and antibody have also been exploited to allow development of the techniques of immuno magnetic separation for cell fractionation. This technique is widely known as immunomagnetic-affinity cell sorting (IMACS).

Immunomagnetic separation is used both qualitatively and quantitatively as a technique to deplete or enrich specific surface antigen positive cell sub-population and has been widely used for the removal or purging of cancer cells from bone marrow (Kemmner *et al.*,1992). Immunomagnetism involves the use of immunomagnetic beads such as Dynabeads (Dynal Ltd.) coated with the appropriate antibody for selection of the complementary surface antigen. For example, studies were carried out on immunomagnetic cell separation by Gee *et al.*,(1991), in which the technique uses the interaction between the antibody and its epitope to identify the cell of interest. The cell of interest is recovered by its binding to a secondary antibody (anti-immunoglobulin coated magnetic bead) which is then subjected to a magnetic field, which does not affect the non-target cells.

Dynabeads are magnetic monosized beads (4.5μm), high in uniformity and with unique paramagnetic properties. Different reactive groups can be attached to the surface of the beads and several methods for covalent attachment of proteins to the beads have been investigated (Lund *et al.*, 1988). The beads are non-porous and provide a low surface area for protein/ligand attachment. The magnetic properties allow the beads to be rapidly and easily separated from the solutions by using a magnet.

The use of Dynabeads in immunomagnetic separations, using immobilised monoclonal and polyclonal antibodies have been described (Swann *et al.*, 1992: Gee *et al.*, 1991). The speed of magnetic separation is thus combined with the specificity of antibodies. Immunological applications based on this concept have been developed for tissue typing and cancer therapy, as well as polyclonal antibody producing cells and separation of sub-cellular components (Uhlen 1989).

The major problems associated with the use of immunomagnetic separations on a large scale are the high cost of the beads, which is compounded by problems of recovering the beads once the separation has been accomplished.

c) Scaling-Up Chromatography

The problems outlined earlier significantly limit the potential for scale up of methods based on both column chromatography and immunomagnetic beads and provide a major incentive for the development of novel approaches for cell separation. An attractive possibility is offered by the work of (Mandrusov *et al.,* 1995) who demonstrated a novel scheme for the separation and live recovery of one cell type from a mixture of cells using a membrane based affinity cell separation system. In this study, the selective chemical force depended on the density of the ligand on the support and on the number of receptor molecules on the cell surface, and the principal mechanical force used to disrupt these interactions was the applied shear. The open nature of the membrane channel (analogous to the flow channel described later and used in this report) allowed a wide range of force to be applied unlike a packed bed. Also the use of a porous membrane allowed the controlled delivery of a non specific eluent (hydrochloric acid) overcoming the problems encountered with biospecific elution of multivalently bound cells.

The success of techniques like this is critically dependent on an understanding of the relationship between ligand and receptor densities and the applied force in determining the attachment of cells to surfaces. This work investigates these relationships using a model system based on the interaction between the lectin Concanavalin A (receptor) and the sugar glucose (ligand).

CHAPTER 2

Theoretical Modelling of Cell Adhesion

The following quote by Rose and Hjortso 1988 describes cell adhesion:

"Specific adhesion is mediated by pairs of molecules that fit each other like pieces of jigsaw. Only molecules with the right shape will be able to form the specific bond, and even small changes in the shape may greatly affect the bond."

The most important factor that determines the strength of the bond between a ligand and its receptor is the affinity of the two molecules involved in the pairing. When a ligand is immobilised onto a solid support the affinity of the interaction will decide whether or not the target protein (receptor) will be retained by the matrix and the effects of external factors such as hydrodynamic shear on bound receptor is an indication of the strength of the bond.

The receptor-ligand interaction is in a state of equilibrium:

$$[Li]+[R]\underset{k_1}{\overset{k_{-1}}{\longleftrightarrow}}[LR] \qquad (1)$$

In equation (1) R is the receptor, and Li is the immobilised ligand, k_{-1} is the "on" constant and k_1 is the "off" constant. The two rate constants, k_{-1} and k_1, describe the formation and break-up of the of the $[LR]$ complex.

The dissociation constant K_d is given by the ratio of the "off" constant to the "on" constant:

$$K_d = \frac{k_{-1}}{k_1} = \frac{[Li][R]}{[LR]} \qquad (2)$$

The total ligand and receptor concentrations are given by the equations (3) and (4), where $[L]$ and $[R]$ are the free ligand and receptor concentrations:

$$[L]_T = [L] + [LR] \qquad (3)$$

$$[R]_T = [R] + [LR] \qquad (4)$$

From these equations K_d can also be represented as:

$$K_d = \frac{([L]_T - [LR])([R]_T - [LR])}{[LR]} \qquad (5)$$

If $[L]_T > [R]_T$ this can be further simplified to:

$$K_d = [L]_T\left(\frac{[R]_T - [LR]}{[LR]}\right) \qquad (6)$$

The possible alteration of the dissociation constant for the interaction due to the immobilisation of the ligand should be taken into account. Usually K_d will be increased, i.e lower affinity, due to the effects of steric hindrance on immobilisation.

The formation rate and the stability of receptor-ligand interactions are of great biological importance. Hormone receptors and antibodies bind monomerically or oligomerically to their respective soluble ligands such as peptides and antigens. These interactions must be stable to allow time for signal transduction or antigen

clearance to occur. The adhesion observed between cells due to the presence of cell adhesion molecules (CAMs) on the surface of the cells is multimeric. CAMs can be divided into five main groups which differ in the duration of the cell-cell interactions that they mediate, e.g. selectins mediate the most transient cell-cell interactions known, the rolling of leukocytes on endothelial surfaces.

Adhesion under hydrodynamic flow is an important step in many physiological processes. The interaction between mammalian cells and solid surfaces plays an important role in a number of biological phenomena. The adhesion of blood borne cells to the vascular surface occurs in the neutrophil-mediated inflammatory response (Harlan 1975), cancer cell metastasis (Pauli *et al.,* 1990) and the homing of lymphocytes to Peyer's patches and lymph nodes (Butcher *et al.,* 1980). In the neutrophil mediated inflammatory response, the adhesion of cells under flow is the initial step leading to margination; a process which involves the neutrophils adhering to the endothelial cells lining the blood vessel adjacent to the infected tissue which is followed by diapedesis which is part of the inflammatory process.

Interest in cell attachment and detachment *in vivo* has led to experiments *in vitro* involving flow-chambers (Forrester *et al.,* 1984: Wattenburger *et al.,* 1990: Cozens-Roberts *et al.,* 1990*a*:*b*:*c*) designed to help elucidate the physical and chemical processes that control adhesion. Also the knowledge that sub-populations of cells express different surface proteins has led to the development of cell separation techniques, such as cell affinity chromatography (Hertz *et al.,* 1985; Hammer *et al.,* 1987). This technique relies on the differential adhesiveness of these sub-populations to immobilised ligands on prepared or derivatized surfaces.

A fundamental and quantitative understanding of the adhesion of cells to surfaces *in vitro* can lead to a greater insight into cell attachment and detachment *in vivo*, interpretation of *in vitro* assays, and analysis and design of biotechnological processes which involve cell adhesion.

The initial phase of interactions between cells and surfaces is usually mediated by ligand-receptor interactions. These interactions are subsequently stabilised by further interactions and often accompanied by morphological changes in the cell. A number of mathematical model systems have been developed in order to understand the relationship between cell surface chemistry and cell adhesion. In these models the surface chemistry is varied systematically and adhesion measured. These systems include antibody coated hard sphere's (Cozens-Roberts *et al.*, 1990*a*: 1990*b*), reconstituted vesicles (Wattenburger *et al.*, 1990) and cellular systems in which substrate chemistry has been varied (Templeman *et al.*, 1994). However the most recent work in this area has been carried out by Hammer *et al.*, (1992: 1993). This group has put forward the "Microvilli Hard Sphere Model" (MHSM) to support their previous "Point Attachment Model" (PAM) (Hammer *et al.*, 1987). All these models tend to predict all or none phenomena rather than the time-dependent detachment observed in practice.

The PAM focuses on the adhesion of cells to a surface when the adhesion is mediated by specific binding between molecules on the cell surface and complementary ligand molecules on the receiving surface. The PAM considers the contact area between the cell and the surface to be a small region that mediates the initial attachment of the cell to the surface. Adhesion is dependent on a number of dimensionless parameters that characterise the interaction between the cell and it's receptors, with the surface and it's ligand. These quantities include receptor-ligand affinity, contact area, and bond formation. Therefore this model allows the prediction of how adhesiveness will depend quantitatively on external factors, including changes in shear stress. The theoretical framework has been built on Bell's work (Bell 1978: 1981: 1984), and the following assumptions were made in this model:

i) The reactions of binding and dissociation occur according to the characteristic rate constants
ii) The rate constants determine how many bonds are formed between the two surfaces.

iii) Receptors diffuse into the contact area between the two surfaces where binding can occur and the rapidity of this accumulation of receptors and size of the contact area determines the number of bonds that are formed.

iv) Cell adhesion occurs under shear flow which is characterised by negligible inertia and low cell density.

v) The contact area is well formed before molecular contact occurs and that this area remains constant throughout the experiment.

vi) There is a short time, called the contact time (T_c), during which the bonds can form unstressed.

vii) The normal stress distribution is such that the bonds are equally stressed in the contact area.

Other quantities expected to influence receptor-mediated adhesion to a surface include the force and torque exerted on the cell by the flow of the fluid.

From these assumptions a set of equations describing the dependence of bound and free receptor densities only on time and not on the position within the contact area were obtained. A balance on bond densities, N_b, and free receptor density, N_a, within the contact area is given by the following equation respectively:

$$\left(\frac{dN_b}{dt}\right) = k_f N_{1o} N_a - k_r N_b \qquad (7)$$

$$\left(\frac{dN_a}{dt}\right) = -k_f N_{1o} N_a + k_r N_b + \Delta(N_{co} - N_a) \qquad (8)$$

N_b = bond density

k_f = rate constant for bond formation

N_{1o} = ligand density on the substrate

N_a = free receptor density

k_r = rate constant for bond dissociation

N_{co} = initial receptor density on the cell

Δ = is a coefficient that accounts for the accumulation of free receptors into the contact area, assuming receptor migration (Hammer *et al.,* 1987).

The reverse rate constant, k_r, and the mass transfer rate, Δ, from equations (7) and (8) have different forms when the bonds are stressed and unstressed, since when the bonds are stressed their lifetime is reduced.

The PAM serves as a starting point for the analysis of cell adhesion systems that are inherently more complicated than the blood borne cell-endothelial cell interactions in the vascular system. The analysis allows for the prediction of when the cell will bind on the basis of fluid mechanical forces acting on the cell, the density of receptors for ligand molecules, the number of cell surface receptors, the speed at which receptors bind the ligand, and the affinity of the receptors for the ligand.

The PAM was later supported by the MHSM (Hammer *et al.,* 1992: 1993:); a mathematical model which is a combination of computer simulation and experimental data, investigating how a population of cells interact with an immobilised ligand under hydrodynamic shear. The cell is modelled as a microvilli-coated hard sphere, where the receptor-ligand bonds are treated as springs (figure 2.1) and the net motion of the cell is determined from a force balance including hydrodynamic, bonding and colloidal forces.

Figure 2.1 The Interactions in the Microville Hard Sphere Model.

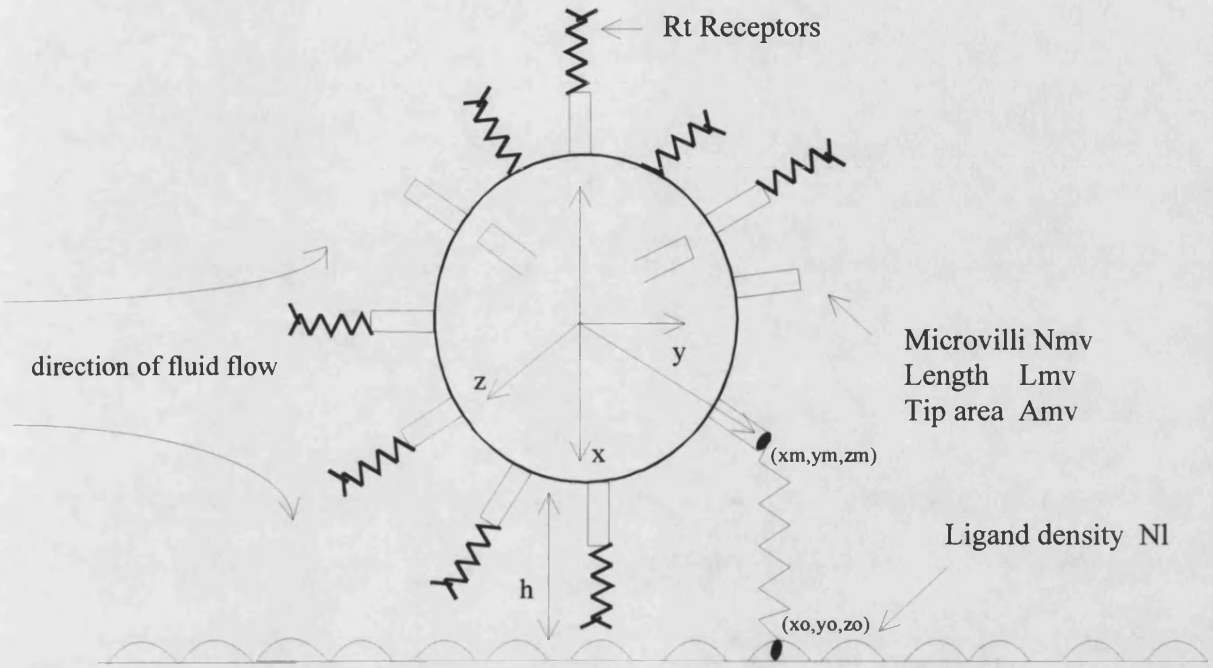

As shown in figure.2.1 the cell is modelled as a microvilli-coated hard sphere which interacts with a ligand coated surface. The cell is modelled as a sphere with radius R, covered with N_{mv} microvilli of length L_{mv} and tip area A_{mv}. In this model R_T receptors are randomly distributed over the cell surface and the density of the ligand immobilised onto the surface is assumed to be N_l. The position of the end of each microvilli is given by the vector (x_m,y_m,z_m) and it's position on the substrate is given by (x_o,y_o,z_o). The distance, h, is a time varying quantity that measures the separation between the sphere and the surface.(Hammer *et al.,* 1993).

The model can simulate the effect of many parameters on adhesion including the following:

i) The number of receptors on the microvilli tips
ii) The density of the ligand
iii)The rates of reaction between receptor and ligand
iv)The stiffness of the receptor-ligand springs
v) The response of the springs to the hydrodynamic stresses

In the inflammatory response, the local neutrophil accumulation is regulated by the concerted action of different sets of neutrophil-endothelial adhesion molecules (integrins-selectins) e.g. LFA-1/ICAM-1 or ICAM-2 and LECAM-1/CD62 (Lawrence *et al.,* 1991). While the resultant inflammation often represents a desirable response to tissue damage, responses of this type can lead to adverse consequences such as the chronic reactions seen during an asthma attack.

Selectins and integrins are adhesion molecules found on the cell surfaces of endothelial cells and neutrophils (leukocytes). The initial leukocyte-endothelium adhesion shows involvement of selectins, an inducible set of molecules. The interaction of selectins with their respective ligands appears to involve carbohydrates. Therefore the use of carbohydrate small molecule mimetics may be beneficial in the modification of the inflammatory process (Parekh. *et al.,* 1994).

The rolling of neutrophils and other leukocytes on endothelial cells was reproduced *in vitro* (Lawrence *et al.,* 1991) on artificial lipid bilayers containing the selectin CD62, that is inducible on endothelial cells. It has been suggested that a progressive decrease in rolling velocity leads to an increase in contact time between the cell and the wall allowing adhesion to occur (Lawrence *et al.,* 1991). The importance of these interactions in a number of clinical conditions is well established and the potential of binding antagonists as potential therapeutic agents has been reviewed (Parekh *et al.,* 1994). The MSHM has been developed (Hammer *et al.,* 1992: 1993) in order to

understand the functional requirements for the CD62/LECAM-1 interactions that promote neutrophil rolling. The MHSM was employed (Hammer *et al.,* 1992) to analyse the neutrophil behaviour on selectin-coated (CD62-coated) surfaces in viscous shear flow reported by Lawerance *et al.,* 1991. This analysis showed that the ability of the bond formed between CD62 and LECAM-1 which causes neutrophil rolling under flow, is the result of its unique response to strain. The adhesion of the CD62-LECAM-1 was studied to further understanding of the initial rolling and adhesion of neutrophils on endothelia. It was suggested from the data obtained that at least three sub-populations were present in these experiments: adherent cells, slow-rolling cells and fast-rolling or non-interacting cells. Understanding the structural and functional characteristics of the CD62-LECAM-1 pair will help elucidate how adhesion in flow is regulated at the molecular level for neutrophils and will provide an insight as to how the lymphocytes and metastasising tumour cells regulate their adhesion as well.

The MHSM shows that a homogenous population of cells with identical numbers of receptors, modelled with parameters suitable to recreate neutrophil rolling, display a distribution of translational velocities. The experimental model (Hammer *et al.,* 1993) investigated the adhesion under hydrodynamic flow and used rat basophilic leukaemia (RBL) derivatized polyacrylamide gels in a flow chamber. This allowed measurements of the distribution of cell binding for a population of cells at different flow rates, indicating that the cell binding decreases as shear rate increases. Experimental data showed that not all cells exhibit the slow rolling characteristic of neutrophils seen during the neutrophil endothelial interactions. Instead the cells appear to exist in a "binary" state in which the cells are either adherent (zero velocity) or non-interacting (moving at a velocity of a free cell), and the transition between these two states is abrupt. Therefore neutrophil binding to CD62 is considered an unusual form of cell-substrate interaction called cell rolling in which cells move at a fraction of the expected hydrodynamic velocity of a free particle.

Experiments with RBL cells coated with a range of densities of the antibody IgE were performed (Hammer *et al.,* 1994), allowing for the number of cell surface binding sites for the antigen to be varied. The densities of the antigen and different antigen-antibody pairs which have different rates of reaction or affinities were used. This allowed for an ideal system for studying the effect of cell surface chemistry on cell attachment in a parallel plate flow chamber when subjected to varying shear rates. It was demonstrated that the forward rate of reaction of the receptor-ligand pair is more important than its thermodynamic affinity in the regulation of adhesion under hydrodynamic flow. Adhesion increased with increasing receptor-ligand reaction rate or decreasing shear rate.

Several groups have attempted to understand the different behaviour observed with neutrophile adhesion *in vivo* (Lawrence *et al.,* 1991: Parekh *et al.,* 1994), but the simulation model appears to be the first method to enable calculation of the statistics of cell populations. Each cell is measured independently which allows determination of single cell statistics as well as population level description by simulating a certain number of cells. The main objective of this paper was to use the simulation method in order to fully comprehend how populations of cells behave. The method of simulation is described in detail in Hammer and Apte 1992.

Neutrophil experiments are shown in Table 2.1 for completeness (Hammer *et al.,* 1993).

Table 2.1 Summary of *in vitro* Cell Adhesion/Attachment Experiments.

Group	Ligand	Receptor	Cell	Behaviour
Lawernce *et al.*, 1991 Schmid-Schoenbien *et al.*, 1987	CD62	LECAM-1	Neutrophils	Rolling and transient attachment
Cozens-Roberts *et al.*, 1990 Tempelman *et al.*, 1990	IgG Dinitrophenol	IgG IgE	Glass bead Rat basophilic leukaemia cells	Irreversible adhesion Irreversible attachment
Dorozosewki 1980	Fibronectin	Integrin	L1210 leukaemia	Irreversible and transient attachment
Wattenbarger *et al.*, 1990	Lectins	Glycophorin	Vesicles	Irreversible adhesion

Leukocytes are normally found flowing in the microcirculation and are constantly coming into contact with the endothelial cell lining. The normal shear flow allows the leukocytes to be swept away off the lining unless the endothelial cells express on their surface receptors specific for leukocyte adhesion. Selectin-ligand bonds have high mechanical strength, allowing initial tethering to the vessel wall through one or more bonds, and have fast on and off rates. This allows rolling in response to hydrodynamic drag (Finger *et al.*, 1996).

If specific receptors are present on the surface, the leukocytes roll with decreasing speed along the endothelial lining until they eventually come to rest, flatten and eventually migrate through the lining of the endothelium.

A greater understanding of molecular events involved in the adhesion of leukocytes to inflamed endothelium has been obtained (Lawrence *et al.*, 1991), allowing emphasis to be placed on antagonism of cell adhesion as a therapeutic strategy to reduce and eventually treat inflammation. These treatments are aimed at the selectins

which are involved in the initial adhesion between circulating leukocytes and the inflamed endothelium. The therapeutic strategies are aimed at reducing chronic or acute inflammation. Enzymes involved or found at the site of inflammation have been the primary area of interest in such treatments (Parekh *et al.,* 1994). Experiments studying selectin-carbohydrate ligand interactions have led to the conclusion that adhesion, *in vivo*, is mediated by selectins, at least in part through binding of a carbohydrate to the selectin in a Ca^{2+} dependent manner (similar to the requirements of the lectin Concanavalin A).

The MHSM model concentrates on the force balance calculations assuming that the ligand receptor interactions can be treated as springs capable of extension prior to breakage. These models do not take into account the co-operative effect of multiple binding interactions on the extent of cell binding or that the deformation and breakage of the bonds implies damage. It has been reported however that there is no change in cells or substrate after prolonged rolling (Lawrence *et al.,* 1991).

Detachment assays have been studied by Cozens-Roberts (1990*a*: 1990*b*: 1990*c*), and have led to the development of an assay known as the Radial-Flow Detachment Assay (RFDA), so called because a radial flow chamber has been used. The progressive detachment effect of receptor-coated latex beads (prototype cells) from a ligand coated glass surface, where the receptors and ligands used are complementary antibodies, was observed under specified experimental conditions. The RFDA allows for the direct observation of cell detachment over a range of shear stresses with quantitative measurement of the adhesive force. The effect of ligand and receptor densities, which can be varied systematically, together with the influences of pH and ionic strength of the medium were also studied. In the RFDA fluid enters at the center point (a thin channel between two discs), and flows radially out from the center such that the fluid velocity decreases from the inlet. This leads to the formation of a fluid shear field decreasing from the inlet and by balancing the flow rate used the shear flow can be matched to the adhesion properties of the cell being studied.

A simple mathematical model cell system has been put forward, which characterises and quantitatively measures the parameters affecting adhesion. The theoretical framework of Bell *et al.,* (1984) and Hammer and Lauffenbuger (1990) for receptor-mediated cell adhesion has been used to analyse the data obtained from the RFDA. Expressions were developed for the critical shear stresses for detachment as a function of the key parameters affecting adhesion. These parameters include the receptor-ligand affinity and the receptor and ligand densities.

The relationship between the surface shear stress (S), the linear velocity (μ) and the Reynolds number (Re) are all inversely proportional to the radial distance from the central point (r) and is given by the following equation:

$$S = \left(\frac{3Q\mu}{\Pi h r^2}\right) \tag{9}$$

where Q is the volumetric flow-rate (cm^3/s), μ is the fluid viscosity (Pa s) and h is the gap width between the two discs (cm).

The critical shear stress is the shear stress at which 50% of the particles remain bound and is determined by using the corrected value for the critical radius (r_c) in Eqn. 9 (there is no global definition for critical shear stress). For a particle to bind to the surface, the net force must balance the torque and force imposed by the passing fluid. In the RFDA, the expressions (Goldman *et al.,* 1967) for a stationary sphere are used to estimate the force and torque exerted on the beads. From their expressions it was predicted that both the torque and the force are linearly proportional to the surface shear stress. The force and torque balance developed by Hammer *et al.,* 1987 in the PAM is employed to estimate the total force exerted by the fluid on an adherent bead. Their model is based on the following assumptions:

i) The adhesive force acts both parallel to the direction of flow and normal to the surface of the particle
ii) Non-specific forces do not play a role in countering the shear force and torque
iii)The force per bond and bond density are constant over the contact area

Cozens-Roberts *et al.,* (1990*b*) observed that at low shears a percentage of beads would "roll" along the coated surface, attaching and detaching several times before either remaining attached or being swept away. Also this behaviour was dependent on the strength of the adhesive bonds: the stronger the bond the higher the shear stress that this behaviour could be observed at. The actual percentage of beads with this behaviour increases with an increase in shear stress. In the RFDA it was the critical radius that provided a quantitative measure of the strength of the adhesive force.

In Cozens-Roberts *et al.,(*1990*b*) work, attachment is due only to reversible receptor-ligand interactions. A deterministic analysis described these results with a simple assumption: that the effective surface ligand concentration is constant due to an excess of the ligand (Cozens-Roberts *et al.,* 1990*c*), and the solution of this equation gives the time-dependent profile of receptor-ligand complexes. The fundamental assumption of this system is that all cells have the same number of interactions with the surface at any given time, and the system is completely homogenous. It is therefore not possible to obtain an accurate description of detachment. This assumption was corrected by the introduction of a probability function which took into consideration the presence of different cell populations with different numbers of ligand-receptor interactions, allowing the progressive detachment behaviour to be explained (Saterbak *et al.,* 1993).

At a constant shear stress, the fraction of latex microspheres coated with anti-goat IgG (which bound to a goat IgG coated surface), show a time dependent detachment which eventually reached a steady-state value that was characteristic of the shear rate being used (Saterbak *et al.,* 1993). This suggests that there is a heterogeneous

population of attached beads, which show different strengths of attachment. At steady-state only a fraction of beads which can balance the forces of the applied fluid is retained, and as cell detachment is a time dependent phenomenon, cells which have formed fewer bonds with the surface will be progressively detached by the applied force. Therefore as the exposure time increases, the cells remaining bound to the surface will have a greater resistive force.

An alternative explanation has been put forward for ligand-mediated interactions on the basis of multiple ligand interactions (Hubble *et al.,* 1995). A cell or a prototype cell with multiple binding sites interacting with ligands on a substrate is analogous to a multi-subunit enzyme with saturated sites, where co-operative binding is a well characterised and understood phenomenon. To describe the interaction between a cell covered with many receptors and a ligand coated surface, the concept of cooperativity used by Yon *et al.,* (1988) to describe multivalent cell/surface interactions, has been extended (Hubble *et al.,* 1995).

Experimental data (Coznes-Roberts *et al.,* 1990*b*) was used in this model (Hubble *et al.,* 1995). Simple analysis of the experimental data showed that neither data or model prediction suggest a normal distribution of binding strengths, where progressive detachment analysis of subpopulations would lead to a sigmoidol curve, (Cozens-Roberts *et al.,* 1990*c*).

This led to the conclusion that a population of cells immobilised only through reversible interactions would show significantly different properties to a population which has started to form covalent attachments and that a different modelling approach is required for each case.

Quantitative relationships based on multivalent ligand receptor binding equilibra have been developed which can describe the enhanced binding observed when polyvalent ligands are employed as inhibitors of cell-cell interactions (Hubble *et al.,* 1996). The enhanced effectiveness of multivalent competitors as inhibitors of

biospecific interactions between cells has been reported, with significant influence in the medical field (Spaltenstein *et al.,* 1991). The quantitative aspects of these interactions has yet to be fully understood as the majority of the literature reports consider the mechanics of the interaction rather than the influence of the binding equilibra.

There are a number of reports considering the multivalent interactions in molecular systems. These include the Co-operative Cluster Theory developed by Yon (1988) which explains the effects of ligand cluster affinity adsorption of multivalent enzymes. The idea of co-operativety was used to develop a model of multi-sited enzyme binding to insoluble affinity supports where ligand densities allowed multivalent interaction.

The Co-operative Theory has been extended to cell systems where ligand binding equilibra have been used to assess the interaction of cells with a surface (Hubble *et al.,* 1995), to predict the extent to which cells will detach by an applied force and the effects of addition of a multivalent inhibitor are also considered (Hubble *et al.,* 1996).

The theoretical development of these relationships described by Hubble *et al.,* 1995 is summarised below:

Consider a cell with multiple receptors (R) capable of interacting with ligands (L). The material balance for the cell receptors, where concentration is defined with respect to area rather than volume, is

$$[R_t] = [R] + [LR] + 2[LR_2] + 3[LR_3] + \ldots\ldots + n[LR_n] \quad (10)$$

where $[R_t]$ is the total cell receptor concentration, $[L]$ is the free ligand concentration, $[R]$ is the unoccupied surface receptor concentration, n is the number

of interactions per cell and $[LR_n]$ is the population of ligand attached to the cell by n ligand-receptor interactions.

Under equilibrium conditions the initial interaction of cell with the ligand complex $[LR]$ can be described by the dissociation constant:

$$K = [L][R]/[LR] \tag{11}$$

Once the cell has undergone the initial binding step, further interactions may take place but will then be spatially constrained. Further attachments will be determined by the presence or absence of a receptor within binding distance of a ligand moiety on the polyvalent complex. While the concentration of ligand and receptor will determine the probability of a possible interaction, the equilibrium position can be quantified in terms of the dimensionless association constant:

$$K' = [LR_n]/[LR_{n-1}] \tag{12}$$

At equilibrium, using these definitions, assuming that the interactions are independent and that the dimensionless constant K' does not vary with the number of cell surface ligands interacting with receptor sites, the concentration of the species identified in equation (10) can be expressed in terms of equations (11) and (12). Solving for $[R]$:

$$[R] = \frac{[R_t]K}{K + [L]\left(\sum_{i=1}^{n} iK'^{(i-1)}\right)} \tag{13}$$

Given that the cell population is assumed to be homogeneous, the occupied fraction of the cell receptor population can be determined:

$$Y = 1 - \frac{K}{K + [L]\left(\sum_{i=1}^{n} iK^{'(i-1)}\right)} \qquad (14)$$

In the case of a monovalent ligand equation 14 simplifies to:

$$Y = 1 - \frac{K}{K + [L]} \qquad (15)$$

Simple inspection of equations (14) and (15) suggest that in the case of a multivalent ligand, the effective concentration is multiplied by the summation term. However, a more realistic comparison must be based on equivalent site densities such that the free ligand concentration is equal to the concentration of the complex multiplied by the number of moieties per complex.

The results obtained in the above study show that the enhanced binding observed with polyvalent ligands can be explained in terms of simple multivalent phenomena.

CHAPTER 3

Theoretical Background to the Flow Chamber and the Affinity Interaction Studied

The adhesive interaction between a cell and a surface, which may involve both non-specific interactions (such as van der Waals, electrostatic and steric stabilisation) and specific receptor-ligand bonds, depends on the cell and the surface properties, the medium composition and the external forces, such as depositional and hydrodynamic forces (Cozens-Roberts *et al.,* 1990*a*). Due to the complexity of this interaction methods have been developed to study cell-surface adhesion, *in vitro*.

Detachment assays are used to compare the ability of adherent cells to withstand a given force. In general hydrodynamic shear assays can be divided into four categories: flow between parallel plates (Forrester *et al.,* 1984: Wattenbarger *et al.,* 1990: Tempelman *et al.,* 1994), flow between a rotating and stationary discs (Pratt *et al.,* 1988), flow between a stationary disc and rotating cone (Worthen *et al.,* 1987) and axisymmetric flow between parallel discs (Duddridge *et al.,* 1982). The parallel plate and rotating cone assays produce only one surface shear stress value per experiment, whereas the axisymmetric assays produce a continuous range of shear stress values within an experiment. Also the parallel plate assays are designed for direct observation during shear, whereas the other three assays are usually not designed for direct observation. In all of these four types of detachment assays, the percentage of cells that remain attached after exposure to a given shear stress is an indication of the adhesive force involved.

3.1 Design of the Apparatus

An experimental rig was designed in order to determine the strength of affinity interactions between Con A and ovalbumin over a range of ligand and receptor densities, which were subjected to various shears. The unit comprises a circular pump flow cell plus a microscope based image acquisition system (figure 3.1).

3.1.1 The Parallel-Plate Flow Chamber

The flow chamber has been designed so that the flow channel generates a laminar flow profile while allowing detachment experiments to be performed at a range of shear values (figure 3.2 A & B).

Figure 3.1 Schematic Diagram of the Experimental Apparatus

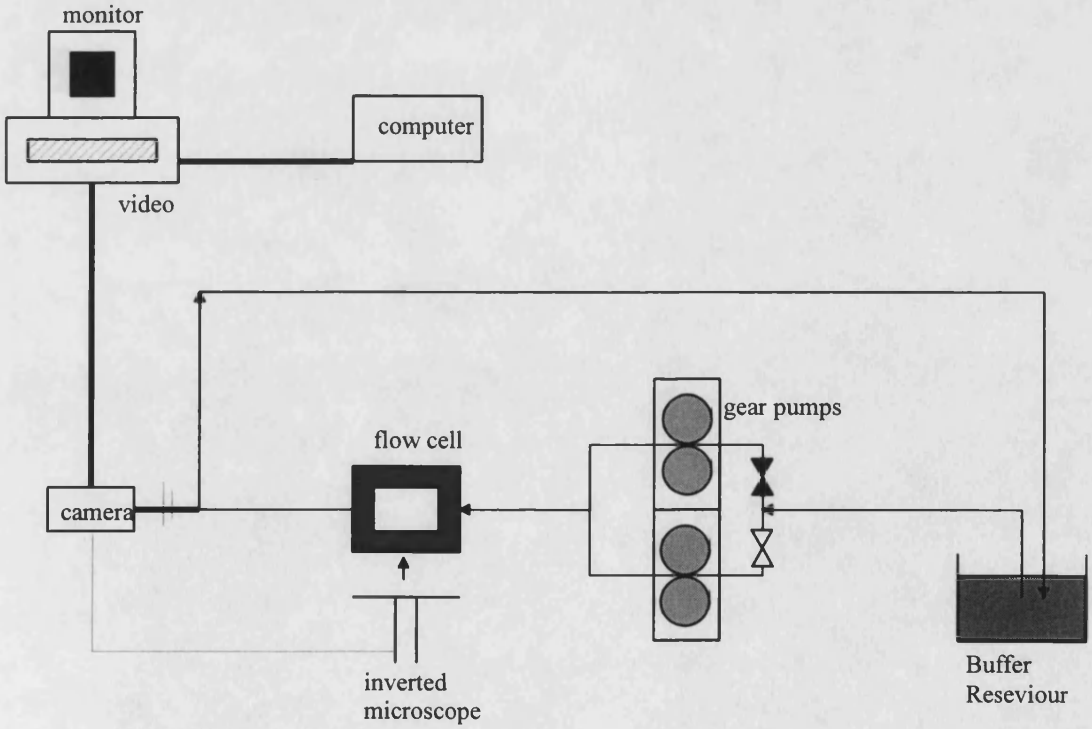

Both peristaltic and gear pumps were used to investigate the full range of shears necessary for the detachment experiments. Initially very low shears (0-0.15dyn/cm^2) were investigated and a peristaltic pump was used, for the higher ranges (0.15-2.25dyn/cm^2) a gear pump was employed. The use of two pump types also allowed the effect of steady and pulsing flow on detachment of beads to be studied. To obtain a pulse free flow at low shears, the pulse needed to be dampened. A pulsation dampener usually takes the form of a cylinder or sphere in which a pocket of air absorbs part of the pumped output during the delivery stroke and restores air to the system during the following suction stroke.

Figure 3.2

(A) A Cross-Sectional View of the Flow Cell.

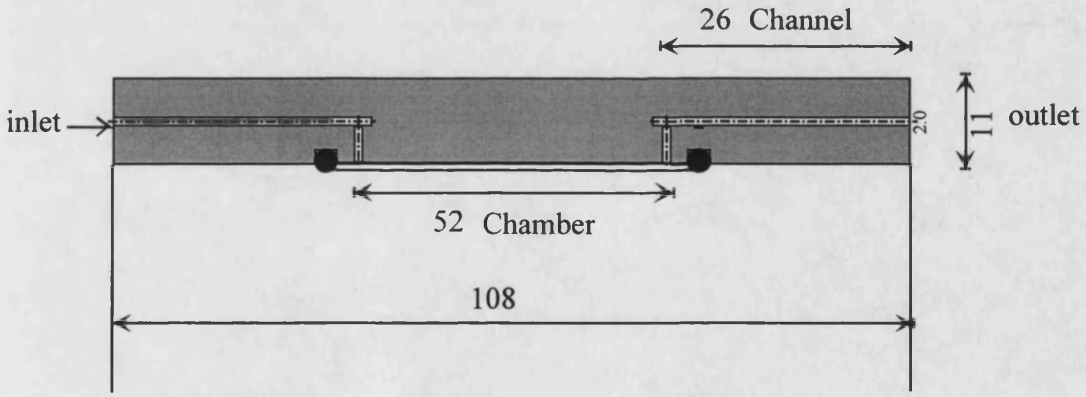

(all the dimensions are measured in mm).

(B) Top View of the Flow-Cell

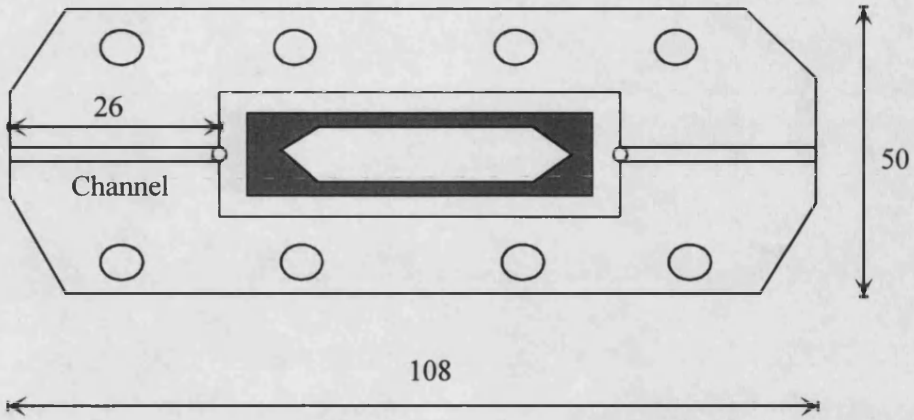

Detailed Schematic of the Chamber

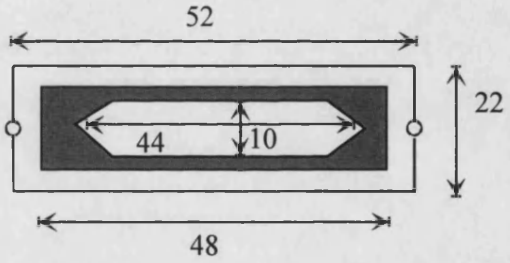

(all the dimensions are measured in mm).

Figure 3.2 gives a detailed schematic of the parallel plate flow chamber. The chamber was constructed from perspex. A standard glass microscope slide fits into a groove cut into the bottom piece. The walls and the top surface of the chamber were formed by a channel 1.0cm wide, 4.4cm long and 0.025cm deep, cut into the top plate. Silicone rubber gasket was used throughout, with chamber dimensions of 1mm in depth, 4.2cm long and 1.2cm wide. The gaskets were used as well as the original chamber. The two halves of the chamber are held together by eight screws. Buffer flow to the chamber is provided by a peristaltic or gear pump. The volumetric flow-rate delivered to the flow chamber was determined, allowing the shear stress

(dyn/cm^2) to be calculated for each experiment. It was important to prevent the beads from settling in the tubing used with the peristaltic pump, therefore tubing with a small sized bore (5mm) was used to ensure high velocities (6.25cm/s).

3.1.2 The Image Analysis System

Detachment experiments were observed using a Diaphot 300 inverted microscope (Nikon Co., Japan) focused on the top surface of the membrane containing attached beads. Data were recorded as a series of images using a video camera connected to the microscope. An U-matic video cassette recorder VO-7630 (Sony Co., Japan) was used to record the images, and a monitor was used to both observe the experiment in real time and to analyse the data collected on the videotape and the number of beads attached at each time frame was counted as described in section 4.2.10(d). In a typical experiment the detachment of the beads across the field of vision was recorded at a magnification of 125x for 45 minutes. The experiments were performed at room temperature (20-25°C). Experiments were repeated over the desired shear range, and the shear stress was adjusted by varying the volumetric flow of the buffer through the cell.

3.1.3 Fluid Flow in the Chamber

The flow of fluid in the flow chamber is said to be laminar, that is all particles of fluid move in distinct and separate lines without turbulence. In turbulent flow velocities fluctuate irregularly producing a turbulent boundary layer. The laminar flow of the fluid is used as a hydrodynamic shearing force to detach cells from the surface.

Transition from laminar to turbulent flow depends on the velocity of the fluid and also on its viscosity, density and the dimensions of the flow chamber. Fluid flow can be characterised using the dimensionless Reynolds number which is defined in equation (1).

$$\mathrm{Re} = \left[\frac{D v \rho}{\mu}\right] \quad (1)$$

where D is the pipe diameter(m), v is the average linear velocity (L/m^2), ρ is the fluid density (kgm^{-3})and μ is the fluid viscosity (Pa s).

The critical Reynolds number marks the upper boundary for laminar flow and laminar flow is encountered at Reynolds number less than 2100. If the Reynolds number is above 4000 under normal conditions turbulent flow is observed. The transition region where flow may be either laminar or turbulent depending on the entrance of the flow chamber is between 2100 and 4000 (or other variable e.g. pipes). The Reynolds number for the flow in the chamber (figure 3.2) at highest shear stress value used was calculated to be 329. This value is well below the transition range of a Reynolds number of 2100 thus confirming laminar flow in the channel under all the conditions used.

The equation for calculating the wall shear rate (S_w, s^{-1}) between parallel-plates is given by the following equation:

$$S_w = \frac{Q}{40Wd^2} \quad (2)$$

where Q is the volumetric flow rate (ml/min), W is the channel height (cm), and d is half-channel depth (cm). Equation (3) was used to calculate the shear stress.

$$S = \mu\left[\frac{du}{dh}\right] \quad (3)$$

S = shear stress (dynes/cm^2), μ = viscosity of the fluid (Pa s), h = height of the channel (cm) and u = linear velocity (cm/sec). Equation (3) can be re-written as $S = \mu\left[\frac{3u}{h}\right]$, when dh is $0.5h$ and $d\mu$/max. is 1.5μ.

The linear velocity is given by the following equation:

$$u = \frac{F}{A} \tag{4}$$

F is the flow rate (ml/sec) and A is the cross-sectional area of the chamber (cm^2).

3.2 Quantification of Affinity Interactions for Use in Cell Sorting

It is the development of cell culture techniques that has led to the recent increase in the interest in cell sorting techniques. Probably their most demanding and exciting application is in therapies for the treatment of cancer (Egland *et al.,* 1993). The ability to extract, separate and culture healthy cells from the marrow of cancer patients offers the potential to remove the need for donors and hence significantly broaden the scope for treatment.

Although a number of affinity based sorting protocols have been qualitatively demonstrated, quantitative assessment of their performance has yet to be rigorously carried out. This project aims to address this by conducting a systematic investigation of the effects of ligand density, strength of binding and system hydrodynamics on the efficiency of affinity based cell sorting techniques.

In this project a model system for the investigation of the effects of ligand and receptor densities was developed. For reasons of economy and availability of existing data on binding constants, this work has been conducted using the lectin Concanavalin A (Con A) as the binding protein.

3.2.1 Concanavalin A

Concanavalin A (Con A) a plant lectin, a globular protein from jack bean (*Canavalia ensiformis*), was first isolated and crystallised by Sumner and Howell (1936). These workers established it to be the phytohaem agglutinin of the jack bean and to be mitogenic for various animal cells and precipitate various polysaccharides. The Con A protomer consists of a single polypeptide chain of 237 amino acid residues. Con A contains no α-helices, and is composed entirely of β-strands (Figure 3.3).

This lectin is a tetramer above pH 7 and a dimer below pH 6. Each monomer (Mr 26 500 Da) has one carbohydrate binding site as well as sites for the transition ions Mn^{2+} and Ca^{2+} (Hardman *et al.*, 1982). The removal of these cations by acidification with 0.1M HCl and dialysis against water abolishes the carbohydrate binding activity and hence the biological function of Con A (Mandal *et al.*, 1994*a*).

Figure 3.3. The Monomeric Structure of Con A. The four β-sheets are shown as ribbons; coloured green, dark green, lavender and red. The N-terminal amide nitrogen of each strand is represented by a light blue sphere and the C-terminal carbonyl carbon atom is similarly represented by a grey sphere. The chelated calcium (CA) and manganese (MN) ions are represented as yellow and range spheres respectively.

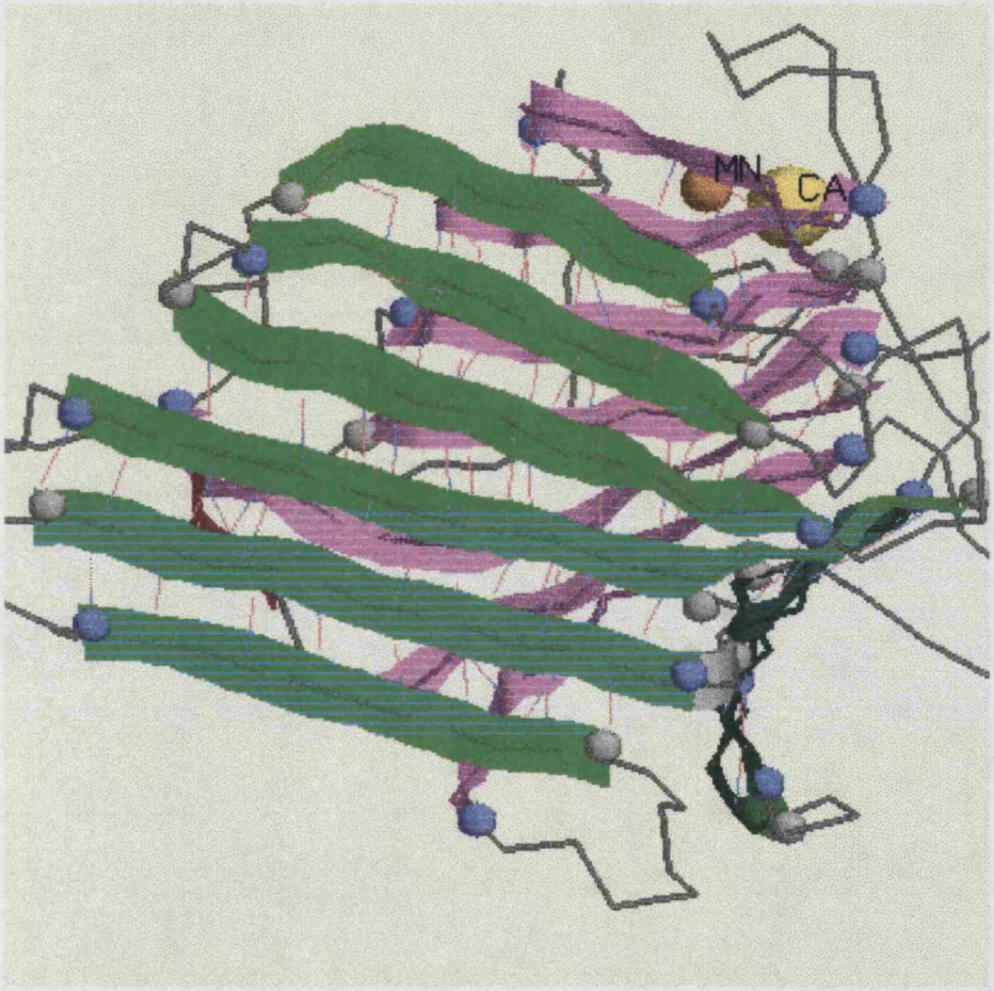

Con A specifically binds mannose and glucose residues present in cell surface glycoproteins. The monosaccaharide with the highest affinity for Con A is methyl-α-D-mannopyranoside ($K_p = 2 \times 10^4\ M^{-1}$), since in it's α-anomeric form, mannose is the monosaccharide most complementary to the Con A sugar binding site. The mannose and glucose binding lectins comprise a group of agglutinins found in the family

heguminosae. On the basis of their molecular structure, the mannose/glucose specific lectins may be classified into two groups. The first group consists of four identical subunits e.g. Con A and the second group is composed of lectins with two light (α) and two heavy (β) chains e.g. pea and lentil lectins, which require metal ions and are rich in acidic and hydroxylic amino acids (Schwarz *et al.,* 1993).

These binding properties allow Con A to be used as a probe for elucidating the structure and function of cell and organelle surface glycoproteins. Con A can also be used for purification of carbohydrate containing macromolecules by affinity chromatographic techniques, itself being the first lectin to be isolated by affinity chromatography (Liener *et al.,* 1986).

a) The Mn^{2+} and Ca^{2+} Binding Sites.

The Mn^{2+} and Ca^{2+} ions are hexa- and pentacoordinated respectively, and are 4.35 Å apart, occupying what is described as a "double site". All the side chains that ligand directly to the Mn^{2+} and Ca^{2+} are found in the first 24 amino acids of the polypeptide chain (figure 3.4 A & B).

Con A sequentially binds a transition metal ion (Mn^{2+}) in the metal-binding site S1 and calcium in the metal-binding site S2 to form it's saccaharide binding site. The conformational change allows for a sugar residue to bind Con A (Hardman *et al.,* 1982).

Figure 3.4. The Interactions at the Mn^{2+} and Ca^{2+} Binding Sites of Con A. The manganese (MN) ion is represented by a green sphere and the calcium (CA) ion by a blue sphere.

(A) The Mn^{2+} Binding Site.

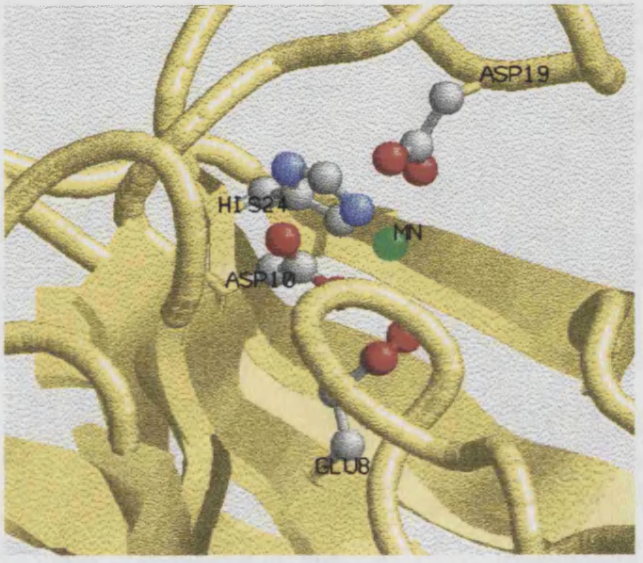

(B) The Ca^{2+} Binding Site.

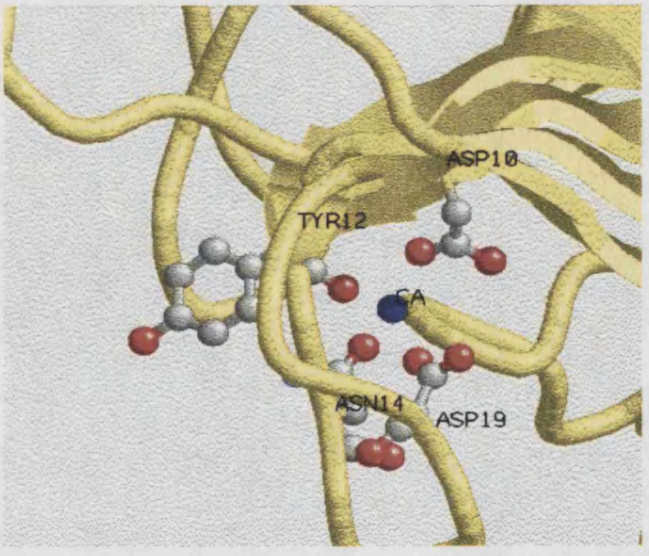

b) The Carbohydrate Binding Site of Con A.

The double ion site is 23 Å from the carbohydrate binding site, which is a distinct cavity and was confirmed in a crystal complex of methyl-α-mannopyranoside (Hardman *et al.*, 1976: Derewenda *et al.*, 1989). The methyl-α-mannopyranoside molecule is bound in the C1 chair conformation and a network of seven hydrogen bonds connect the oxygen atoms of the mannoside to five animo acid residues and two water molecules. These residues act as hydrogen doners and acceptors of the protein (figure 3.5).

Figure 3.5 The Interactions at the Sugar Binding Site of Con A.

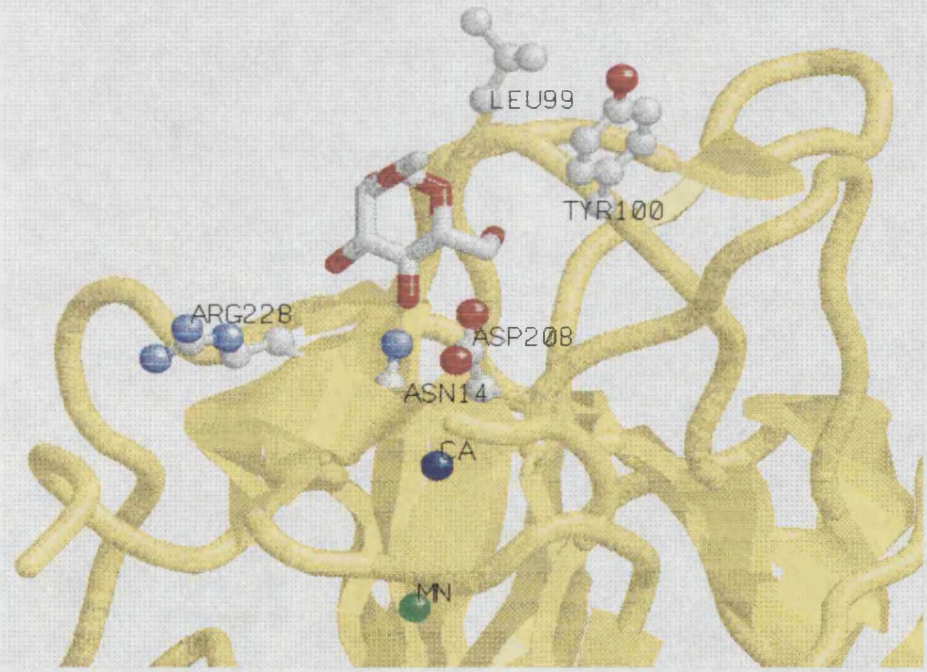

The crystal structure of the Con A-trimannoside complex provides a rationale for the high affinity of Con A for asparagine-linked glycans (Naismith *et al* 1996). The 1,6-linked mannose residue of the trimannoside is bound in the monosaccahride binding site (Derewenda *et al.*, 1989; Mandal *et al.*, 1994*b*). The other two sugars of the trimannoside bind in an extended cleft formed by residues Try-12, Pro-13, Asn-14, Thr-

15, and Asp-16 (Naismith *et al.,* 1996; Mandal *et al.,* 1994*a*). Therefore Con A has an extended binding site which includes a high-affinity site (the monosaccharride site), a lower affinity site and a third site.

The understanding of the molecular interactions involved between the trimannoside and Con A can lead to an insight into the specific interactions of N-linked carbohydrates with the lectin. All N-linked oligosaccaharides contain a common pentasaccharide core consisting of three mannose, the trisaccharide moiety 3,6-di-0-(α-D-mannopyranosyl)-D-mannose, and two N-acetylglucosamine residues (figure 3.6).

Figure 3.6 Structure of the Pentasaccharide.

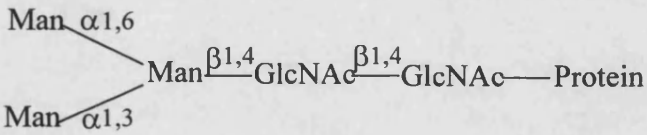

The high affinity of Con A for N-linked carbohydrates allows Con A to be used widely as a tool for investigating the properties of normal and transformed cells, as well as to isolate carbohydrates, glycoconjugates, and cells on a Con A affinity column. It is the trisaccharide moiety 3,6-di-0-(α-D-mannopyranosyl)-D-mannose found in all N linked carbohydrates that is responsible for the high affinity binding between N-linked carbohydrates and Con A (Mandal *et al.,* 1994*b*).

Succcinyl and Acetyl Con A are dimeric derivatives of Con A (both pH independent) and have been used for years as probes of cellular membranes. Differences in the binding and biological behaviour of these derivatives relative to native tetrameric Con A have been attributed to their reduced valence. Derivaitized dimeric Con A posses lower affinity toward some oligomannose glycopeptides found on the cell surface than tetrameric Con A (Mandal *et al.,* 1993). These differences in affinity between tetrameric and dimeric Con A are due to the ability of the longer arms of the Man 7 and Man 9 glycopeptides to jump between adjacent monomer binding sites of

the tetramer, not seen in the dimer because the binding sites are further apart (Mandal *et al.,* 1993).

Extensive experiments with Con A on the binding of ^{13}C-enriched methyl α and β-glycoside to Con A by NMR spectroscopy led to the discovery that different binding orientations exist for these two glycosides (Brewer *et al* 1973; Sekharudu *et al* 1984). For the β-anomer 2-3-, and 4 -OH groups bind at the same position occupied by the 6-, 4- and 3-OH groups of the α-anomer respectively. Chemical modification studies confirmed the involvement of the COOH groups in the Con A carbohydrate binding site.

Plant lectins have been used to define differences between normal and transformed cell surfaces. Several methods have been used to evaluate the interactions of glycoproteins with lectins, including examination of the capabilities of glycoproteins to form insoluble complexes with lectins specific for sugar components of the glycoprotein. Also determination of the ability of a glycoprotein to bind to a lectin which has been covalently attached to an insoluble support such as sepharose or agarose. The support should itself have no specific affinity for the glycoprotein. The glycoprotein can be eluted from the lectin-complex by treatment with a solution of a glycoside for which the immobilised lectin is specific and which removes the glycoprotein by competing for the binding sites of the lectin (Dulaney 1979).

The use of immobilised Con A (e.g. Con A-Sepharose) has proved extremely useful for the isolation and fractionation of glycoproteins and glycolipids. The immobilisation of Con A onto organic membranes e.g. cellulose, may allow the separation of cells depending on their Con A binding properties since different cell populations express different cell surface antigens. This can also be exploited using antibodies used in immmunochemical affinity chromatography.

The kinetics of Con A-sugar interactions show that Con A binds low molecular carbohydrate ligands via monophasic second order kinetics. The rate constants at 25°C of 10^4 -10 M^{-1} sec^{-1} (Gray 1973; Lewis *et al.,*1976), are several orders of

magnitude below what one would normally expect for a diffusion controlled process. This indicates that steric constraints may impede association or that an unstable complex that initially forms at a diffusion controlled rate is subsequently stabilized by a slow rate determining conformational change.

Such low rate constants have also been found in intercellular adhesion phenomena. The formation rate and the stability of an interaction are of great biological importance and are given by the association and dissociation rate constant, respectively. Cell-cell interactions range from the structurally important, long-lasting associations between cells in solid organs, to the transient, highly regulated interactions typical of leukocytes. Affinity and kinetic analyses of cell adhesion molecules (CAM's) have shown that CAM interactions that mediate transient cell adhesion may have surprisingly low affinities and extremely fast dissociation constants (van der Merwe *et al.*, 1994).

Techniques have been developed which allow the attachment of Con A to a number of planar support surfaces and coupling of its complimentary ligand (either in the form of dextran or sugar moieties on the surface of ovalbumin) to a particulate support chosen to mimic a cell's geometry. These techniques have been incorporated into a parallel-plate flow chamber device, to allow the effects of shear on detachment to be studied in a quantitative and reproducible fashion.

CHAPTER 4

Materials and Methods

4.1 Materials

The majority of biochemicals were obtained from Sigma Chemical Co., Poole, Dorset.

Albumin chicken egg (ovalbumin: grade VI), 1,4-butanediol diglycidyl ether, Concanavalin A (type IV), dextran, dextranase, dialysis tubing (cellulose membrane), 4,4-dicarboxy-2,2 biquinoline (bicinchonic acid [disodium salt]), ethanolamine, fluorescamine, Trizma base, Trizma HCl.

The membrane materials used were obtained from Pall,

These included cellulose membranes: Biodyne B an anion-exchange membrane (positively charged Nitrogen groups), and Biodyne C a cation-exchange membrane (negatively charged) and Loprodyne membranes (-OH groups).

All other chemicals used were of analytical grade and were obtained from a number of manufactures.

4.2 Methods

4.2.1 Ligand Coupling to Sepharose 4B

a) Direct Coupling of Cibacron Blue

Initially Sepharose 4B was chosen to mimic cells in the system. The Sepharose was stained with Cibacron blue solely to aid its visualisation under the light microscope.

30ml of the Sepharose CL-4B gel was first washed with distilled water on a sintered glass funnel to remove preservatives and suction dried to a wet cake. The washed gel was placed in 200ml of 200mM sodium carbonate buffer containing 1.0M sodium chloride to which 1g of Cibacron blue was added. The suspension was incubated overnight at 45°C with gentle stirring. The gel was then washed thoroughly with water, packed into a column with a 50ml bed volume (1cm x 65cm) and washed with 300ml distilled water, followed by 500ml 1.0M NaCl, 400ml 50% (v/v) ethanol and 500ml distilled water. Finally, the cibacron modified gel was suspended in water which contained 0.01% (w/v) sodium azide as an antimicrobial agent and stored at 4°C.

b) Epoxy Activation

Sepharose CL-4B was washed as in section 4.2.1(a). The washed gel was suspended in 75ml of 0.6M NaOH containing 150mg sodium borohydride (2mg/ml). An equal volume of 1,4-butanediol diglycidyl ether was slowly added to the gel at room temperature, the reaction mechanism is shown in figure 4.1. This reaction mixture was left at room temperature for 10 hours with constant stirring. The activated gel was extensively washed with water to remove excess reagents, until there was no longer any evidence of an oily film on the surface of the gel which represented the unreacted epoxy compound. Finally the gel was washed with acetone to remove any traces of coupling agents, and the gel resuspended in water for the ligand coupling. A 2ml aliquot was taken at this stage to determine the number of epoxy groups

present on the Sepharose (section 4.2.1(d)). Ligand coupling took place as soon as the gel had been activated.

Figure 4.1. Mechanism of activation of the hydroxylic matrix by 1,4 butanediol diglycidyl ether and subsequent coupling to an amine containing ligand.

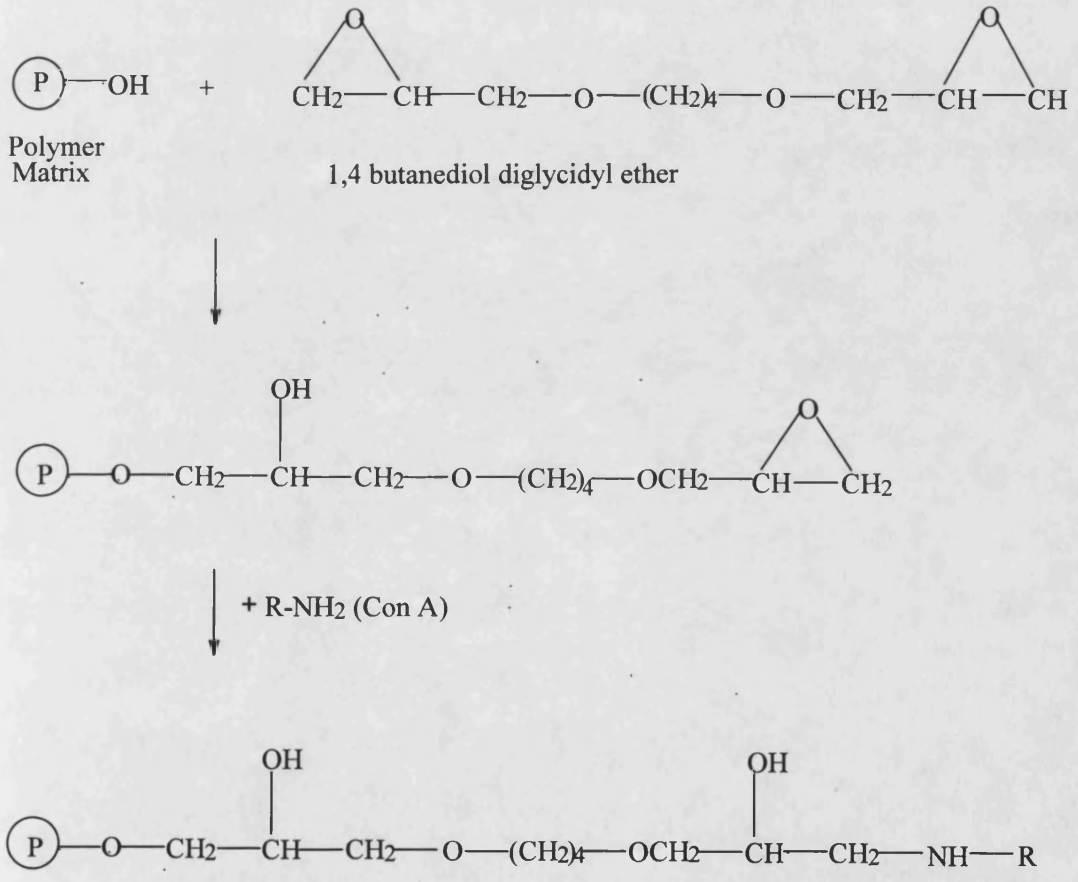

c) Determination of Oxirane Groups

The method suggested by Axen *et al.*, (1967) for oxirane determination uses the reaction between the oxirane ring and sodium thiosulphate to generate an oxidation

product which can be easily detected. Bis-oxiranes are used to introduce oxirane (epoxy) groups into hydroxylic polymers. The reagent used to introduce these active epoxy groups is 1,4-butandediol diglycidyl ether (Sundberg and Porath, 1974). The bond between the bisoxirane and the matrix becomes a stable ether bond, while the other end provides the ligand coupling potential. This terminal epoxy can then react with ligands containing hydroxy, amine, or thiol groups. The reaction between the oxirane ring and sodium thiosulphate is shown in figure 4.2.

Figure 4.2. The Reaction Involved in the Determination of Oxirane Groups.

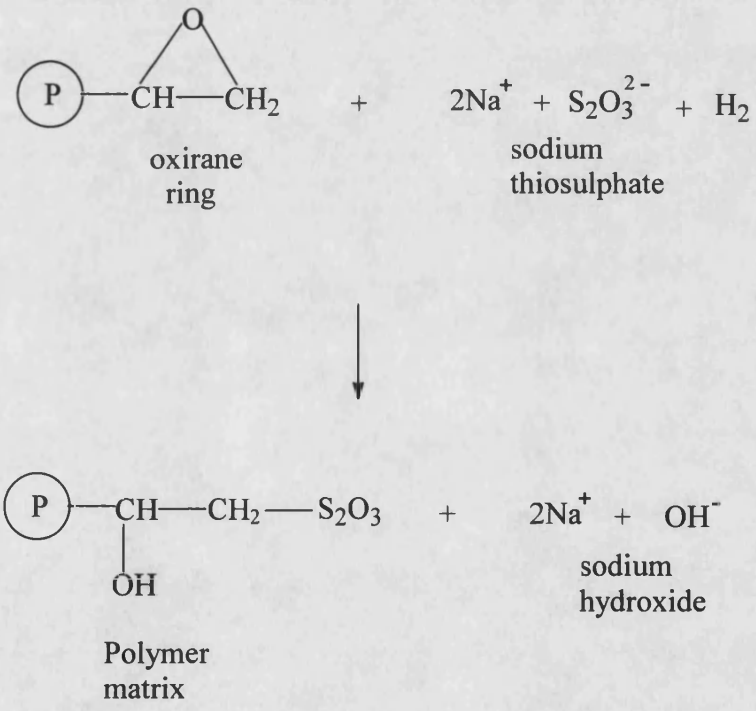

Thus the release of OH^- can be followed by titration with 0.1M hydrochloric acid. This reaction was carried out in an autotitrator (pH stat) to prevent excessive pH fluctuation which could compromise the analysis.

Oxriane concentration in solution was determined as follows. The oxirane containing solution (20µl) was added to 1.0ml of 1.0M sodium thiosulphate solution pH 7.0. The pH was kept constant by the addition of hydrochloric acid until the reaction was complete. The amount of oxirane present in the solution was then calculated from the amount of hydrochloric acid required in order to maintain neutrality.

Oxriane groups in the gel were determined as follows. Wet gel (30g) was added to 1.0ml of 1.0M sodium thiosulphate solution pH 7.0 and the oxirane content of the gel was determined by titration with hydrochloric acid. The agarose gel was suction-dried under vacuum on a sintered glass filter funnel for approximately 5min and weighed. The sample had a dry weight of approximately 21mg.

d) Dextran Coupling to Epoxy-Activated Sepharose

The coupling for 20g of suction-dried oxirane Sepharose, was accomplished by dissolving the desired reactant (dextran) in 30ml of 0.25M NaOH adjusted to a predetermined pH of 14. Dextran was coupled at a temperature of 45°C using a reaction time of 15 hours. The gel was subsequently washed first with 200ml 0.1M NaCl on a glass filter funnel, and then with 200ml distilled water, to remove unreacted ligand. Excess epoxy groups were blocked by suspending the gel in 0.1M ethanolamine, pH 9, with stirring at room temperature for 24 hours. The gel was washed extensively on a glass filter funnel with 1.0M NaCl and water, to removing excess blocking reagent.

4.2.2 Estimation of Bound Dextran

a) Colourimetric Determination

Phenol in the presence of sulphuric acid can be used for the quantitative colourimetric determination of sugars and their methyl derivatives, oligosaccahrides and polysaccharides (Dubios *et al.*, 1956).

Dextran modified Sepharose (from section 4.2.1(c)) was suction dried in a glass filter funnel to a wet cake. A small amount (20mg) of the dextran modified Sepharose was used for the analysis. 50µl of 80% phenol (w/v) was added to the tube containing the Sepharose sample. At this point 5ml of 18.36M concentrated sulphuric acid was added and the mixture allowed to cool for 10 minutes. The tubes were mixed well and incubated for 20mins at 25-30°C. The absorbance was read at 490nm in 1 cm glass cuvettes in a Cecil 272 spectrophotometer. The machine was zeroed against distilled water. A standard curve of dextran was obtained with concentrations ranging from 10-120µg.

b) Dextranase Assay

This method was based on the assay of Jason *et al.,* (1966) in which the enzyme is used to degrade dextran to give isomaltose which can be determined colorimetrically.

Dextran modified Sepharose (from section 4.2.4) was suction dried to a wet cake and 55mg were placed in 2ml of 0.1M phosphate buffer pH 6.0, to which 20µl dextranase (10mg/ml) were added and incubated for 3 hours at 37°C. The incubation period allowed for the hydrolysis of dextran by the dextranase to produce isomaltose. Following the incubation, the gel was allowed to settle leaving the supernatant which contained the isomaltose. The supernatant was allowed to cool before a 600µl aliquot was made up to 2ml with distilled water and the Dubios (1956) colourimetric method was carried out as described in section 4.2.2(a). Unmodified Sepharose was treated as above and used as a control. A standard curve of isomaltose (10-160µg) was constructed, to enable the amount of isomaltose and hence the amount of dextran bound to the Sepharose to be calculated.

4.2.3 Immobilisation of Con A onto Cellulose Membranes

a) Ion-Exchange Coupling

A Biodyne B positively charged membrane with a high density of quaternary amino groups was used. Con A must be negatively charged for the anion-exchange process to occur and the optimum pH for this process was determined as follows.

0.1M bis tris propane, (1,3 bis[tris(hydroxymethyl)-methylamino] propane) and 0.1M sodium acetate buffer solutions were prepared with the following pH values 5.0, 8.4, 8.6 and 9.5, using 1.0M NaOH and acetic acid respectively. These buffers were used to prepare Con A solutions with the following concentrations 0.25, 0.5, 1.0, 2.5 and 5.0 mg/ml.

The Biodyne B membrane was prepared as follows. The membrane was placed in 0.1M buffer (bis tris or acetate) with the appropriate pH for 2 hours and then washed in 0.25M solution of the appropriate buffer (bis tris or acetate). The Con A solutions were added to the membrane and left overnight at room temperature with agitation on a 3-D rotating platform. The amount of Con A bound to the membrane was determined by calculating the difference between the amount of Con A added and that remaining after coupling. The absorbance of the Con A solution before and after the coupling procedure was measured at 305nm in 1cm cuvettes in a Cecil 272 spectrophotometer. The concentrations of Con A present before and after coupling were determined from a standard curve.

b) Epoxy Activation and Covalent Binding of Con A onto a Cellulose Membrane

i) The Epoxy-Activation Procedure.

A piece of membrane (10cm x 16cm) was suspended in a solution of 5ml 0.6M NaOH containing 2mg/ml sodium borohydride. To this was slowly added, with mixing, 5ml 1,4-butanediol diglycidyl ether and the membrane was incubated overnight at room temperature with agitation. The activated membranes were than

thoroughly washed with 50ml distilled water, 50ml of acetone and water 100ml until there was no longer a trace of an oily film.

ii) The Covalent Binding of Con A onto a Cellulose Membrane.

Solutions of Con A with concentrations 1.0, 2.5, 5.0, 10.0 and 25.0mg/ml were prepared in buffers with a range of pH values from 4.5-9.0. A piece of activated membrane ($2cm^2$) was placed in each Con A solution and left overnight at room temperature with agitation on a 3-D rotary platform. The membranes were washed with 50ml of pH 7.4 10mM tris buffer to remove uncoupled Con A from the surface of the membrane and any unreacted sites were blocked with 1.0M ethanolamine in 0.25M $NaHCO_4$. Unmodified membrane was used as a control. Ligand coupling was measured by the difference analysis at 305nm and by the BCA assay (section 4.2.4).

For the difference analysis concentration of Con A before and after incubation with the activated membrane was measured at 305mn in a Cecil 272 spectrophotometer. A standard curve of Con A was constructed and the linear regression equation obtained from the standard curve was used to calculate the amount of Con A bound on the membrane.

The activation and coupling procedure was repeated three times, each time in duplicates. From this data, a binding profile of the Con A onto the membrane was obtained.

4.2.4 Determination of Immobilised Con A

The amount of Con A immobilised on the cellulose membrane (section 4.2.3b) was determined by the following method as well as the difference analysis.

Bicinchonic acid (BCA) is a stable, water-soluble disodium salt, capable of forming an intense purple complex with the cuprous ion, Cu^{2+}, in an alkaline environment. This reaction forms the basis of an analytical method capable of monitoring cuprous

ion production during the reaction of protein with alkali in the presence of copper sulphate (Smith *et al.*, 1985).

The following protocol describes the use of BCA for the determination of immobilised Con A from section 4.2.3 (b).

The Bicinchonic acid working reagent (BCA-WR) consists of Reagent's A and B in the ratio of 50:1.

Reagent A is an aqueous solution of:
1% BCA Na_2
2% $Na_2CO_4.H_20$
0.16% Na_2 tartrate
0.4% NaOH
0.95% $NaHCO_4$

Reagent B consists of 4% $CuSO_4.5H_2O$ in distilled water. Both the reagents are indefinitely stable at room temperature.

A set of protein standard solutions were prepared using the soluble form of Con A and BSA as a standard protein. At least 5 concentrations, ranging from 0.1-2.0 mg/ml of the standard protein were prepared. To 100µl of the standard samples, 2ml of BCA-WR were added. As the sample protein to be assayed was immobilised onto an organic membrane, 2ml of the BCA-WR were added directly to the Con A modified membrane ($2cm^2$). The samples and the standards were mixed, sealed with parafilm and incubated at 37°C for 30min. After this time they were cooled to room temperature, and the absorbance of the supernatant was measured in 1cm plastic cuvettes at 562nm in a Cecil 272 spectrophotometer. The standard curve of BSA was used to calculate the amount of protein bound onto the membrane.

4.2.5 Determining the Binding Capacity of Immobilised Con A

The glycoprotein ovalbumin was used to determine the binding capacity of immobilised Con A, which has a carbohydrate binding site per monomer. The binding between Con A and ovalbumin is an indication of the availability of Con A active sites.

The binding capacity of Con A involved a contacting or adsorptive step, which loaded the ovalbumin onto the Con A modified membrane, a washing step to remove residual unabsorbed material, desorption or elution of ovalbumin with a suitable solvent and washing to remove residual eluant.

a) Binding of Ovalbumin onto Immobilised Con A

The binding capacity of Con A was determined by measuring the amount of ovalbumin bound to Con A modified membrane over a fixed period of time, with ovalbumin concentrations ranging from 0.2-10mg/ml.

Con A was immobilised onto an organic membrane, Loprodyne, at an initial concentration of 5mg/ml (67μg/cm^2) as in section 4.2.3(b). The membrane was placed in 5ml tris buffer pH 7.4 containing 10mg/ml of ovalbumin in the presence of 1mM $CaCl_2$ and $MnCl_2$ since Ca^{2+} and Mn^{2+} ions are required for Con A binding (Hardman *et al.,* 1982), and left for 2 hours at room temperature with agitation. Controls were set up with unmodified and modified Con A membranes to which no ovalbumin was added. The experimental and control membranes were washed with PBS (50ml) and the amount of ovalbumin bound to the membrane was determined using the BCA assay (section 4.2.4) and an adsorption isotherm constructed.

b) Removal of Ovalbumin Bound to Immobilised Con A with Glucose

Ovalbumin loaded membranes were produced as above and a control was also set up with an unmodified membrane (6cm^2), and a Con A modified membrane (6cm^2) with no ovalbumin added. Both the control and experimental membranes were washed

with 50ml PBS and 50ml 0.5M glucose solution in tris buffer pH 7.4 was added to the membranes. The solution was changed at regular intervals of 30min in order to prevent depletion of glucose. The membranes were washed with 50ml PBS and the BCA assay was performed on both the control and the experimental membranes (Section 4.2.4).

The above experiment was repeated with tritiated glucose to confirm that competitive elution of ovalbumin was taking place.

c) Binding of ^{3}H-Glucose to Immobilised Con A

The binding of tritiated glucose, with a specific activity of 2.6Ci/mmol, to immobilised Con A was performed in order to confirm the binding activity of Con A. Con A modified membranes ($4cm^2$) were prepared as described in section 4.2.5(a) and placed in different concentrations of ^{3}H-Glucose, ranging from 2-6mM, containing 5mg/ml unlabelled glucose, Ca^{2+} and Mn^{2+} ions and the total buffer volume was made up to 3ml. At regular time intervals (0, 15, 30, 60, 120 and 180 minutes) 10µl samples were taken and opti-phase scintillant was added. These samples were placed in a scintillation counter and cpm readings were obtained.

The above experiment was repeated, this time cold glucose was omitted and 2mM were added after 60 and 120 minutes time interval samples had been taken. This was in order to see continuous binding of ^{3}H-glucose to the Con A modified membranes. Controls were set up with unmodified membrane and with no membrane.

4.2.6 Determining the Stability of Covalently Bound Con A

An organic membrane, Loprodyne, 10×16cm was covalently modified with Con A (Section 4.2.1). Excess reactive sites were blocked with sodium cyanoborohydride 0.01% (w/v) in 50ml 1.0M ethanolamine. The membrane was washed with 100ml PBS, and stored at 0-4°C. At regular intervals over a period of several weeks, a $2cm^2$ piece of the membrane was cut out at random and the BCA test was performed to establish the amount of Con A bound to the membrane.

4.2.7 Coating Dynabeads with Ovalbumin

Ovalbumin was immobilised onto Dynabeads; which are 4.5μm polystyrene paramagnetic beads, using the methods below. The dynabeads were supplied as ethanol washed beads in distilled water at a concentration of 4 x 10^8 beads/ml by Dynal Ltd,.

a) Adsorption of Ovalbumin onto Uncoated Dynabeads

Uncoated Dynabeads (50μl) were washed with 200μl of 0.1M sodium phosphate buffer pH 7.5 and spun for 2 minutes in a centrifuge at room temperature. The supernatant was discarded and the washing procedure repeated twice. Ovalbumin at a concentration of 100μg/ml was added to the beads in a total volume of 200μl of sodium phosphate buffer pH 7.5. The mixture was left for 24 hours at room temperature. The coated beads were washed twice for 5mins with PBS and then finally left for 24hrs in PBS. The coated beads were stored in PBS containing 0.02% (w/v) sodium azide. Bound ovalbumin was estimated using the methods described in Section 4.2.8.

b) Coating Dynabeads with Ovalbumin using Gluteraldehyde

Uncoated dynabeads were placed in a 2% (v/v) gluteraldehyde solution in 0.1M sodium phosphate buffer pH 5.0, using a ratio of 1μl beads to 50μl buffer and incubated for 24hrs at room temperature (figure 4.3). These were washed thoroughly with PBS. Ovalbumin solution in 0.1M sodium phosphate buffer pH 8.0 at 5mg/ml was added to the washed beads in the same ratio as above. The beads were left for 24hrs at room temperature with mixing. The coated beads were washed carefully with 10ml 0.1M phosphate buffer pH 8.0, followed by 10ml 0.15M NaCl. The excess activated sites were blocked with 1.0M ethanolamine containing 0.01% (w/v) sodium cyanoborohydride in 10ml 0.1M phosphate buffer pH 8.0 and left overnight. The beads were washed with 25ml PBS pH 7.0, resuspended with 5ml PBS and stored at

0-4°C with 0.01% (w/v) sodium azide. Ovalbimin bound was estimated by the methods outlined in section 4.2.8.

Figure 4.3 The Steps Involved in the Immobilisation of Ovalbumin onto Dynabeads via Glueraldhyde Derivatization of the Beads.

a) The gluteraldeyhde polymerization step.

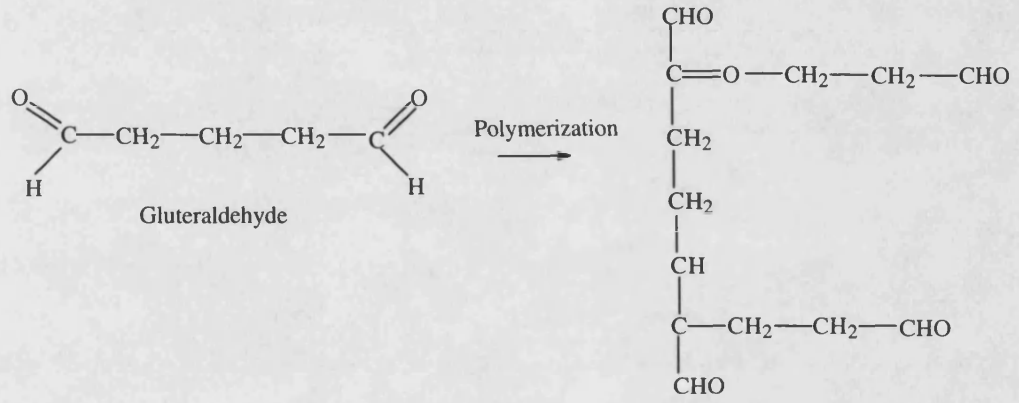

b) Ovalbumin Immobilisation onto Dynabeads

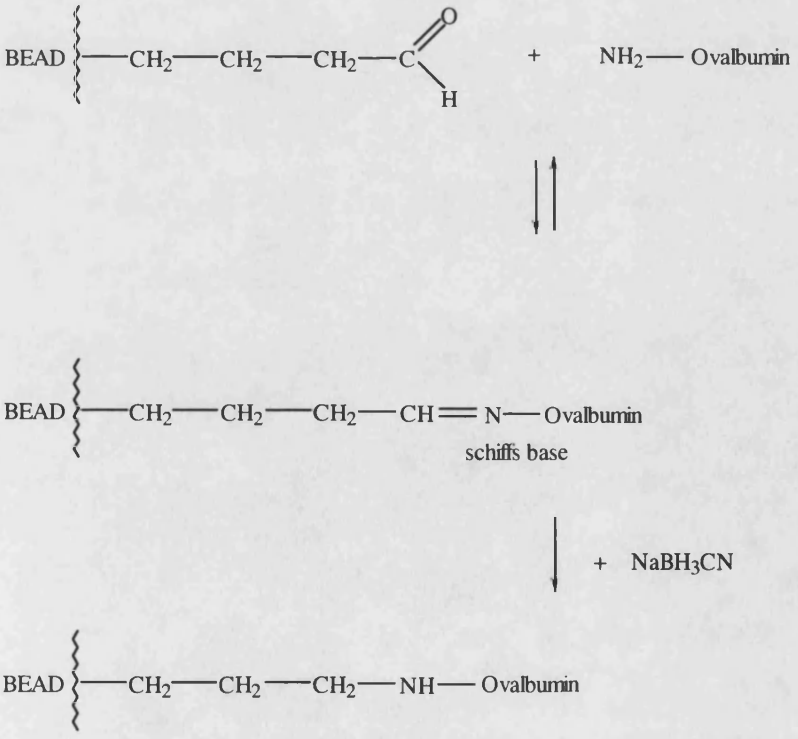

c) Coating Tosyl-activated Dynabeads with Ovalbumin

Tosyl activated dynabeads were used to covalently bind ovalbumin to the beads. The tosyl groups on the beads react with primary amino acids on proteins. In ovalbumin this interaction occurs via the twenty-four lysine residues per ovalbumin molecule.

Figure 4.4. The Tosylation Step of Dynabeads and the Subsequent Binding of Ovalbumin.

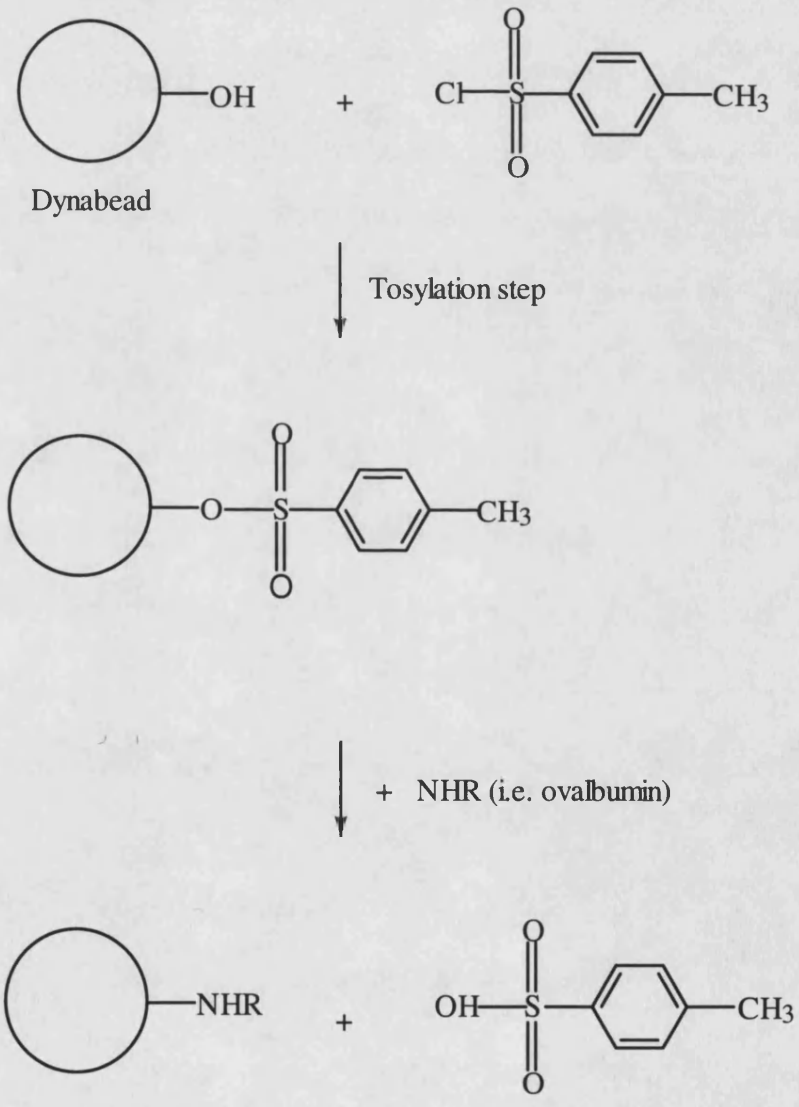

The dynabeads (4×10^8 beads/ml) were vortexed and resuspended in 1ml 0.17M borate buffer pH 9.5, and then washed three times in 1ml borate buffer. Ovalbumin at a concentration of 5mg/ml in 10ml 0.17M borate buffer pH9.5 was added to the washed beads and left for 24 hours at room temperature with mixing. The beads were washed three times for 10 minutes, and then for 30 minutes, and finally overnight at 4°C. All the washes were carried out in 10ml PBS. The excess activated sites were blocked with 10ml 1.0M ethanolamine containing 0.01% (w/v) sodium cyanoborohydride in 0.17M borate buffer pH 9.5, and left for 3 hours. Ethanolamine reacts with any tosyl sites that have not reacted with the NH_2 groups of lysine as shown in figure 4.4. The beads were washed with 10ml PBS pH 7.4 and resuspended in PBS containing 0.01% (w/v) sodium azide and stored at 0-4°C.

d) Binding Ovalbumin Coated Beads to Con A Modified Membranes

The stability of ovalbumin bound onto the dynabeads from the three binding methods previously described (4.2.7a-c) was compared by placing each sample of ovalbumin-coated beads onto Con A modified membranes overnight in a petri dish in tris buffer pH 8.5. Controls were also set up with unmodified membranes. The beads were washed gently with the buffer to remove any unsettled and non-specifically bound beads off the membrane. A qualitative assessment was made as to the stability of the ovalbumin-Con A bonds formed by amount of the beads that remained bound on the membrane after several washes with the buffer.

4.2.8 Development of a Protein Assay: Estimation of Immobilised Ovalbumin

The amount of ovalbumin bound to the dynabeads (from Section 4.2.7) was estimated by the methods described in the following section. Initial attempts involved estimation by mass balance by calculation of the difference between ligand added and ligand remaining in the washings described as the "difference analysis method". As the amount of ovalbumin bound, calculated by mass balance gives an indirect estimate, trypsin digestion and acid hydrolysis protein assays were also performed on the immobilised ovalbumin. Fluorescamine, (4-phenylspiro[furan-2-

(3H,1-phatalan)]-3-3'dion) was used to react with the ovalbumin and used for the protein assays.

Fluorescence resulting from the reaction of a protein with fluorescamine is an indication of the number of free amino groups in that protein. Fluorescamine is a non-fluorescent molecule that reacts with primary amines e.g. lysine to yield an additional product that is highly fluorescent under UV irradiation (figure 4.5). The resulting fluorescence is proportional to the amine concentration and the fluorophores produced are stable over several hours

Figure 4.5 The Structure of Fluorescamine and its Subsequent Reaction with Primary Amines.

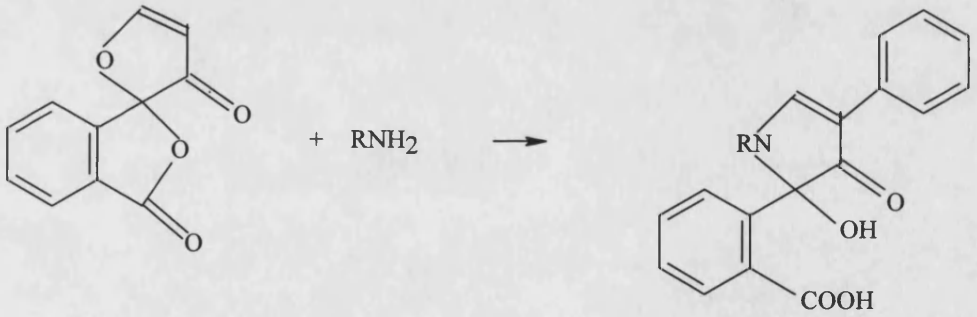

Fluorescamine
(non-fluorescent)

Fluorescent product

a) Difference Analysis

The concentration of ovalbumin before and after incubation with tosyl activated beads was measured using Fluorescamine. Tosyl-activated dynabeads samples of $4x10^8$ beads/ml were incubated overnight with ovalbumin at a range of concentrations of 2.5-40mg/ml. The ovalbumin concentration before and after incubation was determined using Fluorescamine. A standard curve of ovalbumin

with fluorescamine with a concentration of 18mg/ml in acetone was obtained (Chen *et al.,* 1978). The fluorescence was measured in a fluorometer with excitation and emission wavelengths of 390nm and 475nm respectively (Evans *et al.,* 1984). A linear regression equation was used to calculate the amount of ovalbumin in the samples. Uncoated beads were used as a control against the ovalbumin coated beads. The experimental and control reactions were carried out in 0.05M tris buffer. To determine the most suitable pH for this reaction, ovalbumin standards in 0.05M tris buffer with the pH values of 7.0, 7.5, 8.0, 8.5 were tested.

As this is also an indirect method of protein determination, the following, direct methods were attempted in order to quantify the exact amount of ovalbumin bound to the beads.

b) Trypsin Digestion of Dynabead Immobilised Ovalbumin.

Ovalbumin ranging in concentration from 25-100mg/ml in 0.05M tris pH 8.5 was immobilised to tosyl-activated beads (as described in section 4.2.7c). The beads were resuspended in tris buffer pH 8.5 to which 10µl of fluorescamine (18mg/ml) was added and left for 15min. The hydrolysis products of fluorescamine were washed with tris buffer, 20µl trypsin (10mg/ml) was added to the resuspended beads. These were left overnight at room temperature allowing the immobilised protein to be cleaved by the trypsin. The fluorescence in the supernatant containing peptides was measured and a linear regression equation derived from a standard curve was used to determine the amount of protein in the supernatant. For initial ovalbumin concentrations of 50 and 100mg/ml, stable fluorescence was being observed. The process was repeated for lower ovalbumin concentrations, ranging from 2.5-40mg/ml.

Further research on this assay suggested that tris buffer can interfere with the reactions of protein with flourescamine (Evans *et al.,* 1984). Therefore the use of tris buffer was suspended and borate buffer pH 8.5 was used for later experiments.

c) Acid Hydrolysis of Immobilised Ovalbumin

Ovalbumin coated beads (4×10^8 beads/ml) prepared section (4.2.7c) were placed in a solution of 6M HCl and frozen on dry ice before being vacuumed for 2min. The tubes were sealed with parafilm and left overnight at 110°C in an oven. Sample pH was brought up to 9 with 5.8M NaOH to which 10µl of fluorescamine (18mg/ml) had been added. The fluorescence was measured as in section 4.2.8(b). A standard curve of acid hydrolysed ovalbumin was used to relate fluorescence to total protein concentration.

4.2.9 Determining the Binding Capacity of Immobilised Ovalbumin

The binding capacity of immobilised ovalbumin on dynabeads was determined by measuring the amount of Con A bound to the immobilised ovalbumin.

Con A (5mg/ml) in 0.1M borate buffer pH 8.5 was added to 1ml ($4x\ 10^8$ beads) of ovalbumin (27µg/ml of beads) coated beads and left overnight at room temperature. At pH 8.5 Con A is in it's tetrameric form (Gray *et al.*, 1973). Samples of supernatant containing unbound Con A were taken every five minutes over a period of 30 minutes. A Con A-fluorescamime standard was used to determine the amount of Con A present in the supernatant thus allowing the amount of Con A bound to the immobilised ovalbumin to be calculated. The bound Con A was competitively eluted off the ovalbumin coated beads overnight using 1.0 M D-glucose pH 8.5 at room temperature. The Con A eluted off the beads was measured using fluorescamine and Coomassie blue. This assay was repeated with ovalbumin-coated beads that had been incubated in varying ovalbumin concentrations (1.0, 2.5, 5.0, 10.0, 25.0, 50.0, 100.0, 250.0µg/ml)

4.2.10 Parallel-Plate Flow Detachment Assays

The parallel-plate flow chamber (section 3.1) provides a controlled environment for the determination of the shear stress at which ovalbumin coated beads (cell mimics) can detach from the Con A modified membrane. By increasing the flow-rate of the

buffer (0.05M tris pH8.5) over the Con A membrane to which beads are bound, and assessing the number of beads detached at each shear stress, the relationship between the shear force and effect of Con A and ovalbumin densities can be determined. All the detachment assays were carried out at room temperature of 19-22°C.

a) Detachment Assays

Ovalbumin solutions at concentrations of 1.0, 2.5, 5.0, 10.0 and 25.0μg/ml in 0.05M tris buffer pH 8.5 were prepared and bound onto tosyl activated beads as in section 4.2.7(c), the activity of bound ovalbumin was determined as described in 4.2.8 Con A solutions at concentrations of 1.0, 2.5, 5.0, 10.0 and 25.0mg/ml were prepared in buffer Na_2CO_3 as outlined in section 4.2.3 and the amount of immobilised Con A was determined (table 5.1) by the BCA assay as described in section 4.2.4.

Ovalbumin coated beads were attached to a Con A modified membrane (1.7cm x 4.7cm, 78μg/cm^2 i.e. an initial Con A loading of 1mg/ml) in a petri dish containing 0.05M tris buffer pH 8.5, $CaCl_2$ and $MnCl_2$ and sodium azide. This was left at room temperature overnight to allow Con A and ovalbumin to bind, the membrane was placed in the flow cell. A section of beads was viewed under an inverted microscope at a magnification of 125 (section 3.2.2) and the beads were subjected to the following five shear stresses 0.15, 0.46, 1.00, 1.65, 2.25dyn/cm^2, which were generated using a gear pump to vary the volumetric flow through the cell. Buffer (0.05M tris pH 8.5) was used in the system for all the detachment assays. A low flow wash was used prior to the detachment assay in order to remove any settled and non-specifically bound beads from the membrane.

The membrane was first subjected to the lowest shear of 0.15dyn/cm^2 for 40min, during which at regular intervals of 0, 1.0, 2.5, 5.0, 10.0, 20.0, 30.0 and 40.0 minutes, images of a chosen section of the beads on the membrane were captured using the image analysis package (see section 3.3.2) and printed for subsequent counting of the number of beads bound at that time. This was repeated for a further four shear values of increasing magnitude. Between each detachment experiment the flow-chamber

was cleaned with 0.05M tris buffer pH 8.5 and a duplicate was performed. This allowed a detachment profile to be obtained for chosen Con A and ovalbumin concentrations at the five shear stresses selected (chapter 6). This shear sequence was repeated for Con A concentrations at each of five ovalbumin concentrations. A silicone rubber gasket were used to obtain a leak free system and also to give variance in cross-sectional area of the chamber. Control experiments were performed to test for non-specific adhesion under flow with unmodified membrane and beads. Ovalbumin coated beads (4×10^8beads/ml) were placed onto an unmodified membrane(1.7cm × 4.7cm), and subjected to the lowest shear of 0.15dyn/cm^2. This was also performed with unmodified beads and a Con A modified membrane (67μg/cm^2).

Initially a peristaltic pump was employed but only covered a range of shears, 0.08, 0.17, 0.24, 0.35 and 0.48dyn/cm^2. The use of the a peristaltic pump also allowed the effect of pulsatile and steady flow (delivered by a gear pump) on the detachment behaviour of the beads to be investigated. The gear pump was used to obtain steady flow at higher shears (>0.46 dyn/cm^2) and was used for all the detachment experiments. The membrane with attached beads was placed in the flow cell with the original chamber.

b) The Effect of Pre-Incubation Contact Time on Detachment of Beads.

The following experiments were performed to assess the effect of pre-incubation time on the strength of attachment.

Five pieces of (1.7cm x 5cm) Con A modified membrane (Con A loading concentration of 5mg/ml: 67μg/cm^2) to which ovalbumin beads (25μg/ml initial loading) were added were prepared. These pieces of membrane were left at room temperature for 4, 8, 16, 24, 48, 72 and 96 hours, and subjected to a shear of 1.00dyn/cm^2 for 40 minutes and frames captured at regular time intervals.

c) Competitive Elution with Glucose

To determine the effect of introducing a competitor into the system, glucose was used at various concentrations to compete with the bound ovalbumin coated beads off the Con A modified membrane.

Ovalbumin coated beads with a loading concentration of 25μg/ml were bound to a Con A (10 mg/ml; 119.5μg/cm^2) modified membrane (8cm^2) for twenty four hours at room temperature. Glucose solutions with the following concentrations were employed in this experiment: 0.01, 0.025, 0.05, 0.1 and 0.25M.

The glucose solution (0.01M) was passed over the membrane with the bound beads for 40min at 1.00dyn/cm^2. Each concentration was run until a steady state had been obtained (i.e. when no further detachment was observed over a period of 15 minutes) on the same piece of membrane. The images were captured as described in section 3.3, for the following times: 0. 1.0, 2.5, 5.0,10.0, 20.0, 30.0 and 40.0 minutes, this allowed for a detachment profile to be constructed of the percentage of beads bound against glucose concentration (results section). This experiment was also performed in the absence of glucose solution as a control experiment. The difference in the detachment profiles for the beads in the presence and absence of glucose was observed (chapter 6).

d) Bead Counting

The image analysis system described in section 3.1.2 allowed for each time frame to be printed. For each given time, the captured frame was printed. Allowing the number of beads attached at that time to be counted. A clear plastic sheet with a grid was placed over the printed frame enabling each bead to be marked whilst counted on a manual counter.

For each set of 40 minute experiments the following methodology was carried out. The first frame to be studied was that obtained at end of each of 40 minute experiment for each shear stress value, therefore the last frame to be taken at that

shear stress value. This was replaced by the time frame for 30 minutes with the same grid sheet to which additional beads found were marked, This subsequent marking of beads with the time frames was carried out until the time frame zero, that is the frame printed before the experiment was started. From this the percentage and hence the fraction of beads bound over the 40 minute experiment were calculated (chapter 6).

CHAPTER 5

Surface Immobilisation and Characterisation of Con A and Ovalbumin

A study of the systematic effects of ligand and receptor densities on cell surface interactions requires techniques which allow controlled immobilisation to derived surfaces. The flow-cell used in this work is designed to take replaceable flat sheets containing the ligand or receptor.

To ensure reproducible support properties synthetic membrane materials were used as the surface for immobilisation. Although originally designed for purely size based separations recent interest in affinity membrane adsorption has resulted in a range of membranes designed for ligand attachment. A number of these were evaluated in this study.

Several methods can be employed for the immobilisation of cells and proteins, but the most common ones used are either adsorption or covalent attachment. Successful immobilisation ensures that there is efficient contact between the phase containing the immobilised cell or protein and the phase carrying substrate in and away from the biologically active region. Membranes are commercially available which allow both covalent and ion-exchange adsorption to be investigated.

Ion-exchange membranes, as well as cellulose membranes rich in hydroxyl groups were used to compare the ease of attachment and the binding capacity for Con A. Ion-exchange adsorption is a mild, relatively low-cost, and efficient method of attachment Although more costly. the advantage of covalent binding over ion-exchange is the generation of a stable conjugate which is unlikely to dissociate during subsequent use. Although the conditions under which covalent links form often disrupt the delicate three-dimensional structure of the protein. This almost inevitably

results in a loss of a significant proportion of binding activity during coupling. This can only be justified when the superior stability of the conjugate is important, or the activated support is supplied in a convenient and reliable form. Thus covalent attachment is used most frequently where it is essential that no activity leaks into the system. Pre-activated supports are commercially available but it is also normal practice to pre-activate the support material under sever conditions , any corrosive reagents are then removed and the activated material contacted with the protein of interest under mild conditions.

Selection of a good support is as important as the chemistry of the linkage. In principal it is possible to synthesise ready-activated polymers but producing a material with good physical characteristics at the same time is not easy. Therefore it is more common to activate a ready-made support which has the desired physical properties. Natural polymers such as cellulose, cross-linked dextran and agarose provide a suitable hydrophilic environment for the protein.

5.1 Immobilisation of Con A onto Organic Membranes

5.1.1 Comparison Between an Ion-Exchange and Covalent Binding Method

Con A was immobilised onto both ion-exchange and covalent membranes and the binding capacity of the membrane for Con A was obtained over a range of pH values. The binding of Con A was studied to determine the optimum conditions for immobilisation onto an organic membrane. Con A exists as a dimer below pH 6.0 and as a tetramer above pH 7.0 (Mandal *et al.,* 1994*a*). Therefore the binding capacity, in mass terms, is expected to be greater above pH 6.5 where Con A exists in its tetrameric form. Con A was adsorbed onto Biodyne B cellulose ion-exchange membranes as described in section 4.2.3 and covalently coupled to a cellulose membrane (Loprodyne membrane, supplied by Pall). Immobilised Con A was determined spectrophotometrically (section 4.2.3) and with the BCA assay as described in section 4.2.4. The BCA assay was also employed in the characterisation of Con A's binding activity (section 4.2.5). The spectrophotometric method assumes

that Con A in solution, is in equilibrium with the bound Con A and all the sites on the membrane are available for binding. The results of these loading experiments are shown in tables 5A and 5B respectively (where the term loading refers to the initial protein concentration the membranes are incubated with).

Table 5A The Binding Capacity of Con A for an Ion-Exchange Membrane against pH where C_o is the Initial Concentration of Con A, C_s is the Solution Con A Concentration after Binding in Solution has Occurred and C_b is the Amount Bound.

pH	C_o (mg/ml)	C_s (mg/ml)	(C_o-C_s) (mg/ml)	C_b (mg/cm^2)
	5.00	5.336	0.664	0.221
5.0	2.5	2.209	0.291	0.094
	1.0	n.d	n.d	n.d
	1.00	0.7714	0.228	0.076
8.4	0.50	0.4095	0.090	0.030
	0.25	0.200	0.050	0.016
	5.00	5.39	0.61	0.2030
8.6	2.50	2.47	0.031	0.0103
	1.00	n.d	n.d	n.d
	1.00	n.d	n.d	n.d
9.5	0.5	0.409	0.091	0.0303
	0.25	0.171	0.079	0.026

The values of Con A binding that could not be determined are labelled "n.d". This was due to insufficient amount Con A present in the sample to be detected in the linear region, that the absorbance reading was taken for.

Table 5B The Binding Capacity of Covalently Immobilised Con A for Loprodyne Organic Membrane against pH.

pH	C_o (mg/ml)	C_o mM	C_s (mM)	(C_o-C_s) (mM)	C_b (mg/cm^2)
	5.00	0.0465	0.0312	0.015	0.5400
9.5	2.50	0.0230	0.0187	0.0043	0.1548
	1.00	0.00925	0.00827	0.00096	0.03456
	5.00	0.0465	0.0407	0.00545	0.19262
8.6	2.50	0.0230	0.0221	0.00093	0.0334
	1.00	0.00925	0.0100	n.d	n.d
	5.00	0.0465	0.0423	0.0038	0.1360
5.0	2.50	0.0230	0.0227	0.00023	0.0828
	1.00	0.00925	0.0100	n.d	n.d

The binding capacity of the ion-exchange membrane for Con A is lower than the binding achieved using covalent coupling. This probably reflects the greater site density of attachment points for covalent derivatisation compared with the number of ion-exchange groups in the pre-derviatised membrane. In addition the reversible nature of ion-exchange adsorption will mean that adsorbed capacity will be a function of both dissociation constant and site. There appears to be no obvious correlation between pH and binding capacity. The covalently bound capacity of Con A is highest at pH 9.5, which can be attributed to the greater nucleophilic nature of the lysine groups at the higher pH leading to a more effective reaction.

Figure 5.1 A Comparison of the Binding Capacity of Con A (2.5mg/ml) Immobilised via an Ion-Exchange and Covalent Method.

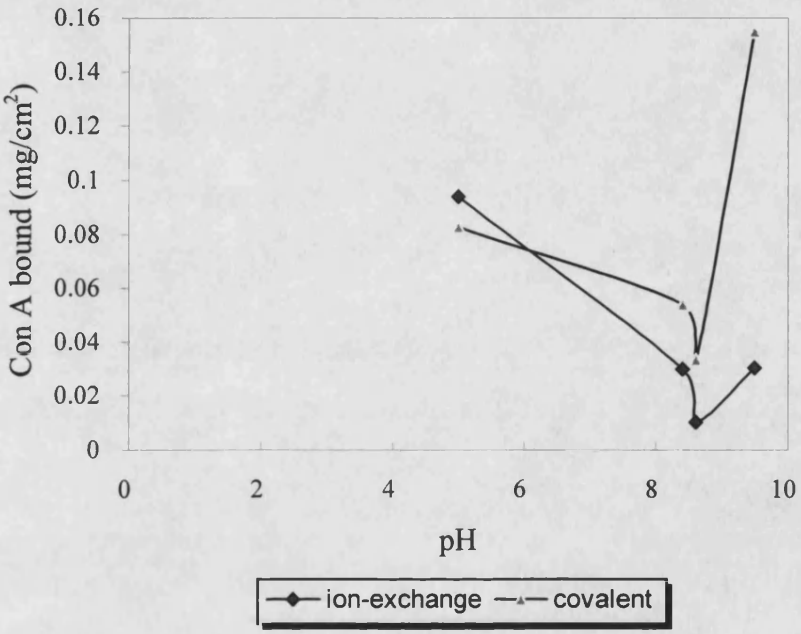

Duplicates were performed for the data shown in figure 5.1

The lowest binding capacity of Con A was observed between pH's 8.0-8.5, this is consistent with the fact that Con A is known to precipitate in the pH range of 6-8 (Liener *et al.,* 1986). The decrease in the binding capacity for both the ion-exchange and covalent membranes can be seen from figure 5.1 as a dip in the binding curves. These results demonstrate that despite its greater complexity, the covalent binding protocol gives significantly higher loading. As the Con A binding will be more stable using the covalent binding, this form of immobilisation was employed for future experiments.

5.1.2 Binding of Con A to Dialysis and Opaque Cellulose Membranes

Original experiments were conducted with membranes because of the mechanical strength and ease of derivatisation. However, the opaque nature of these membranes made subsequent particle visualisation difficult. As an alternative a transparent cellulosic dialysis membrane was investigated as a support surface. As the coupling chemistry is similar to that used for the Loprodyne membrane a direct comparison is possible.

The binding capacities of the dialysis and opaque membranes was determined over a range of Con A concentrations as outlined in section 4.2.3. The binding capacity of the dialysis and the opaque cellulose membranes for Con A is shown (figures 5.2 & 5.3) and were performed in triplicates. From these data the number of moles and molecules of Con A bound per unit area (cm^2) of the dialysis membrane were calculated and the concentrations of immobilised Con A were calculated using BCA-Con A standards.

Figure 5.2 The Binding Capacity of Con A for the Cellulose Dialysis Membrane.

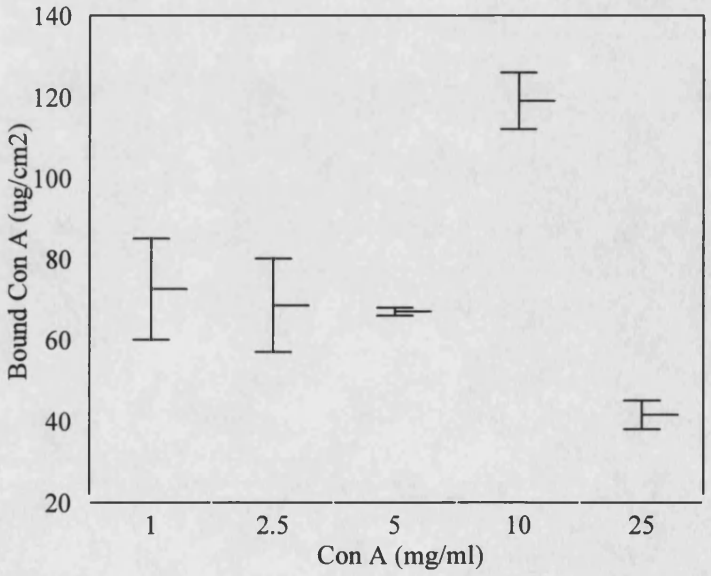

Figure 5.3 The Binding Capacity of Con A for the Opaque Cellulose Membrane.

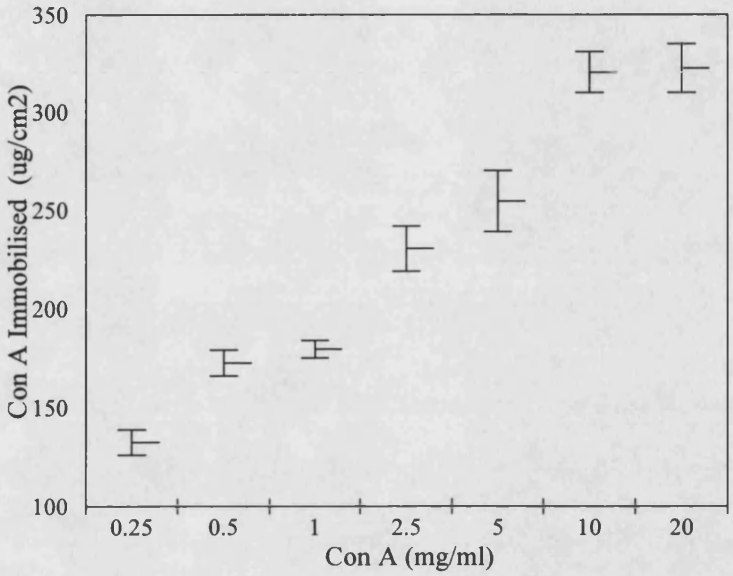

Figure 5.3 shows a definite increase in the amount of Con A immobilised onto the membrane with increasing initial Con A loading, but saturation appears to be reached at the higher Con A concentrations of 10-20 mg/ml. Therefore binding experiments were carried out in the lower Con A concentration range. This allowed a greater difference to be observed in the attachment of ovalbumin coated beads to the immobilised Con A.

The binding of Con A onto the dialysis membrane does not give the same binding profile as the opaque membrane. The greatest binding of Con A is seen at the Con A loading of 10mg/ml, there appears to be an optimum initial loading for this membrane. The highest Con A loading of 25mg/ml gives a lowest reading for the amount of Con A bound (table 5C).

The different wettabilities of the membranes employed for Con A binding may account for the difference in binding capacity. The most hydrophobic of the two cellulose membranes (Loprodyne opaque membrane) has the highest amount of Con A bound, whereas the dialysis membrane, which is extremely hydrophilic has a considerably lower amount of Con A bound, that of 119μg/cm^2 compared to 311μg/cm^2. This is supported by Uyen *et al.,* 1990 who showed that the adsorption of albumin to substrata with a broad range of wettabilites in a parallel-plate flow chamber in a stationary phase was always highest on PTFE, the most hydrophobic material employed and decreased with increasing wettability of the substrata. Adsorption of albumin onto the substrata of interest was performed by flowing the protein solution over the substrata in the flow cell and allowing an adsorption period of 120 minutes.

It was also observed that the protein was mostly adsorbed in island like structures on the hydrophobic substrata. The tendency to form island like structures was shear stress and concentration-dependent and disappeared gradually as more hydrophilic material was employed (Uyen *et al.,* 1990).

The difference in binding between the two cellulose membrane can also be attributed to the fact that the dialysis tubing is not made specifically for protein binding experiments as the Loprodyne membrane is derivatised for that purpose. Due to the batch to batch variation of immobilised Con A on the dialysis membrane, protein determination was performed using the BCA assay with each new batch of membrane. Also, with the hydrophilic membrane although the total amount of Con A bound is lower, the active figure may well be higher as proteins are more easily denatured on immobilisation onto a hydrophobic membrane (Doran 1985).

Table C The Number of Moles and Molecules of Con A Bound on the Dialysis Membrane per unit area (cm^2).

C_o (mg/ml)	C_m (nmoles/cm^2)	C_{mol} (molecules/cm^2) $\times 10^{15}$
1.0	6.97	4.22
2.5	6.58	3.98
5.0	6.44	3.90
10.0	11.44	6.93
25.0	3.9	2.4

The number of molecules per cm^2 of membrane is highest for the Con A loading of 10mg/ml with 6.93x 10^{15} molecules/cm^2. Previous work has shown that a monolayer of the lectin wheat germ agglutinin (WGA) covered a glass slide with 43μg over an area of 6.5cm^2 assuming that all of the lectin binds to the surface and that each lectin molecule occupies 0.7ηm^2 (Wattenburger *et al.*, 1990). On this basis it can be calculated that Con A has covered the dialysis membrane to the equivalent of at least a monolayer, as the range of Con A bound (41-119μg/cm^2) is within the range found for the WGA lectin.

5.2 Determining the Activity of Immobilised Con A

The number of Con A molecules on the surface of the membrane which are available for binding is expected to limit the number of bonds formed and therefore the number of adhering beads at low lectin surface coverage.

It is difficult to measure the number of available binding groups for a particular receptor present due to the small surface area involved, the monolayer coverage, and

the difficulty in labelling an active site without altering the receptor's binding behaviour. The total amount of protein may be measured, but the number of active sites may not always be directly related to the amount of protein present because of denaturation or incorrect orientation of the binding site.

The activity of immobilised Con A was determined by following its interaction with the glycosylated protein ovalbumin which has two N-linked glycosylation sites. Quantification of the amount of ovalbumin bound to the Con A modified membrane was determined by performing the BCA assay (section 4.2.4). The protein BSA was used as a standard.

The activity of the immobilised Con A was calculated from the ratio of Con A to ovalbumin molecules bound. The results obtained for ovalbumin binding showed that for Con A density of 67μg/cm^2 addition of 10mg/ml ovalbumin resulted in 135μg/cm^2 of bound protein. This shows an approximate mass ratio of 1:1 of Con A to ovalbumin, and a mole ratio of 1:1.5 of Con A to ovalbumin. Previously reported ratios of quail ovalbumin to monomeric Con A (in solution) at the point of maximum precipitation is 1:2, showing that the oligomannose chains present on ovalbumin are bivalent for Con A binding (Mandal *et al.,* 1992). The mass ratio obtained of 1:1 for Con A to ovalbumin is not surprising as one would have expected a lower binding ratio due to the lack of accessibility of the Con A binding sites imposed steric constraints then for the ratio obtained for Con A in solution.

5.2.1 Competitive Elution with ^{3}H-Glucose

Competitive elution of the bound ovalbumin with excess glucose (section 4.2.5c) confirmed the binding of ovalbumin to the immobilised Con A. The absorbance reading obtained after elution of ovalbumin with glucose was identical to that obtained from a control with no ovalbumin. This confirmed that the ovalbumin had been specifically bound to the Con A. The binding of ^{3}H-glucose to immobilised Con A (section 4.2.5c), shown in figures 5.4 and 5.5, confirmed that elution of ovalbumin was taking place and that the immobilised Con A was active.

Figure 5.4 The Binding of Tritiated Glucose to Con A Modified Membrane.

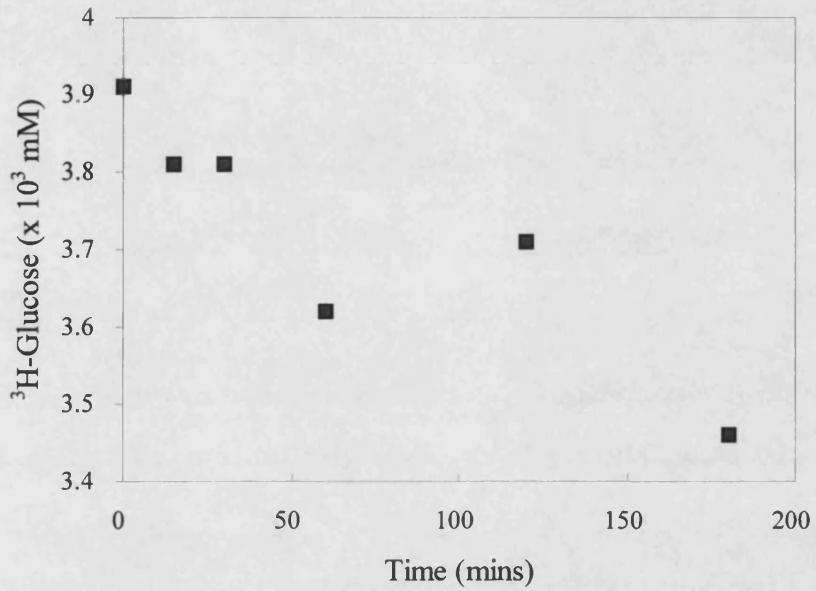

From figure 5.4 it can be seen that over a period of three hours glucose is binding the Con A and a decrease in the radioactive glucose present in solution can be observed suggesting that binding is occurring. The decrease is not very large (11%) and is not conclusive in showing that the binding of glucose to the immobilised Con A is specific. This could possibly be due to too much radioactive glucose present initially therefore a steady decrease is not likely to be observed. To overcome this problem the amount of radioactive glucose present initially can be reduced. The experiment was repeated with a Con A modified membrane in the presence of both radioactive and non-radioactive glucose (figure 5.5).

Figure 5.5 The Binding of ^{3}H-Glucose to Immobilised Con A.

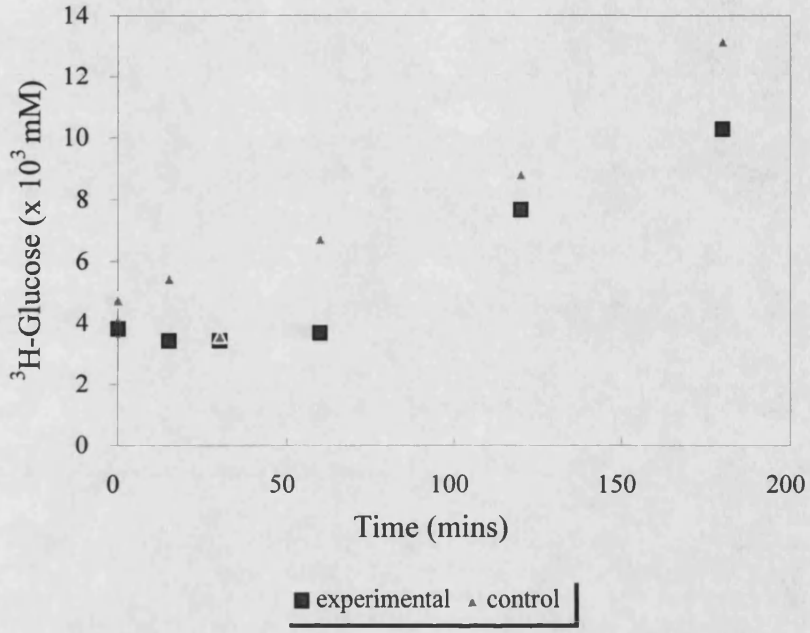

The control contains unmodified membranes. A definite decrease can be observed in the amount of radioactivity present in the experimental solution between 0-60 minutes. The amount of radioactivity present between 60 and 120 minutes is greater in the control than in the experimental solution as expected as at these time intervals 2mM of ^{3}H-glucose was added in order to maintain a constant level of glucose in the solution (see section 4.2.5c). Therefore in the control only unmodified membrane is present and the glucose concentration is expected to increase, whereas in the experimental the increase in glucose concentration is likely to be due to the fact that the Con A binding sites on the modified membrane are saturated with glucose and any addition of glucose, at time intervals 60 and 120 minutes will not lead to any further binding.

5.2.2 Ovalbumin Adsorption Isotherm.

An adsorption isotherm of ovalbumin was obtained and is shown below in figures 5.6 & 5.7. The amount of ovalbumin present in solution at equilibrium was determined using a standard curve constructed with native ovalbumin.

Figure 5.6 The Adsorption of Ovalbumin onto Immobilised Con A.

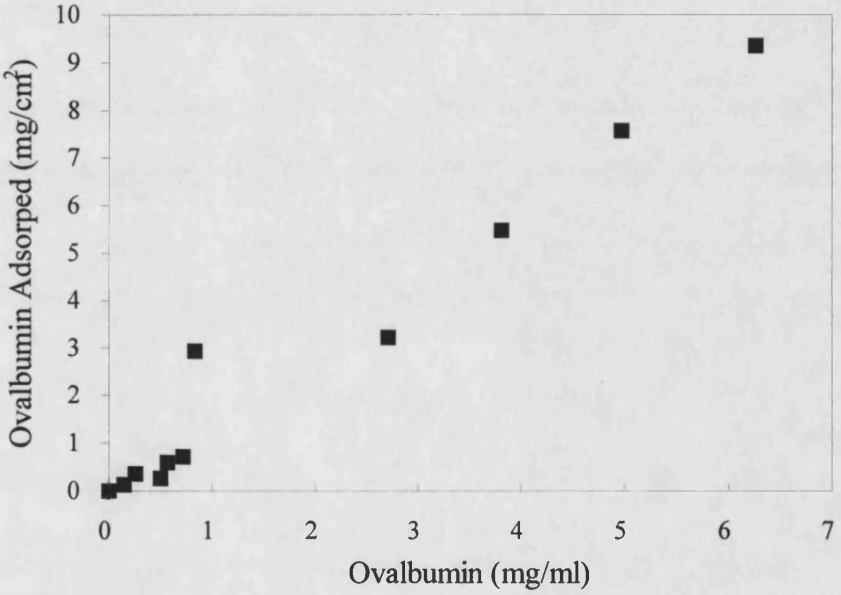

Figure 5.6 suggests saturation of ovalbumin below the concentration of 1 mg/ml, above this initial loading concentration of ovalbumin an increase in adsorption of ovalbumin occurs. The increase is likely to be due to non-specific binding of ovalbumin to the Con A modified membrane. Saturation kinetics for the adsorption of ovalbumin to immobilised Con A suggests that the Con A binding sites are active and accessible for binding. Therefore the process of immobilisation has not interfered with the binding activity of Con A.

Saturation occurs when all the accessible sites have been occupied by the ovalbumin. Initially, at lower ovalbumin concentrations a rapid increase is observed in the amount of ovalbumin adsorbed as the binding sites on the Con A are being occupied by the ovalbumin. Eventually the amount adsorbed begins to level out as no more sites are available for binding regardless of the increased ovalbumin concentration.

The non-specific binding observed is likely to be due to the presence of hydrophobic regions and ionic charges present on the surface of ovalbumin. This would explain the adsorption observed at ovalbumin concentrations higher than 1mg/ml, leading to the formation of non-specific layers on the Con A modified membrane.

Figure 5.7 The Adsorption of Ovalbumin at the Lower Loading Concentrations.

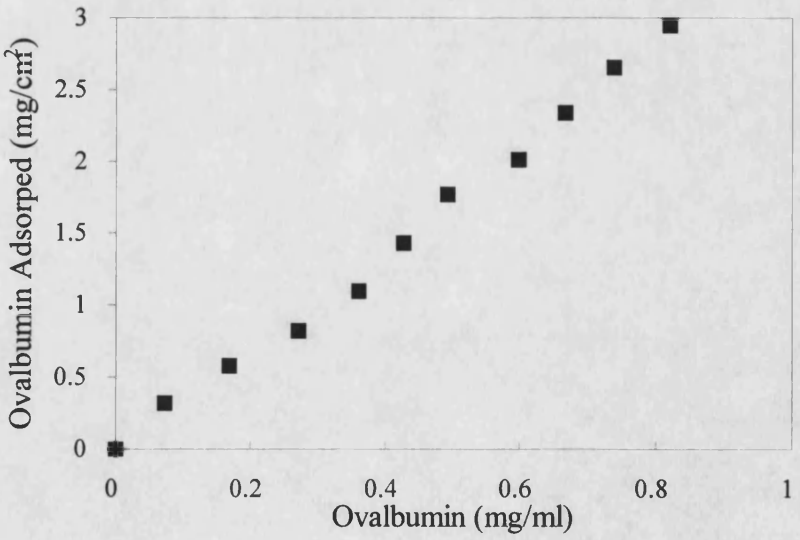

The value of the dissociation constant, K_d could not be calculated as the graph in figure 5.7 did not fit the theoretical model of the saturation curve. Usually a sharp increase is observed in adsorption at the lower protein concentration, which is due to

the high affinity of the protein for the immobilised molecule. From figures 5.6 & 5.7 a slight "kink" in the curve can be observed in the initial ovalbumin concentration region of 0.3mg/ml,. This may be due to a switch from specific to non-specific binding indicating a K_d value in this region implying a high affinity between Con A and ovalbumin. From this concentration of 0.3mg/ml the surface saturation value can be calculated to be approximately 1 x 10^{-5} M which is in agreement for the dissociation constant for the chromophoric derivative, *p*-nitrophenyl-α-D-mannopyranoside to Con A which was studied and the dissociation constant was measured to be 5 x 10^{-5} M (Gray *et al.,* 1973). The interaction of the sugar moieties could be compromised by the bulk of the protein backbone.

5.3 Ovalbumin Immobilisation onto Dynabeads

In order to minimise complications resulting from bead size heterogenetity it was important that beads with a uniform size distribution were used. Dynabeads (Dynal Ltd.,) are ideal for this purpose as they are available in a defined size distribution, they are coloured making visualisation simple, and they are provided in a chemically activated state to allow easy coupling of proteins. A number of coupling procedures was tried.

5.3.1 Ovalbumin Immobilisation onto Dynabeads

Ovalbumin immobilisation onto dynabeads was carried out employing three different methods and the quantification of the immobilised ovalbumin was attempted by proteolysis and acid hydrolysis. Dynabeads were used as they are easily visualised under the light microscope being brown in colour. Dynabeads are magnetic and are employed in immunochemical based separation of proteins (Swann *et al.,* 1992).

a) The Direct Binding Method

Ovalbumin was bound directly to the beads and was left in a solution of Con A and also with a Con A modified membrane for several hours to allow binding between ovalbumin and Con A to occur following a protocol provided by Dynal Ltd., (section 4.2.7a). The beads did not bind to the Con A modified membrane implying that the ovalbumin was not accessible to the beads and that ovalbumin has not bound to the dynabeads sufficiently allowing for the binding interaction between Con A and ovalbumin to take place.

b) Binding via Gluteraldehyde.

Gluteraldehyde can be used to activate amino or amide functions and then coupling of primary amines can be carried out. This method is simple, inexpensive and suitable for ligands sensitive to alkaline pH. The linkage is stable and simultaneously introduces a spacer arm (figure 4.3).

Dynabeads coated with gluteraldehye before ovalbumin binding (section 4.2.7b) were found to bind to Con A modified membranes. Uncoated beads did not bind to the Con A modified membrane. The bound beads were washed several times with tris buffer pH 8.5 (section 4.2.7d) and most of the beads remained bound onto the membrane.

c) Binding to Tosyl-Activated Dynabeads.

The chemically bound ovalbumin to tosyl activated beads (section 4.2.7c) was observed to withstand the greatest number of washes with tris buffer (section 4.2.7d). The ovalbumin coated beads bound to Con A modified membrane whereas the control beads (uncoated beads) did not bind to the Con A modified membrane indicating that the binding between the ovalbumin-coated beads and Con A modified membrane was taking place specifically and was due to the interaction between ovalbumin and Con A.

The stability of ovalbumin bound onto the dynabeads from the three binding methods previously described (4.2.7a-c) was compared by placing each sample of ovalbumin-coated beads onto Con A modified membranes overnight in a petri dish in tris buffer pH 8.5. The beads were washed gently with the buffer to remove any unsettled and non-specifically bound beads off the membrane. A qualitative assessment was made as to the stability of the ovalbumin-Con A bonds formed by amount of the beads that remained bound on the membrane after several washes with the buffer. From this assessment it was found that beads that had been bound via the direct binding method did not attach to the Con A modified membrane thereby indicating that the ovalbumin had not adsorbed onto the beads. With the gluteraldehyde method attachment was observed to a Con A modified membrane but the beads were removed with the first wash, whereas ovalbumin that had been covalently bound via the tosyl groups on the beads was not removed with the washing. This led to the conclusion that the covalent binding method was most suitable for the subsequent study of bead detachment from Con A modified membranes.

5.3.2 Quantification of Immobilised Ovalbumin

The quantification of immobilised ovalbumin on the dynabeads was attempted by using the fluorescent reagent fluorescamine. The effect of pH on the fluorescence intensities obtained from the ovalbumin-fluorescamine interaction was studied over a range of pH's (section 4.2.8a) to determine the optimum pH (figure 5.8).

Fluorescence resulting from the reaction of a protein with fluorescamine is an indication of the number of free amino groups present in the protein. The resulting fluorescence is proportional to the amine concentration and the fluorophores are stable over several hours. The relative fluorescence of individual fluorescamine derivatives is constant from pH 4-10. Variations depend on the reactivity of each amine at different pH values and on differences in quantum yield for various fluorphores (Lorenzen *et al.*, 1993).

Figure 5.8 The Effect of pH on the Fluorescence Intensity of Ovalbumin.

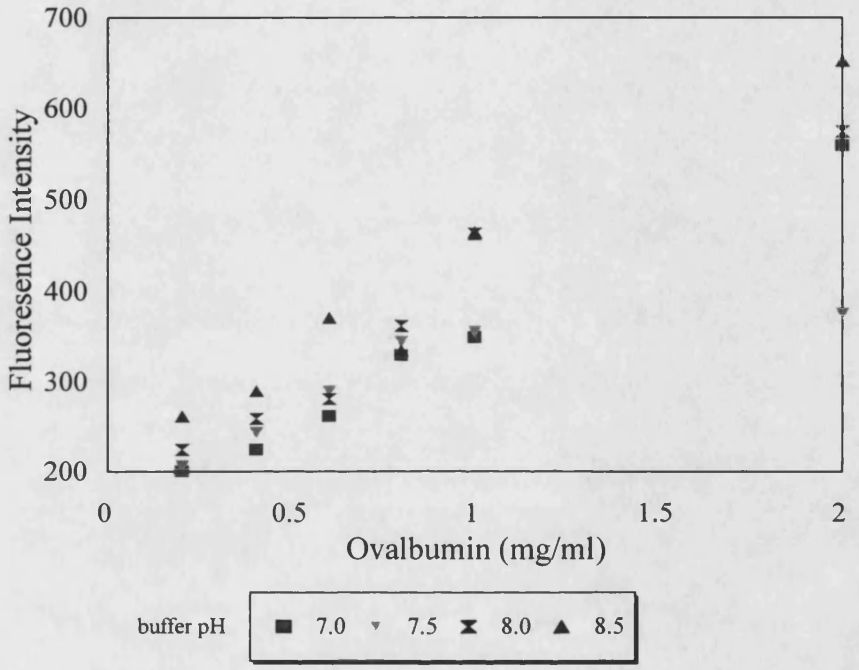

The above figures were obtained from duplicates.

There wasn't a great difference between the pH's but the highest fluorescence was obtained at pH 8.5, therefore this pH was used for future work. This result fits in well with the fluorescamine assays which are usually prepared between pH 8.5-8.8 and offer slightly more reproducible results than pH 9.0. Lysine is the only amino acid with a free amino group in ovalbumin, therefore covalent binding of ovalbumin to the tosyl groups is through the lysine side chains only.

A standard curve was constructed of free ovalbumin-fluorescamine at pH 8.5 (figure 5.9). This was performed twice in duplicates and the linear relationship was obtained between the ovalbumin concentration and the fluorescence intensity as expected. An

increase in the fluorescence intensity is observed with an increase in the ovalbumin concentration as the number of free primary amino groups present are greater.

Figure 5 9 The Standard Curve of the Ovalbumin-Fluorescamine Reaction.

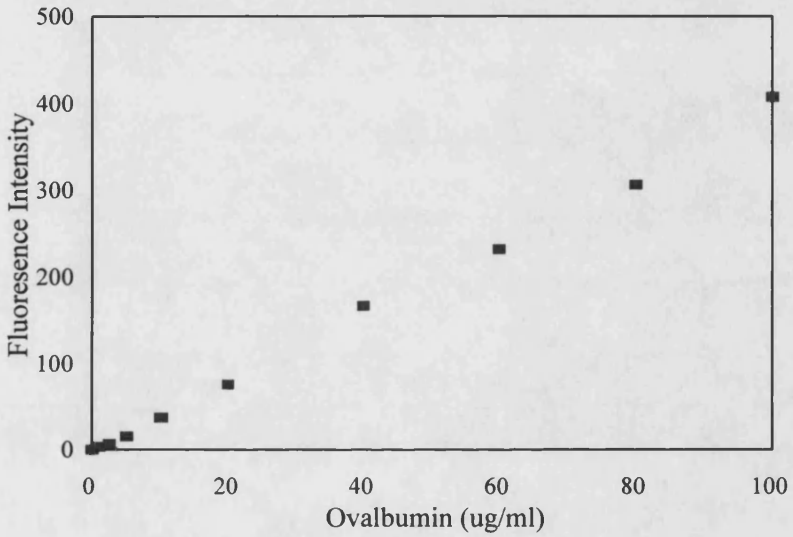

The above figure shows that the reaction of fluorescamine with ovalbumin is as expected.

5.3.3 Trypsinisation

Proteolytic enzymes are employed in the protein determination of the protein of interest . Such enzymes cleave the polypepetide chains of specific amino acids found in the protein producing several polypeptide chains which can be assayed. The enzyme trypsin was used to digest the ovalbumin bound to the beads to allow the quantification of the ovalbumin cleaved off the beads. Trypsin is a proteolytic enzyme from pancreatic juice and cleaves polypeptide chains on the carboxyl side of arginine or lysine residues (figure 5.10).

Figure 5.10 Trypsin Hydrolyzes Polypeptide on the Carboxyl side of Lysine and Arginine residues.

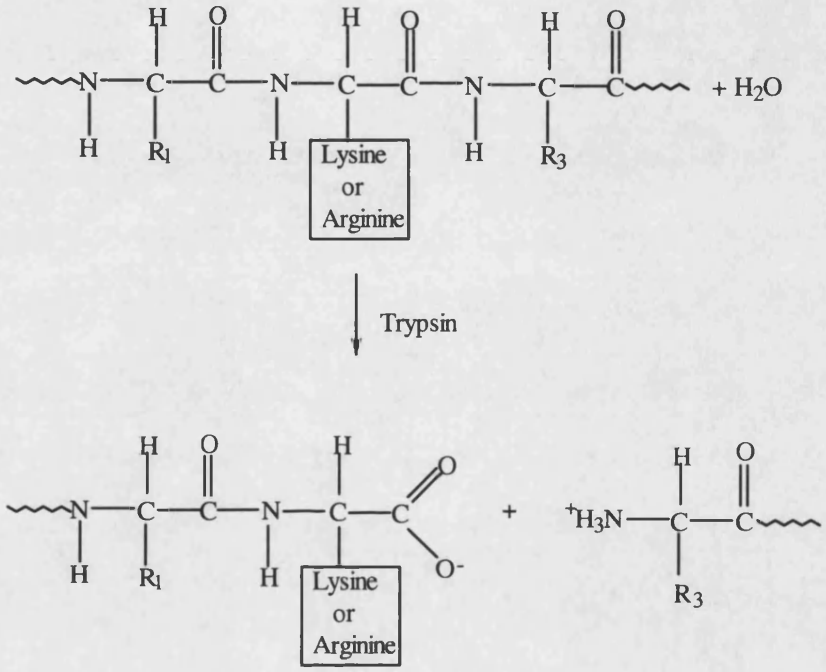

A standard curve of native trypsin digested ovalbumin was performed where fluorescamine was used to determine the amount of peptides and amino acids present. The results show a higher protein concentration present than originally used in the sample (table 5D). This can be attributed to the increase in the number of free amino groups available for interaction with fluorescamine. Although limited proteolysis was performed on the ovalbumin, the results obtained with this set of experiments were not consistent.

Table 5D The Fluorescence Intensity of the Fluorescent Derivative of Ovalbumin after Trypsinaisation where Co is the Initial Ovalbumin Concentration the Beads were Incubated in. Each assay was repeated five times (F_{1-5}) and performed in duplicates.

C_o (mg/ml)	Average Fluorescence				
	F_1	F_2	F_3	F_4	F_5
2.5	145.4	178.8	235.9	192.2	40.5
5.0	269.4	292.6	291.0	177.7	20.7
7.5	113.1	125.3	202.5	305.1	5.5
10.0	166.2	145.1	325.3	251.2	55.5
12.5	58.7	60.2	311.4	367.3	56.1
15.0	145.4	155.9	238.0	191.6	83.1
20.0	226.5	242.4	235.0	312.6	97.5
35.0	20.6.5	228.4	305.9	189.8	70.2
40.0	166.4	213.2	268.1	313.0	57.6

The data represented in table 5D do not show an obvious trend or correlation between the initial ovalbumin concentration and the proportional fluorescence obtained. This could be due to too much protein being present initially allowing protein layers to form on the dynabeads, further experiments were carried out with reduced initial concentration of ovalbumin (5.0-80.0μg/ml) shown in table 5E. A standard was used to calculate the amount of protein found.

At this stage of the analysis it was important to determine the range where the dependence of the fluorescence signal on the protein content of the sample is linear; this defined the range of measurable protein concentrations. This problem which is easily solved with highly sensitive spectrofluorimeters, becomes more complicated with standard laboratory fluorimeters equipped with interference filters. With such fluorimeters, determination of sensitivity sharply decreases, and the range of linear dependence of the determination signal on protein concentration is reduced.

Table 5E The Fluorescence obtained with Reduced Initial Ovalbumin Concentration. Each assay was repeated four times (F_{1-4}) and performed in duplicates.

Co (μg/ml)	Average Fluorescence			
	F_1	F_2	F_3	F_4
5.0	65.5	46.9	45.3	65.0
10.0	50.9	42.1	42.1	32.9
20.0	212.0	33.3	28.7	8.7
40.0	52.3	42.8	39.6	27.2
60.0	47.8	19.2	22.5	25.3
80.0	85.2	18.7	17.0	29.3

Reducing the amount of initial ovalbumin the beads are incubated with gives less variation than the data obtained for the higher ovalbumin concentrations (table 5D). The results obtained are not conclusive in showing a trend between the initial ovalbumin concentration and the amount that has been trypsinized off the beads.

Table 5F The Initial Ovalbumin Concentration against the Fluorescence Obtained using Borate buffer pH 8.5. Each assay was repeated twice in duplicates (F_{1-2}).

Co (μg/ml)	Average Fluorescence	
	F_1	F_2
1.0	183.5	382.4
2.5	201.1	80.4
5.0	218.4	95.0
10.0	159.6	267.7
20.0	253.1	297.7
40.0	215.1	289.5
60.0	187.8	202.5
80.0	252.8	117.4

It is possible that the concentration of fluorescamine being used is not sufficient but this is unlikely as the amounts being used have been used previously for protein concentrations in the same range (Horowitz *et al.*, 1984). Fluorescamine is subjected

to both fluorescent and non-fluorescent interference (Bohlen *et al.,* 1974), and the reaction conditions can affect the observed fluorescence intensities (Castell *et al.,* 1979). Factors affecting the amount of fluorescence obtained from the interaction of fluorescamine with primary amines include the following: the amine involved, the pH of the solvent, solvent composition and the amount of fluorescamine added. The last factor is very important in that even though the reaction will be driven to completion by large amount of fluorescamine, the excess reagent will quench the fluorescence of the product. The sequential addition of fluorescamine is more effective than the same amount being added all at once, suggesting that fluorescamine is inactivated by a process whose rate depends on the concentration of fluorescamine (Chen *et al.,* 1978). These experiments were repeated where fluorescamine was sequentially added to the samples, but the data obtained did not show any improvement in consistency and reproducibility.

This method of protein quantification was considered to give an inaccurate amount of ovalbumin bound. This is because even though ovalbumin-trypsin samples were left for a limited time (limited proteolysis), one could not be sure that all the ovalbumin had been cleaved or where it had been cleaved. That is, it is not possible to be sure if the standard ovalbumin-trypsin samples are a true reflection of the bead-ovalbumin-trypsin samples. Also as there is no specific enzyme for the cleavage of the lysine-tosyl bond, this type of method for quantification of bound ovalbumin was not considered to be simple and easy.

5.3.4 Acid Hydrolysis

Although acid hydrolysis is generally used for the determination of the total number of amino acids found in a particular protein, it can also be employed for the determination of the total amount of protein present. Therefore acid hydrolysis of the bound protein would allow all the amino acids to react with the fluorescamine giving a more accurate indication of the total amount of protein bound to the beads. The

assay outlined in section 4.2.8c was carried out to quantify the total ovalbumin immobilised onto the beads.

Table 5G shows the florescence obtained from acid hydrolysed ovalbumin immobilised onto the beads over a wide range of ovalbumin concentrations. As can be seen the results are not very reproducible, the experiment was performed in tris buffer pH 8.5.

Table 5G Fluorescence Intensity of Acid Hydrolysed Immobilised Ovalbumin.

Co (mg/ml)	Average Fluorescence	
	F_1	F_2
2.5	123.5	66.7
5.0	101.1	17.2
10.0	101.7	46.8
12.5	85.9	41.2
20.0	96.0	109.0
35.0	100.7	26.9
40.0	87.6	26.0

The same experiment was repeated with lower initial ovalbumin concentrations used for incubation with tosyl beads. The data obtained are shown in table 5H.

Table 5H The Fluorescence Intensity obtained after Acid Hydrolysis of Immobilised Ovalbumin from Dynabeads at lower loading concentrations of Ovalbumin.

Co (μg/ml)	Average fluorescence	
	F_1	F_2
0.01	258.7	115.9
0.10	258.1	111.6
1.00	256.4	110.5
10.00	260.5	95.4
20.00	261.4	92.7
40.00	265.8	90.8

The above data were obtained using tris buffer pH 8.5, similar results were obtained with the borate buffer pH 8.5. At this point it was decided to discontinue with this assay as it was too time consuming and reproducible results were not being obtained.

The fluorescamine-trypsin and fluorescamine-acid hydrolysis assays were discontinued as it was decided that progress was being delayed in the quantification of immobilised ovalbumin. Though several different methods were employed in the determination of immobilised ovalbumin, the data obtained from all the methods were inconclusive as it was not reproducible. The errors found were too great to allow those assays to be used with confidence.

5.4 Determination of the Active Binding Sites on Immobilised Ovalbumin.

The problems encountered in determining the total ovalbumin immobilised as described in the previous section led to the determination of the active sites present on the immobilised ovalbumin, although this would not have been obtained from the total protein quantification assays. The activity of immobilised ovalbumin is very important as it will be these active sites which interact with Con A. The determination of the number of active sites on immobilised ovalbumin was attempted by the addition of Con A to a suspension of ovalbumin coated beads (section 4.2.9). The amount of Con A molecules/beads was calculated (table 5I & figure 5.11), no Con A was found to bind uncoated dynabeads indicating that the Con A is specifically binding to the immobilised ovalbumin which is active.

Con A bound to immobilised ovalbumin was eluted with glucose. Several elution's were required to be confident that all of the immobilised Con A had been competed off, and the amount of Con A present in the elution's was not detected with Comassie blue or fluorescamine.

Table 5I The Number of Moles and Molecules of Con A bound per Ovalbumin Coated bead where C_o is the Initial Ovalbumin Loading, C_b is the Amount of Con A (μg) per ml of beads, where a ml of beads contains 4×10^8 beads, C_m is the number of moles of Con A per Ovalbumin Coated Bead and C_{mol} is the Number of Molecules of Con A per bead.

C_o (μg/ml)	C_b (μg/4 $\times 10^8$beads)	C_m (moles/bead) ($\times 10^{-17}$)	C_{mol} (molecules/bead) ($\times 10^6$)
1.0	57.10	1.37	8.30
2.5	95.90	2.30	13.90
5.0	48.50	1.17	7.06
10.0	32.89	0.79	4.79
25.0	35.76	0.85	5.21
50.0	58.20	1.38	8.47
100.0	54.13	1.32	7.88
250.0	56.88	1.36	8.28

The initial Con A concentration used for binding to the ovalbumin-coated beads of 5mg/ml is well excess of the incubation loadings of ovalbumin. Therefore it can be assumed that all the Con A is in excess and saturation of Con A is not occurring.

Figure 5.11 The Binding Profile of Con A in the Presence of Ovalbumin Coated Dynabeads. The Con A Concentration used was 5mg/ml in a total volume of 10mls. The data were obtained from duplicates.

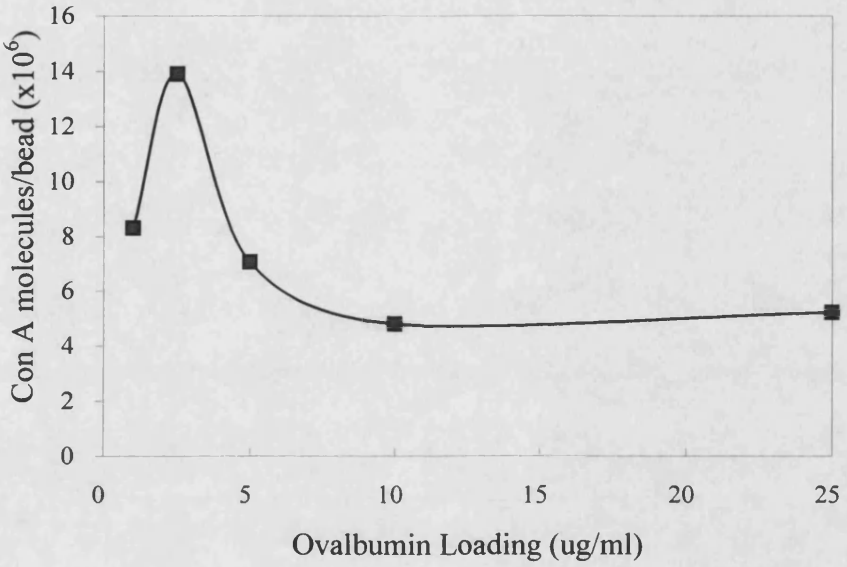

It is more important to know the activity of the immobilised ovalbumin than the exact amount of ovalbumin bound as it is the active sites that will be accessible to the Con A molecule for binding. Therefore it is of greater importance to determine the amount of free Con A that can bind the immobilised ovalbumin as this will be an indication of the binding to be expected with the immobilised Con A surface. The amount of Con A bound to the ovalbumin coated beads is much less then amount bound of Con A immobilised onto the membrane ($2.4\text{-}6.93 \times 10^{15}$molecules/cm^2). In other words there may have been more than enough Con A to bind all the available ovalbumin molecules even at the lowest Con A concentration. It would appear that the ovalbumin coated beads have the highest capacity for Con A with an ovalbumin loading of 2.5μg/ml. This appears to be the optimum loading concentration as an increase in the ovalbumin concentrations does not lead to an increase in the amount of Con A bound to the ovalbumin coated beads. It is possible that steric hindrance of adjacent ligands at the higher ovalbumin concentrations may lead to the masking of

others preventing them from being available for interaction with Con A. Therefore at the ovalbumin loading of 2.5μg/ml the ovalbumin is bound in such a manner to allow a greater number of the N-linked glyco groups to be available for binding with Con A. This loading may be considered the critical ligand density at which the Con A molecules can bind only one ligand at a time and only the Con A-ovalbumin interaction would be stron enough to lead to the binding.

The binding profile of Con A in the presence of increasing amounts of ovalbumin coated beads shows a bell shaped profile (figure 5.11) also obtained in the precipitation of Con A in solution with quail ovalbumin, (Mandal *et al.*, 1992) and is similar to that observed for oligomannose type glycopeptides and the lectin (Bhattacharyya *et al.*, 1987). The highest precipitation of Con A was observed at a concentration of 5.4μg/ml of ovalbumin (Mandal *et al.*, 1992) compared to half that of 2.5μg/ml as seen in figure 5.11. This difference in the ovalbumin concentration at which the greatest amount of Con A binds or precipitates to the ovalbumin explains the lower mass ratio obtained for Con A to ovalbumin of 1:1 (section 5.2.3).

Binding of Con A to the immobilised ovalbumin is an indication of the amount of active ovalbumin sites on the beads. Similar methods have been employed in the determination of immobilised antibodies and proteins to polystyrene beads. To date the quantification of immobilised proteins on beads has been determined by the introduction of a "flag" or maker protein as well as or in conjunction with methods such as flow cytometry and acid/alkaline hydrolysis (Kuo *et al.*, 1993; Templeman *et al.*, 1994). The marker protein is usually a secondary antibody or the protein to which the immobilised protein is to bind in the experiment. An example is the determination of receptor number on beads coated with IgG, the coated beads were incubated with Protein A (Sp A) and flow cytometry was used to determine the number of receptors on beads. Sp A is the ligand immobilised onto a glass surface and the force required to detach the IgG coated beads from the Sp A covered glass surface was being studied (Kuo *et al.*, 1993).

5.4.1 Estimation of the Number of Receptors and Ligands in the Contact Region Between Bead and Surface.

As shown in figure 5.12 the contact area for a smooth, relatively non-deformable particle can be estimated using geometrical considerations (Cozens-Roberts et al., 1990*b*).

Figure 5.12 Schematic Diagram Showing Geometrical Determination of Contact Area of a Non-Deforamable Bead with a Surface, where *hs* is the Separation Distance Between the Surfaces, *H* is the Maximum Separation Distance, *r* is the Radius of the Bead, and *a* is the Radius of the Contact Area (Cozens-Roberts *et al.*, 1990*b*).

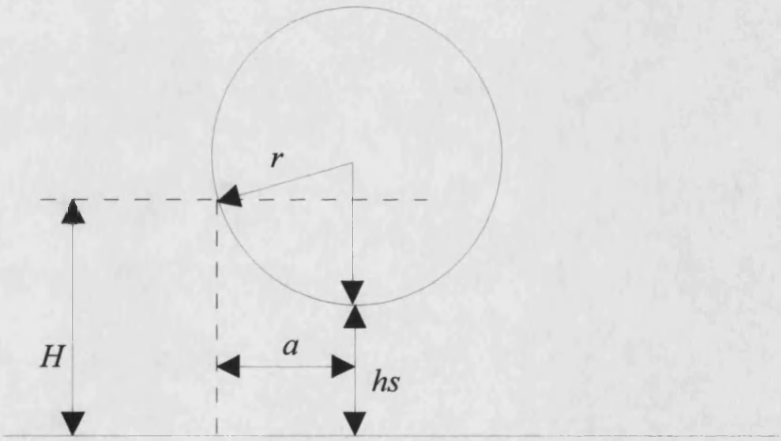

An estimate of the contact area between cell and surface was determined using the equation by Saterbak *et al.*, 1993 who found the value for the contact area to lie between πa^2 and $2\pi a^2$, depending on the extent of bead curvature where a is the radius of the contact area (10% of the original radius). The factor of 2 was considered to be within the level of uncertainty. Therefore for the calculations of the contact area used here a factor of 1.5 was used. From this value, the total surface

area of the bead, and the ligand and receptor densities the number of receptors and ligands in the contact region were calculated (table 5J).

Table 5J The Number of Ovalbumin and Con A molecules in the Contact Region where L_c and R_c are the number of Con A and ovalbumin molecules in the contact region respectively, and R_T is the total Receptor number per bead.

Con A ($\mu g/cm^2$)	L_c ($x10^6$)	R_T ($x10^6$)	R_c ($x10^4$)
41.5	5.70	4.76	1.78
67.0	9.28	5.21	1.94
68.5	9.47	7.09	2.65
72.0	10.04	8.31	3.11
119.0	16.49	13.90	5.20

As can be seen from table 5J the number of Con A molecules in the contact region in comparison to the number of ovalbumin receptors is greater by a factor of 100. This implies that it is the ovalbumin concentration in the contact region that will determine the number of bonds formed between Con A and ovalbumin (chapter 8).

From the data obtained on Con A and ovalbumin binding studies it can be concluded that the two proteins can be assayed and the amount of active immobilised protein can be determined. The quantification of active immobilised proteins allowed for detachment experiments to be carried out using different receptor (ovalbumin) and ligand (Con A) concentrations at various shears. This is possible as the flow cell provides a controlled environment for determinations of the shear stress at which beads (cells) in suspension can bind to Con A modified membrane. By increasing the flow rate of the buffer over the Con A membrane with ovalbumin coated beads attached and assessing the number of "cells" bound at each shear stress, the relationship between shear force and binding efficiency can be determined.

CHAPTER 6

Detachment Assay Results

A model experimental system was used with ovalbumin coated dynabeads as cell mimics and a Con A modified membrane as an affinity surface. This allowed the effects of systematically varying both the ligand and receptor densities on the affinity interaction to be investigated. This experimental system was used to quantify the effects of shear stress, receptor density and ligand density on "cell" detachment. Detachment assays were performed in the parallel-plate flow chamber (as described in chapter 4, section 4.2.10) allowing the measurement of the force required to detach the beads from the surface.

A further set of experiments was performed to see if a variation in adhesion strength was observed on addition of glucose as a soluble inhibitor of the affinity interaction. The effect of incubation contact time on the strength of adhesion was also investigated to establish the optimum time required for stable bonds to form between Con A and ovalbumin and to evaluate the kinetics of multivalent bond interactions. Finally given the widespread use of peristaltic pumps in biotechnological studies a preliminary assessment of the effects of pulsatile flow on cell detachment was conducted.

6.1 The Effect of Hydrodynamic Shear, Ligand and Receptor Densities on Detachment

6.1.1 Applied Hydrodynamic Force.

It has been shown that, in cell-surface interactions, the number of bonds is directly proportional to the number of receptors (Hammer *et al.*, 1992). If it is assumed that all the bonds are equally stressed by an applied shear force, the total bead binding force (F_S) will be a resistant force countering the applied force, and can be considered as the product of force per bond (F_b) and the number of bonds (c).

For a particle to adhere to the surface, the net adhesive force must balance the force and torque imposed by the passing fluid. The total force exterted by the fluid on an adherent particle is given by the force and torque balance developed by Hammer et al., (1987) for receptor-mediated cell adhesion. Their model is based on the following assumptions: the adhesive force acts both parallel to the direction of flow and normal to the surface of the particle, the non-specific forces play a negligible role in countering the shear force and torque, and the force per bond and bond density are constant over the contact area. Thus the total applied hydrodynamic force (F_T)exterted by the passing fluid on an adherent bead is given by the following equation which has been widely used to relate applied force to the shear stress:

$$F_T = \left[\frac{110Sr^3}{a}\right] \qquad (1)$$

where S is the fluid shear stress; r is the radius of the bead (2.25μm) and a is the radius of the contact area (0.225μm) where the estimated value for the contact radius is approximately 10% of the bead radius (Hammer *et al.*, 1987: Saterbak *et al.*, 1993). Thus the total force is a function of both flow rate and bead diameter.

A specimen calculation is shown below for both the shear stress and the total force exerted on the bead for a shear stress value of 2.25dyn/cm^2:

The shear stress was calculated (section 3.1.3) with a fluid velocity of 93.75cm s^{-1}, fluid viscosity of 0.001dyn s cm^{-2}and a channel depth of 0.125cm:

$$S = \frac{3 \times 93.75}{0.125} \times 0.001 = 2.25 \text{ dyn/cm}^2$$

From this the F_T value was calculated using the dimensions of the bead given above:

$$F_T = \frac{110 \times 2.25(2.25 \times 10^{-4})^3}{2.25 \times 10^{-5}} = 12.5 \times 10^{-5} \text{dyn}$$

Table 6A The Total Force Applied to the Beads at each Shear Stress.

S (dyn/cm^2)	F_T (dyn) ($\times 10^{-4}$)
0.15	0.083
0.46	0.250
1.00	0.550
1.65	0.918
2.25	1.250

Therefore the greatest force applied to the adhered beads under the conditions reported here is 1.25 x 10^{-4}dyn.

The effect of fluid shear on detachment profiles obtained for a range of Con A loading concentration was studied over a range of ovalbumin densities (table 6B) and the detachment profiles obtained are shown in figures 6.1-5(A). From these data the steady-state fraction of beads attached, remaining at each shear, were calculated and

plotted against shear stress in figures 6.1-5(B). The plots of attached fraction against shear stress allowed a qualitative view of the affect of ligand/receptor densities with respect to shear to be obtained. These data also provide the basis for a quantitative assessment of the mathematical model presented in chapter 2 which will be developed in chapter 7.

Table 6B The Density of Immobilised Con A and Ovalbumin Receptors per bead against the Initial Loadings of Con A and Ovalbumin. Where C_o is the initial loading concentration, C_b is the amount of Con A immobilised onto the membrane and R_T is the number of ovalbumin receptors (assayed using the method outlined in section 4.2.9 in chapter 4).

C_o [Con A] (mg/ml)	C_b Con A ($\mu g/cm^2$)	C_o [Ova] ($\mu g/ml$)	R_T/bead ($\times 10^6$)
1.0	72.5	1.0	8.30
2.5	68.5	2.5	13.90
5.0	67.0	5.0	7.06
10.0	119.0	10.0	4.79
25.0	41.5	25.0	5.21

From the receptor number per bead an estimate of the receptor separation distance on the bead (b) can be calculated using the following equation (figure 6.1):

$$b = \left[\frac{S_A}{R_T}\right]^{1/2} \qquad (2)$$

where S_A is the bead surface area ($63.6\mu m^2$) and R_T is total number of receptors per bead (Cozens-Roberts *et al.*, 1990*a*).

Figure 6.1 The Mean Distance (b) Between Receptors on an Ovalbumin-Coated Bead Against the Total Receptor Number (R_T)

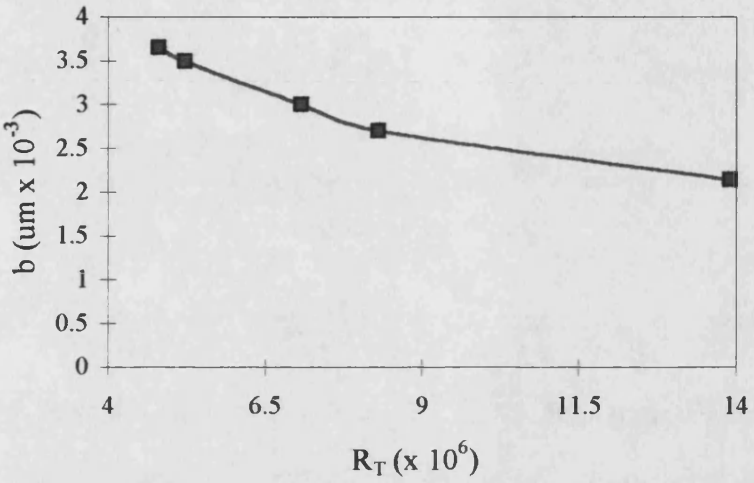

The mean receptor distance is inversely proportional to the total receptors bound per bead. Therefore the greatest distance between ovalbumin receptors is found at the lowest receptor concentration and the effects of bead distance on cooperativity between receptors is discussed further in chapter 8.

Figure 6.1 (A) The Effect of Increase in Shear Stress on Bead Detachment with a Con A Covering of 41.5μg/cm^2 over a period time.

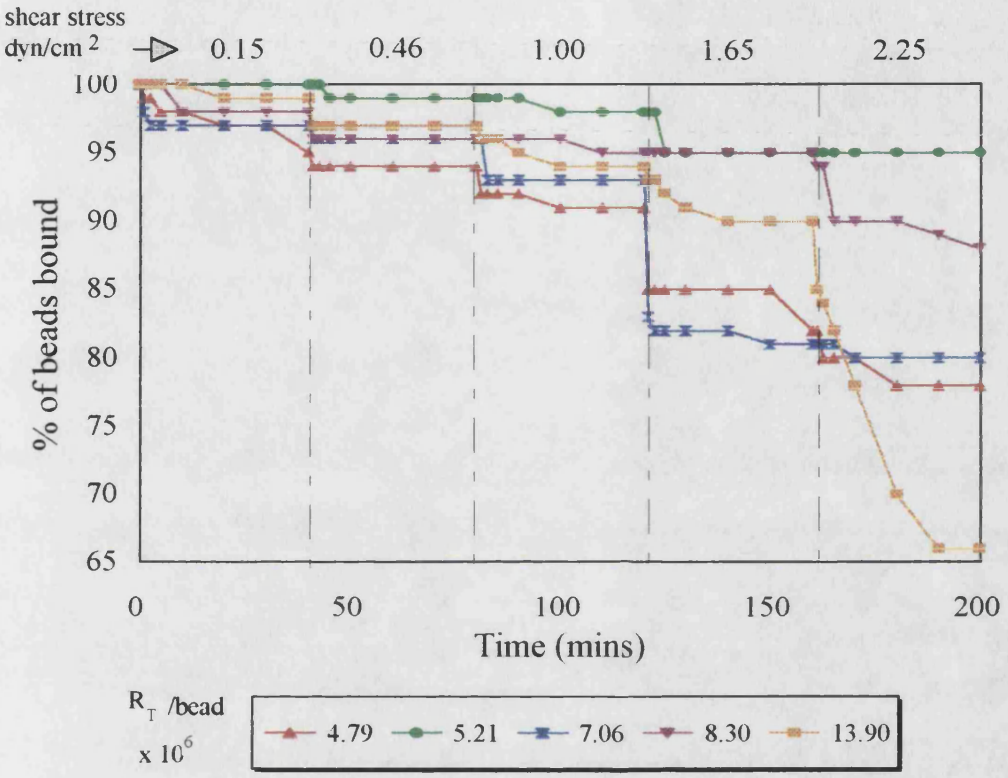

A step-wise decrease in the percentage of beads bound is observed at each shear stress. The beads progressively detach as shear force is applied but a steady-state is reached over the 40 minutes used for each shear stress when no more detachment is observed. This indicates that the number of beads that remain bound have a greater capacity to withstand the hydrodynamic force applied and would require a greater shear force to be detached.

Figure 6.1(A) shows the lowest Con A density of 41.5μg/cm^2 and the trend observed from the detachment profiles indicates the strongest binding in comparison to the other Con A densities. The greatest detachment of beads is observed with ovalbumin concentration of R_T 13.9 x 10^6 molecules/bead where 65% of the beads remain attached. This is the smallest percentage of attached beads.

Figure 6.1(B) The Fraction of Beads Bound against Shear Stress with a Con A covering of 41.5μg/cm^2.

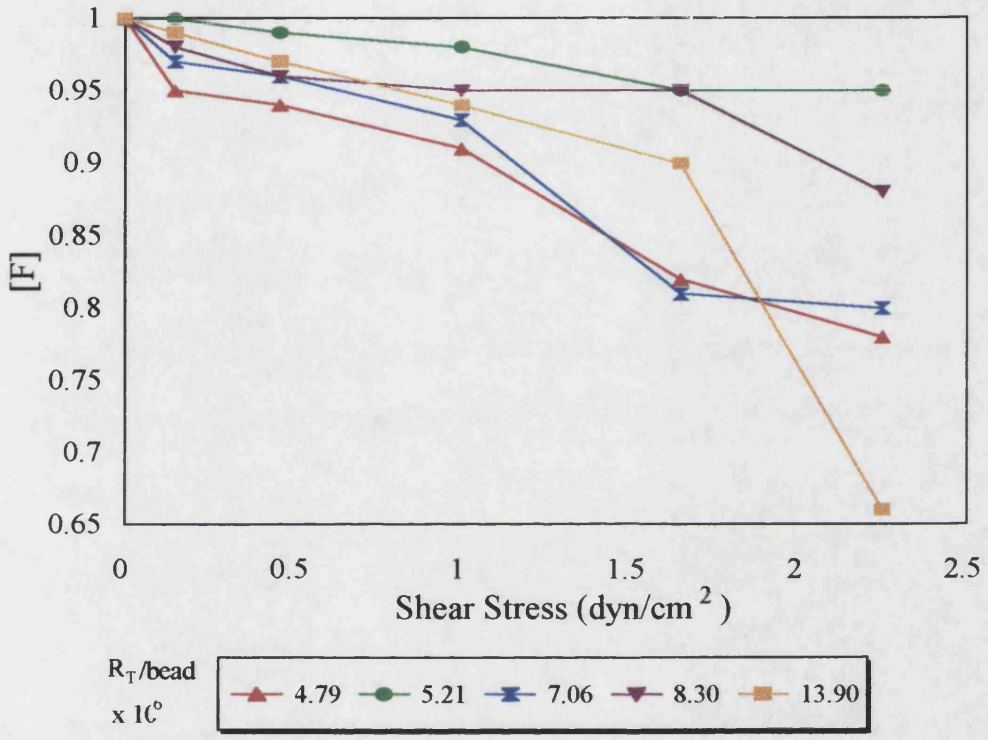

Figure 6.1(B) shows the fraction of beads bound at each shear stress at the end of the 40 minute detachment assay. From this information we can determine the effect of ovalbumin density on the beads on detachment in relation to the increase in shear stress. The overall trend of detachment is as expected with a decrease in the fraction of beads bound as shear stress is increased.

Figure 6.2 (A) The Effect of Shear Stress on Bead Detachment with a Con A Covering of 67.0μg/cm^2.

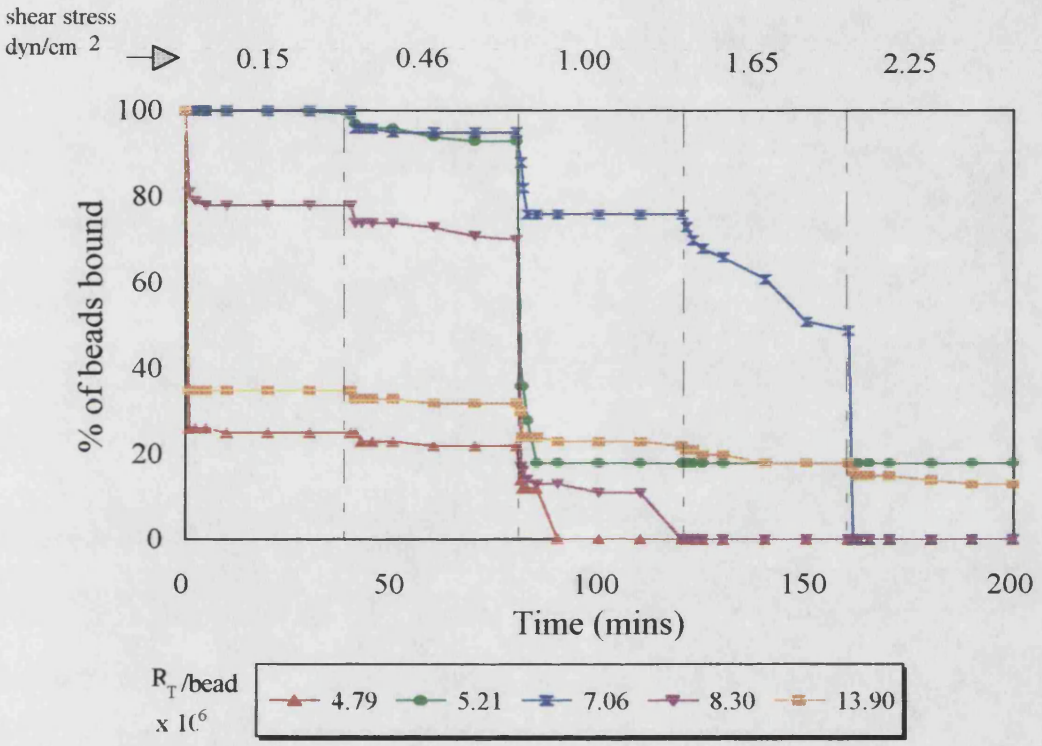

The detachment profiles obtained all show the expected step-wise detachment of the beads. A sharp drop in the percentage of beads bound is seen for both 4.79 and 13.90 ovalbumin molecules/bead. The highest percentage of attached beads at the greatest shear stress is 20% in comparison to 65% for the Con A density of 41.5μg/cm^2.

Figure 6.2 (B) The Fraction of Beads Bound against Shear Stress with a Con A Covering of 67.0μg/cm^2.

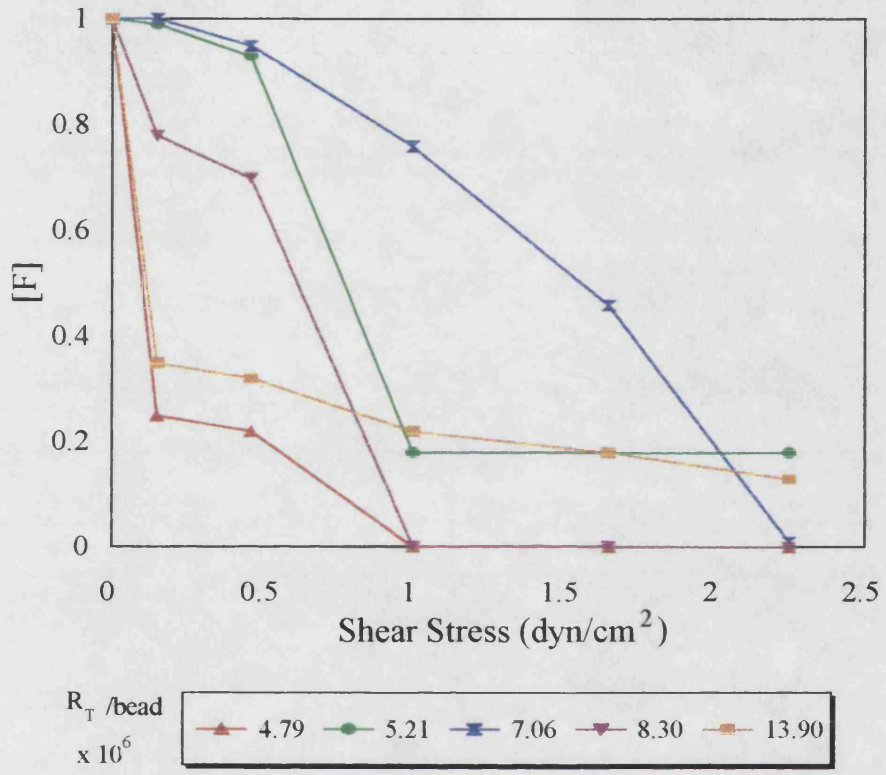

Two different types of detachment curves are obtained (figure 6.2B). These different types of curves obtained are discussed further in chapter 8.

Figure 6.3 (A) The Effect of Shear Stress on the Detachment of Ovalbumin-Coated Beads with a Con A Covering of 68.5μg/cm^2.

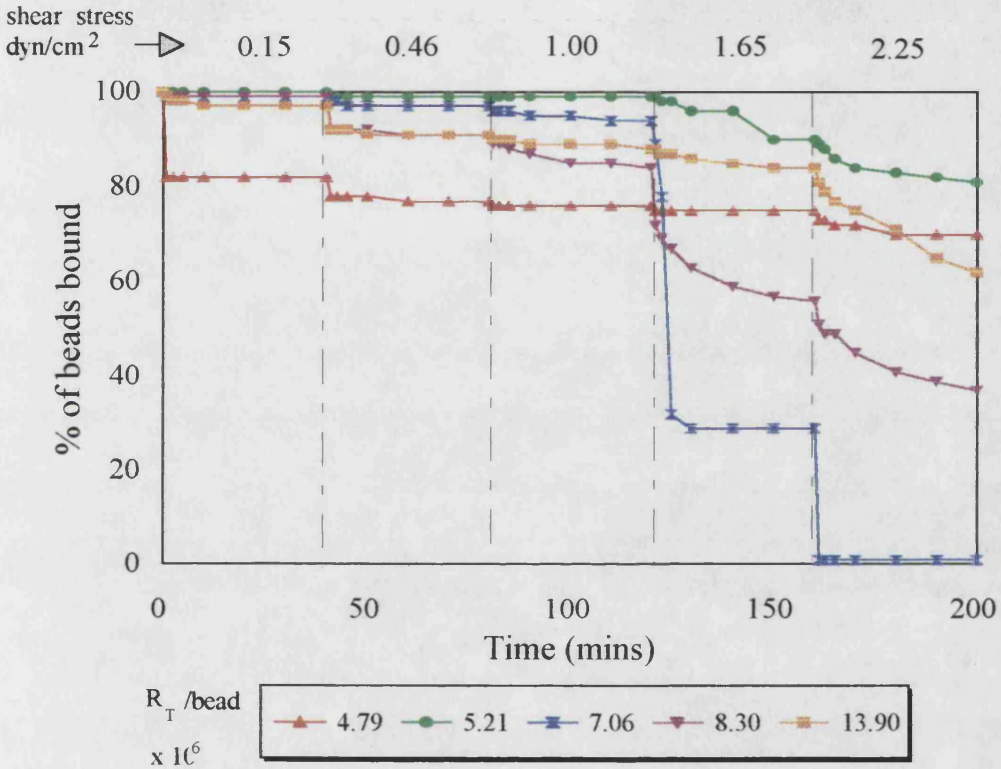

The greatest detachment is observed in the shear range of 1.65-2.25dyn/cm^2. In the lower shear ranges (0.46-1.00dyn/cm^2) only the beads with an ovalbumin loading of 10μg/ml show any significant detachment, this is to be expected as the least number of receptors (4.79molecules/bead) are present on this set of beads. Therefore the least number of bonds are likely to form requiring a lower applied force for detachment to occur.

Figure 6.3 (B) The Fraction of Ovalbumin-Coated Beads Bound on a Con A (68.5μg/cm^2) covered membrane against Shear Stress

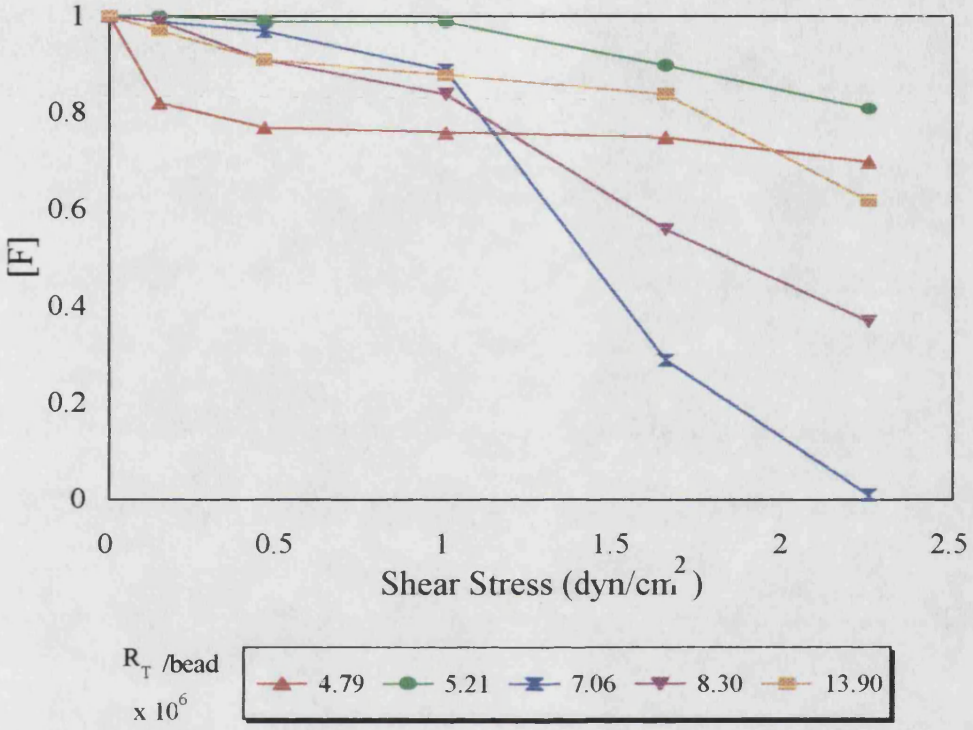

The fraction of beads bound for a Con A density of 68.5μg/cm^2 is higher for all five ovalbumin densities in comparison to that of 67.0μg/cm^2. Although the difference in Con A coverage is only 1.5μg/cm^2 it is enough to increase the fraction of adhered beads. The greatest percentage of beads attached for the three Con A densities of 41.5, 67.0 and 68.55μg/cm^2 is seen at the ovalbumin concentration of R_T of 5.21 x 10^6 ovalbumin molecules/bead.

Figure 6.4 (A) The Detachment of Ovalbumin-Coated Beads with Increase in Shear Stress off a Con A covered membrane (72.5μg/cm^2) against Time.

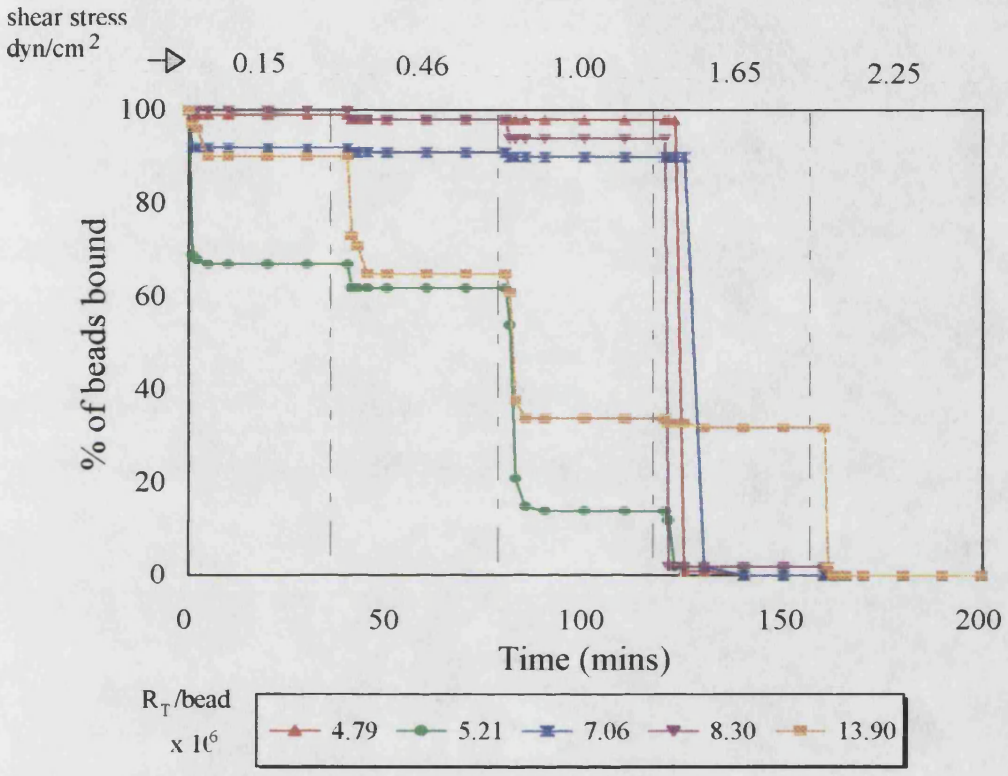

The ovalbumin-coated beads with the greatest number of ovalbumin receptors bound (13.9 x 10^{6}molecules/bead) would be expected to form the greatest number of bonds. As seen from figure 6.4(A), approximately 40% of the beads are still bound at this loading at 1.65dyn/cm^2 whereas with the other loadings little or no beads are found attached at this shear. It can also be noted that ovalbumin-coated beads with R_T of 5.21 and 13.90 x 10^6 molecules/bead follow the same detachment profile of steady decrease in the number of beads bound over the shear range. The progressive detachment of beads implies differing numbers of bonds and possibly differing strengths of bonds formed.

The other three ovalbumin receptor concentrations (4.79, 7.06, & 8.30 x10^6) show little or no detachment when subjected to the first three shears, but on application of a shear

stress of 1.65dyn/cm^2 100% detachment occurs within the first few minutes of the run. This sudden detachment pattern implies that the same number of bonds with the same strength were formed. The bonds appear to require the one shear stress for detachment to occur where the applied force would be greater then the net adhesive strength.

Figure 6.4(B) The Fraction of Beads Bound against Shear Stress for a Con A covering of 72.5µg/cm^2.

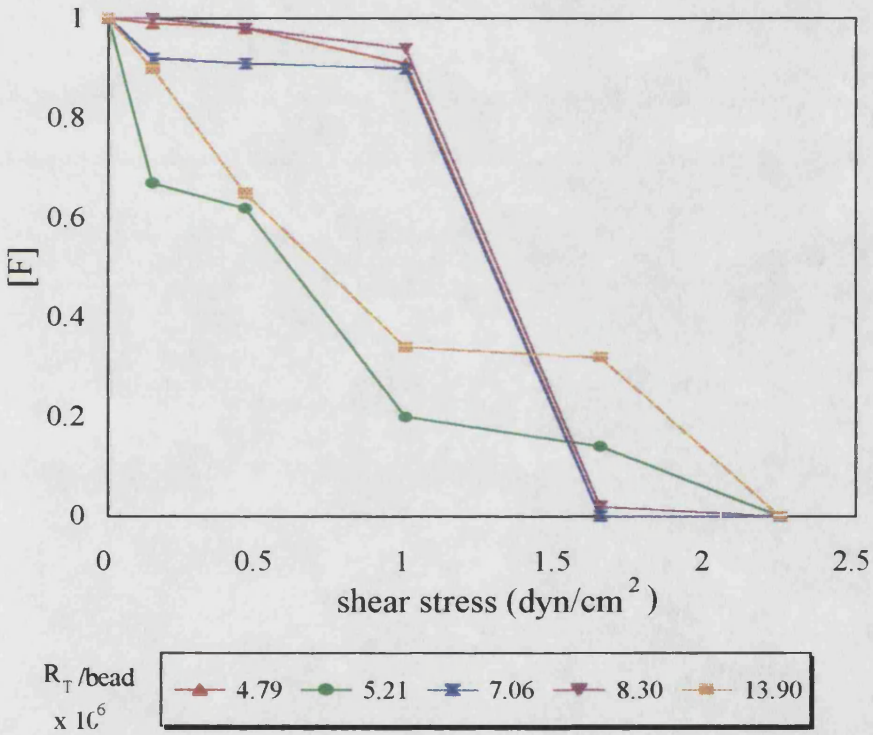

In comparison to the detachment profiles obtained with a Con A coating of 72.5µg/cm^2 the profiles in figure 6.3(B) for Con A covering of 68.5µg/cm^2 show a more gradual decrease in adherent beads. This may be explained by the lower amount of Con A bound leading to less possibilities of bond formation, therefore a lower shear is required for detachment to occur.

Figure 6.5(A) The Detachment of Ovalbumin-Coated Beads against Time with an Increase in Shear Stress with a Con A covering of 119μg/cm^2.

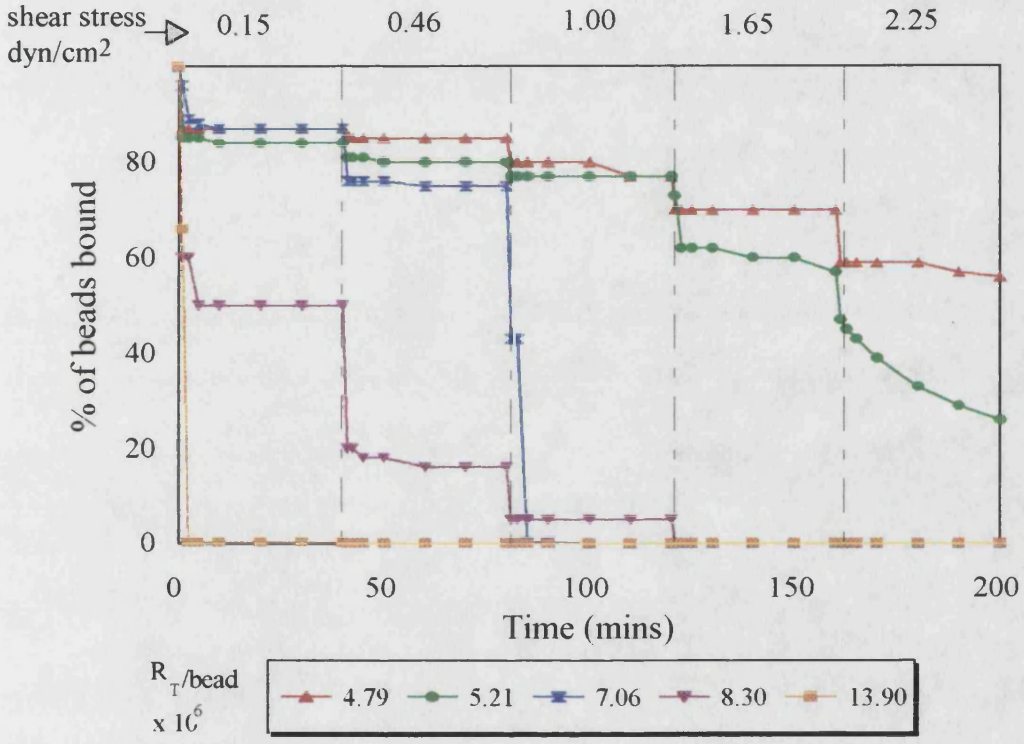

A sharp decrease in the number of attached beads for 68.5μg/cm^2 ovalbumin is observed. As this ovalbumin loading and the Con A coverage (119.0μg/ cm^2) are the highest loadings for both the proteins it would have been expected to observe a much larger percentage of attached beads. One possible explanation is that a high coverage of proteins may lead to masking of available sites for binding thereby reducing the number of bonds that can form. A shear stress force of 0.15dyn/cm^2 is enough to detach all the beads bound for this ovalbumin loading.

Figure 6.5(B) The Fraction of Beads Bound against Shear Stress with a Con A covering of 119μg/cm^2.

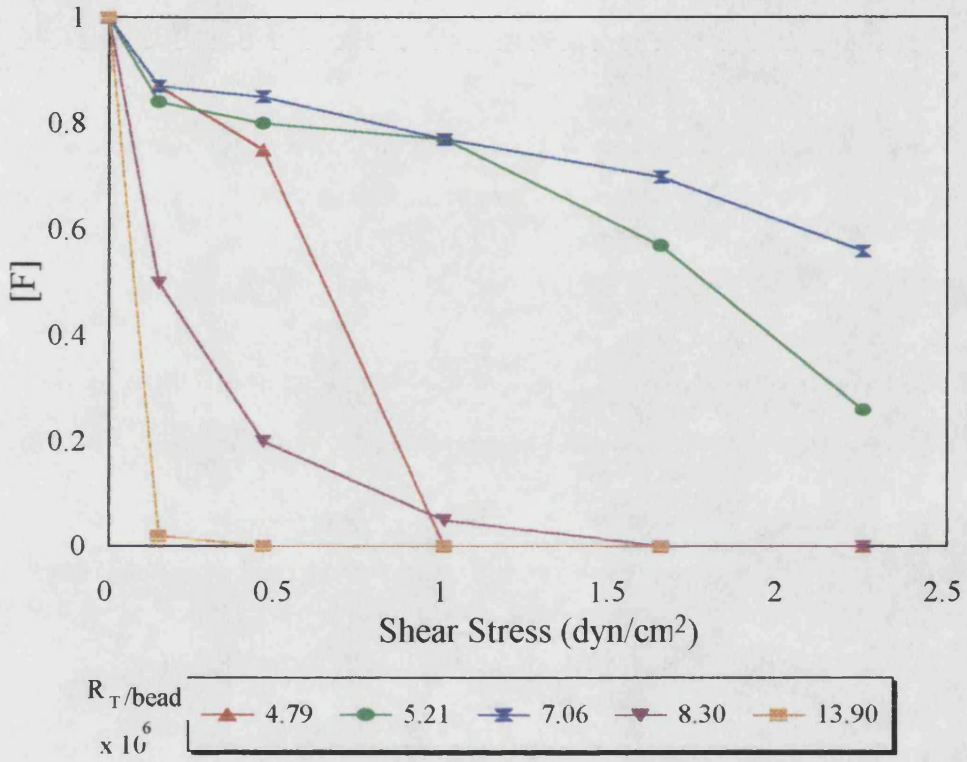

The greatest attachment is observed at the Con A density of 41.5μg/cm^2, therefore it could be considered to be the optimum density. This is the lowest Con A density employed in the detachment experiments and from the results obtained allows the most suitable orientation for the immobilised Con A for interaction with ovalbumin. This is discussed further in chapter 8.

6.1.2 Detachment Behavior

At the lower range of shear stresses, a percentage of beads "roll" along the coated surface, attaching and detaching several times before either remaining attached or being swept away. There are several noticeable trends in this behavior. First, the shear stress

range for this behavior depends on the strength of the interaction between the beads and the coated surface: the greater the adhesive strength the higher the values of shear stress supporting this behavior. Second, the actual percentage of beads with this behavior increases then decreases with shear stress: at the highest shear stresses, the beads detach and are swept away from the surface and at the lower shear stresses only a percentage of beads detach. Also observed was that an attached bead acted as a nucleation site for a attachment. Beads were seen to detach and "roll" to a new position next to an adherent bead , where it remained attached. This type of detachment behavior was also observed by Cozens-Roberts *et al.*, (1990*b*) in the detachment of antibody-coated latex beads off a ligand coated surface in a radial flow device.

The fraction of adherent beads is reported as a function of time for a range of applied fluid shear stress (figures 6.1-5A). From a typical detachment profile two major observations can be noted. First, there is a continuous loss of beads from the surface which slows down asymptotically over a period of time for a given shear stress. Second, the fraction of beads remaining attached to the surface at 45 min decreases with increasing applied fluid shear stress. A "plateau" region in the plot of the fraction of adherent beads versus detachment time is seen. Radial-Flow Detachment Assay (RFDA) work of Cozens-Roberts *et al.*,(1990*a*: 1990*b*) in which detachment runs involved a 65-min period during which the beads were subjected to fluid shear stress and the same detachment patterns were observed. Saterbak *et al.*, (1993), found that at a constant shear stress, the fraction of anti-goat IgG-coated latex beads which attached to a surface with goat IgG, showed a time dependent detachment which also reached a steady-state value characteristic of the shear rate used. This suggests that there is a heterogeneous population of attached beads showing different strengths of attachment, this is discussed in greater detail in Chapter 8.

6.2 Bead-Surface Pre-Incubation Contact Time

The effect of contact time on the stability of the bonds formed between Con A and ovalbumin was investigated (section 4.2.11). Given that the forces applied to the beads in

the previous experiments greatly exceeded the estimated force for a single bond (1×10^{-5} dyn, Bell 1978) it would appear that there is a multiple bond interaction between bead and surface which may well take time to develop. This is an important factor in optimising the attachment stage of an affinity cell separation process. The percentage of beads bound over the 40 minutes against each shear was plotted for each time dependent membrane (figure 6.6A).

Figure 6.6 (A) The Effect of Bead-Surface Contact Time on Bead Detachment.

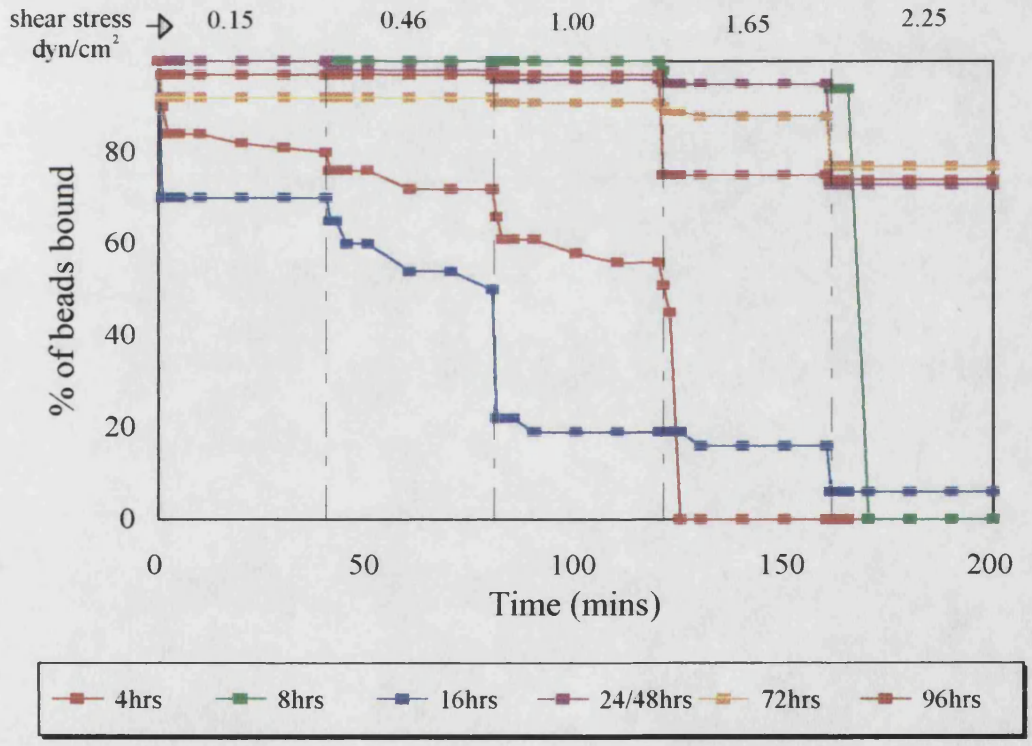

From figure 6.6(A), the fraction of beads left bound at each shear stress was obtained, and this was plotted against the shear stress for each time course experiment as shown in figure 6.6(B).

Figure 6.6 (B) The Fraction of Beads Bound against Increased Contact Time over the range of the Shear Stress used.

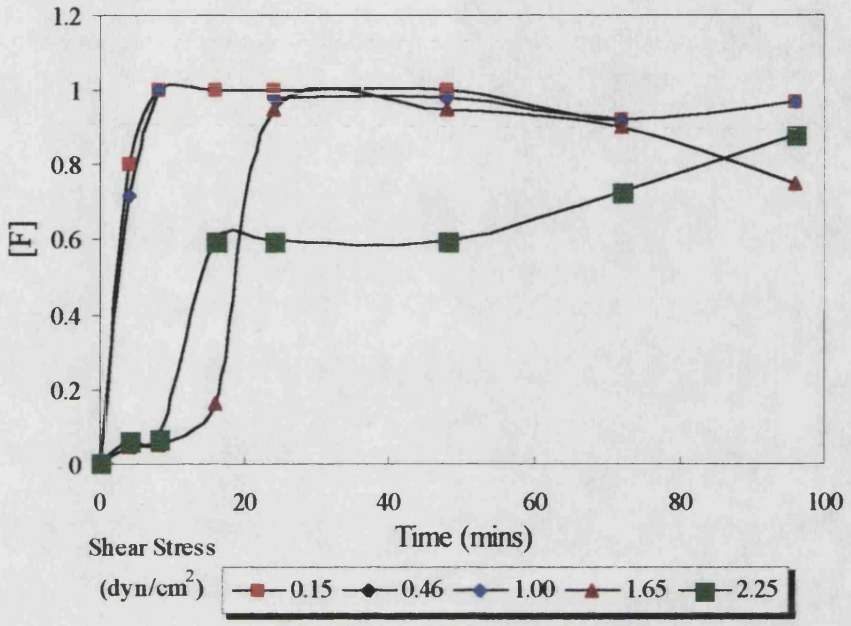

The data obtained on the time course detachment assays indicate that the bonds formed between the start of the incubation period and up to 24hours are unstable and most of the beads will detach at the highest shear used (2.25dyn/cm^2). For beads incubated for 24hours and more the stability of the bonds formed appears to have increased as the fraction of beads bound at the highest shear is not below 0.95. This indicates that detachment assays should not be performed on beads that have only been incubated for 24hours or less as the strength of the bond formation is still unstable and has not yet fully formed to it's maximum strength and stabilisation of additional bond formation requires a longer period of contact time. The fraction of beads bound increases with increase with incubation time and also the fraction of attached beads is lower at the higher shear stress value of 2.25dyn/cm^2.

6.3 The Effect of Glucose Competition on Bead Detachment

As Con A has a high affinity for the monosaccharide glucose (Mandal *et al.*,1994*a*), the effect of the addition of glucose on the detachment of ovalbumin-coated beads was studied.

Glucose Competition detachment assays were performed as described in section 4.2.10(c). The Con A loading concentration was 5mg/ml (67.0μg/cm^2) and the shear stress at which all the experiments were performed was 1.00dyn/cm^2. The graphs below show the detachment of ovalbumin coated beads (R_T 7.06 x 10^{6}molecules/bead) in the presence and absence (as a control) of glucose and also the effect of increasing glucose concentration on the detachment profile.

Figure 6.7 (A) The Effect of Glucose as a Competitor on Bead Detachment against Time.

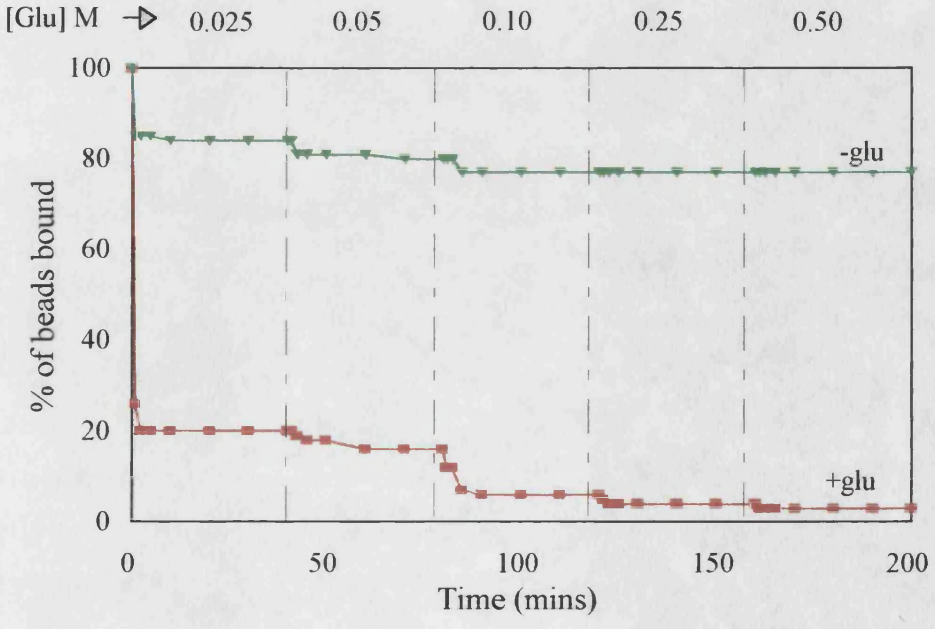

On addition of glucose, detachment of beads was increased to almost 100% in comparison with 20% in the absence of glucose. This suggests that glucose is competing with the glyco groups of ovalbumin for the sugar binding site of Con A. The stepwise detachment of beads is due the increased glucose concentration. This behavior supports the detachment profiles obtained for the beads on subjection to increased shear stress. Initial detachment is observed in the control experiment, in the absence of glucose due to the applied shear force. Detachment reaches a steady-state as the beads that remain bound require a greater applied force for detachment.

The fraction of beads bound at the end of each experiment with the glucose concentration was plotted against the glucose concentration as shown in figure 6.7(B).

Figure 6.7(B) The Fraction of Beads Bound against Increasing Glucose Concentration.

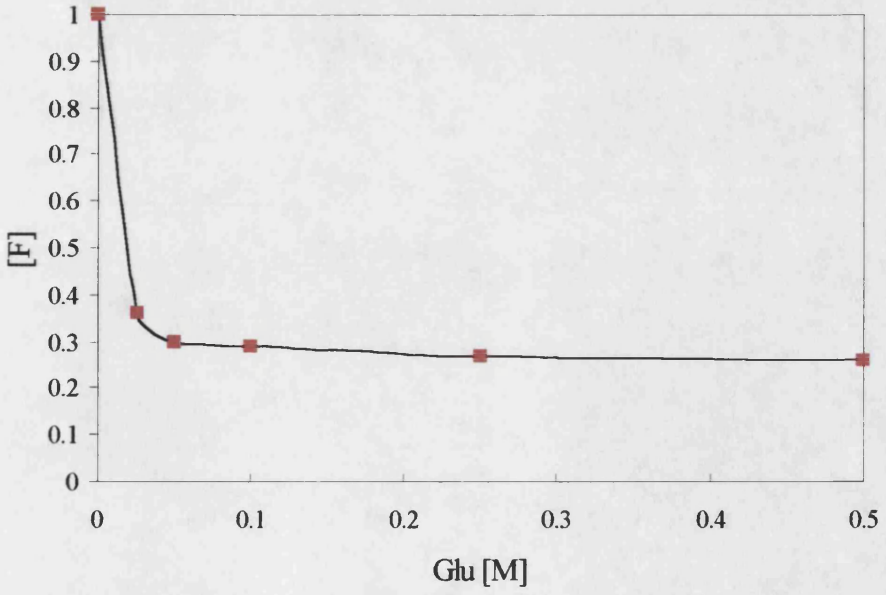

bound on addition of glucose. As the glucose concentration is increased further detachment is observed. This behavior indicates a difference in the strength of Con A and ovalbumin binding, hence requiring different concentrations of glucose.

6.4 Effect of Steady and Pulsatile Flow on Detachment

The effect of pulsatile flow on the detachment of ovalbumin coated beads was studied. A peristaltic pump was used instead of the gear pump and detachment experiments were performed with Con A and ovalbumin surface concentrations of 119μg/cm^2 and 8.30 x 10^6 ovalbumin molecules/bead respectively (figure 6.9).

Figure 6.8 The Effect of Steady and Pulsatile Flow on Detachment.

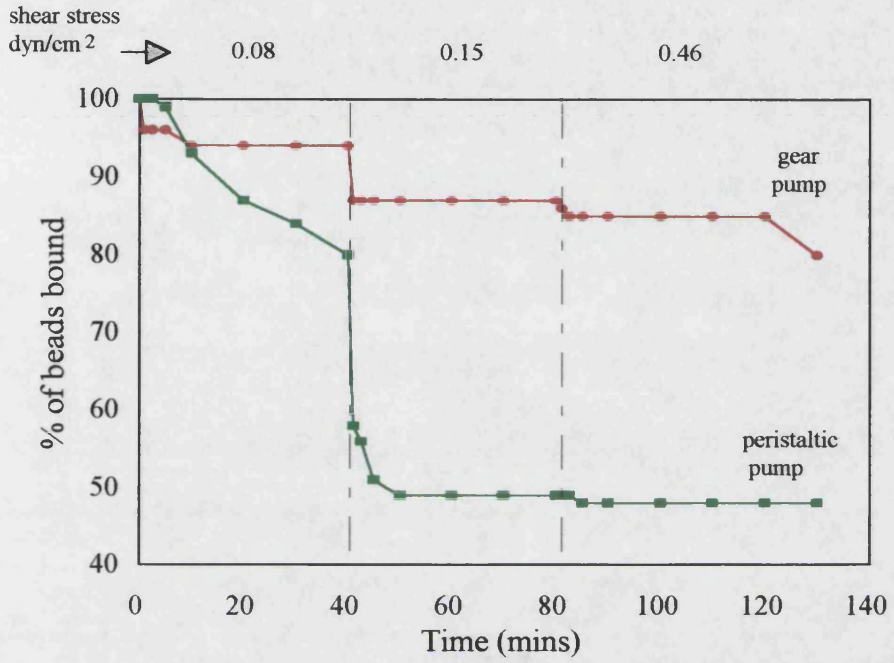

There are two possible explanations for the enhanced effect of the pulsatile flow. The most obvious is that despite giving the same average applied force, the force at the peak of the peristaltic cycle will be higher than the average value and will be more disruptive. The second is that there will be an oscillatory force applied to the beads which will enhance the "peeling" effects as bonds are disrupted.

CHAPTER 7

Modelling for the Estimation of Con A-Ovalbumin Adhesion Strength

A theoretical multi-site binding equilibrium model has been developed and used to quantify the relationship between applied shear and the attached bead fraction in bead-surface interactions (Hubble *et al.,* 1996). Unlike earlier models used to describe this phenomena this model considers the extent to which multiple interactions show surface cooperativity such that the attached fraction can be described in terms of a number of sub-populations linked via differing ligand-receptor interactions. An explanation for ligand-mediated interactions has been proposed on the basis of multiple ligand interactions as outlined in chapter 2 (Hubble *et al.,* 1995).

The model uses two parameters, the critical shear stress, S_c, required for detachment of the total attached bead population, and a surface association constant, K_p, based on the estimated strength of the bead interaction force.

7.1 Model Development and Evaluation

After a cell/bead is attached to a solid surface via ligand interactions, the strength of the attachment will be a function of the number of bonds formed between the bead and the solid surface. For removal of the attached beads, a force equaling the net adhesive force must be applied. After exposure to an applied force the number of detached beads will be non-linearly dependent on the magnitude of the applied fluid

force. As the applied shear force approaches a limit, the number of attached beads falls sharply until all the beads have detached.

Taking a cell population immobilised via 1 to n ligand receptor interactions where C represents the suspended cell concentration:

$$C_{tot} = C + C_1 + C_2 \ldots\ldots\ldots + C_n \qquad (1)$$

Equation 1 can be expressed in terms of the surface ligand concentration, the dimensionless dissociation constant describing the first interaction between a free cell and the surface, (K_d) and the association constant describing the equilibrium between $C_{n-1} \Leftrightarrow C_n$, ($K_p$).

$$C_{tot} = C + \frac{C[L]}{K_d} + K_p \frac{C[L]}{K_d} + K_p^2 \frac{C[L]}{K_d} + \ldots\ldots\ldots + K_p^{n-1} \frac{C[L]}{K_d} \qquad (2)$$

The first term on the right hand side is the free cell population, with each successive term representing an attached cell sub-population. Depending on the value of K_p the population fraction attached by a given number of bonds can either show an increase with bond number ($K_p > 1$) or decrease with bond number ($K_p < 1$). As shear is applied to the system those cells held with the lowest number of bonds will be removed first with successive sub-populations being sequentially removed until the attachment force resulting from the number of bonds remaining balances the applied force.

Assuming identical bonds or an average bond strength, the maximum number of bonds per cell can be calculated from the force required to remove the most tightly bound cells (i.e. the force resulting from the critical shear) and the individual bond strength. The number of bonds for the cells just detached by an intermediate applied shear is given by the applied force divided by the bond strength. Therefore we can write:

$$Cb_{tot} = \Sigma_{i=1}^{ntot} K_p^{i-1} \frac{C[L]}{K_d}$$ Total bound cells (3a)

$$Cb = \Sigma_{i=1}^{n} K_p^{i-1} \frac{C[L]}{K_d}$$ Bound cells removed by a given shear force (3b)

The number of bonds required to maintain attachment, *n,* must be calculated from estimates of the applied force and the individual bond strength. Applied force is given by Hammer and Lauffenburger (1987).

$$ftot = 110\, s\, r^3/a \qquad (4)$$

where s applied shear, r (particle radius 2.25 x 10^{-4} cm), a (radius of contact area, 2.25 x 10^{-5} cm).

Number of bonds

$$n = ftot/fb \qquad (5)$$

(ntot is the number of bonds determined from ftot when the critical shear is used)
where fb = 1 x 10^{-5} dynes (Bell 1978). The value of fb was derived with work carried out on the interactions between antibodies and antigens, as this study is concerned with the interactions between a lectin and a glycoprotein the value for fb is considered a close estimate.

When steady state has been reached the fraction of attached cells (F_{eq}) remaining on the surface can be given as

$$F_{eq} = \left(\frac{\left(Cb_{tot} - Cb\right)}{Cb_{tot}} \right) \qquad (6)$$

Substituting for Cb_{tot} and Cb using equations 3a & 3b, and simplifying

$$F_{eq} = \left(\frac{\Sigma_{i=1}^{ntot} K_p^{i-1} - \Sigma_{i=1}^{i=n} K_p^{i-1}}{\Sigma_{i=1}^{ntot} K_p^{i-1}} \right) = \frac{K_p^{ntot} - K_p^n}{K_p^{ntot} - 1} \qquad (7)$$

The term $\frac{C[L]}{K_d}$ which cancels out in this step can be assumed to be independent of applied force in a detachment experiment as it will define only the last, monovalent, interaction between cell and surface. This expression suggests that in a detachment experiment the shear effect should be independent of the suspended, i.e. unattached, cell concentration. The effect of ligand and receptor density will be observed in changes in the value of K_p reflecting the probability of adjacent ligands and receptors being sufficiently close to form additional bonds once the cell is attached.

The data describing the variation of fractional attachment with increasing applied shear can be fitted to equation (7) using an appropriate non-linear least square algorithm. A commercial package based on Powells method was used for this purpose (Scientist - MicroMath Ltd.). The following sections describe the results obtained from applying this model to the data presented in chapter 6.

7.2 Description of Experimental Detachment Data

7.2.1 The Effect of Hydrodynamic Shear

The data obtained from the fraction [F] of adherent beads against shear stress (figures 6.1-5B) were used to determine the critical shear stress (S_c) and the surface association constant (K_p) for the interaction between Con A and ovalbumin.

As some of the experimental data do not fit the model the values of critical shear stress and association constant have not been given.

a) Con A Density of 41.5μg/cm^2

Figure 7.1 (A) R_T 4.79 x 10^6 ovalbumin molecules/bead

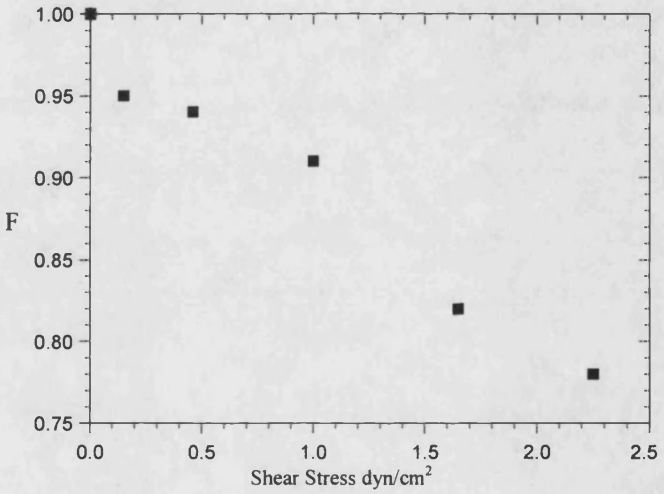

Figure 7.1 (B) R_T 5.21 x 10^6 ovalbumin molecules/bead

S_C=4.67

K_p=1.03

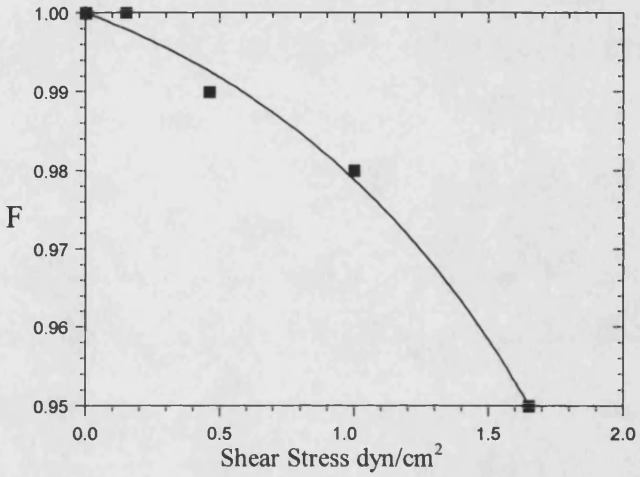

Figure 7.1 (C) R_T 7.06 x 10^6 ovalbumin molecules/bead

S_C=3.30

K_P=1.03

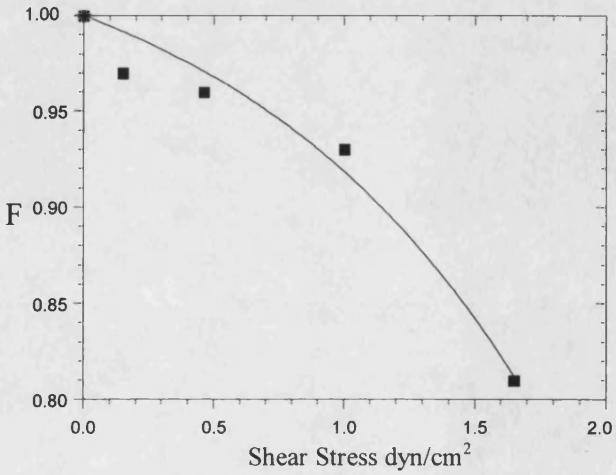

Figure 7.1 (D) R_T 8.30 x 10^6 ovalbumin molecules/bead

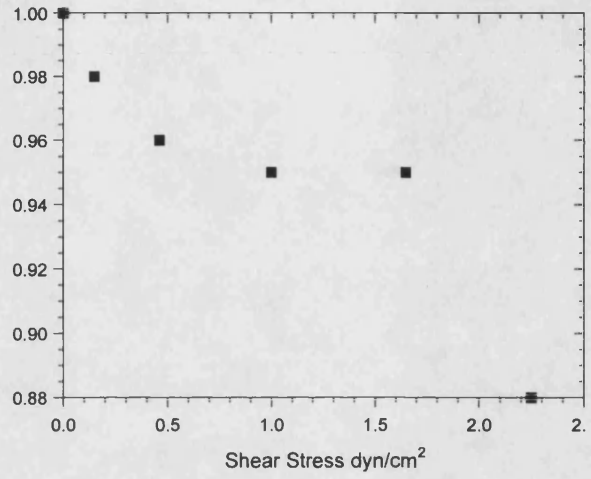

Given the fit of the data the value for the critical shear is likely to be meaningless.

Figure 7.1 (E) R_T 13.90 x 10^6 ovalbumin molecules/bead

S_C=2.80

K_P=1.06

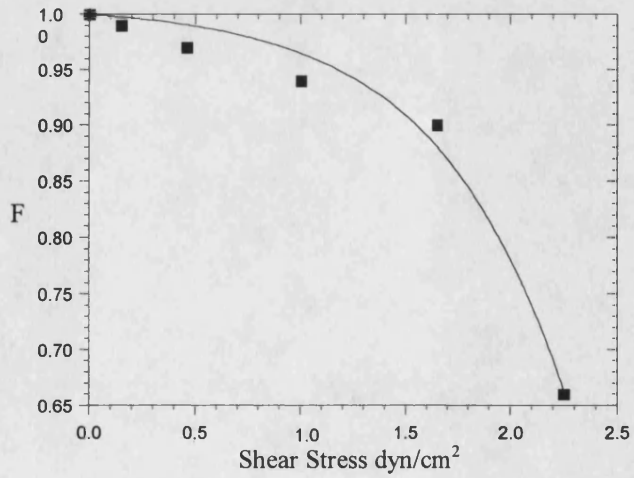

b) Con A Density of 67.0μg/cm^2

The following graphs show the simulated curves for the all ovalbumin concentrations except ovalbumin R_T value of 13.90 x 10^6 ovalbumin molecules/bead as it did not fit the model or show a curve of any significance.

Figure 7.2 (A) R_T 4.79 x 10^6 ovalbumin molecules/bead

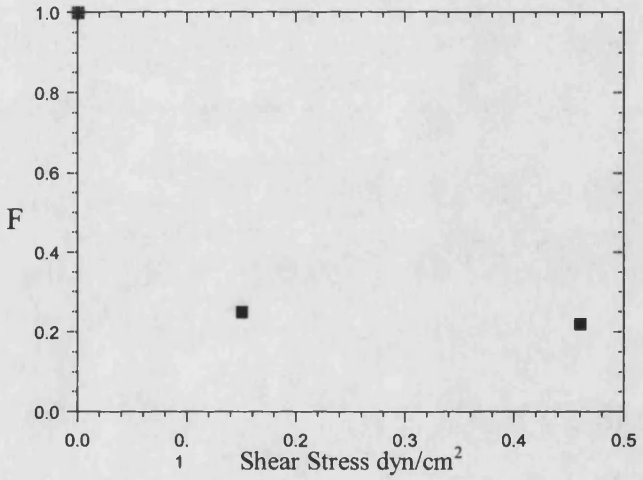

The critical shear value could not be determined.

Figure 7.2 (B) R_T 5.21 x 10^6 ovalbumin molecules/bead

S_C=1.70

K_P=1.00

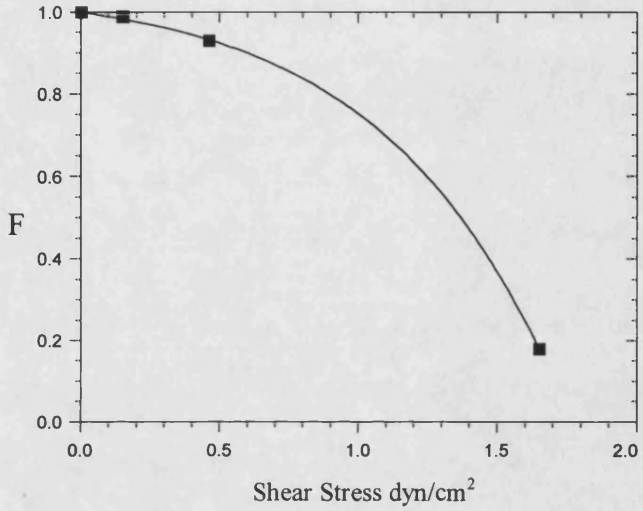

Figure 7.2 (C) R_T 7.06 x 10^6 ovalbumin molecules/bead

S_C=1.84

K_P=1.00

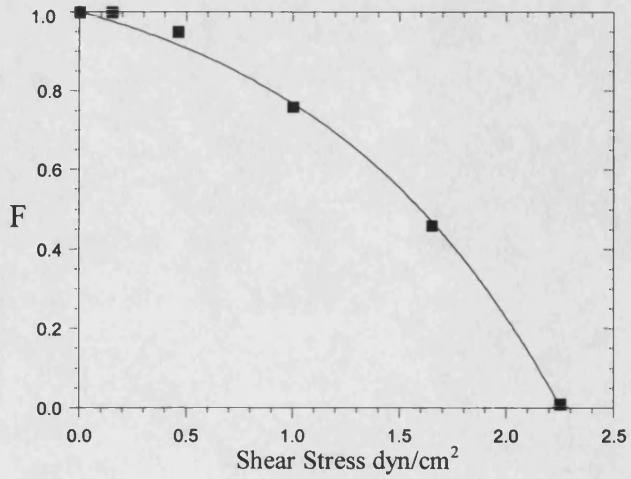

Figure 7.2 (D) R_T 8.30 x 10^6 ovalbumin molecules/bead

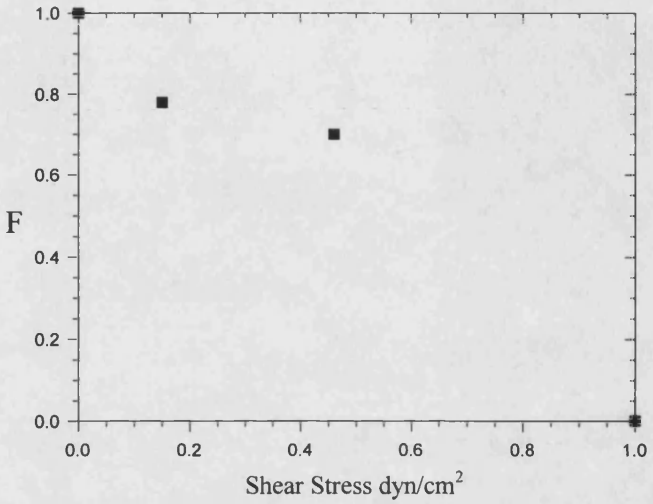

c) Con A Density of 68.5µg/cm^2

The following graphs (figures 7.3 A-E) show the fraction of beads bound against shear stress at the five ovalbumin receptor concentrations.

Figure 7.3 (A) R_T 4.79 x 10^6 ovalbumin molecules/bead

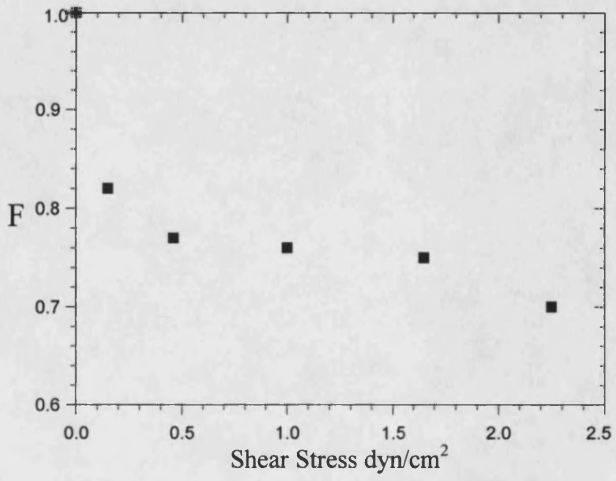

Figure 7.3 (B) R_T 5.21 x 10^6 ovalbumin molecules/bead

S_C=2.89

K_P=1.04

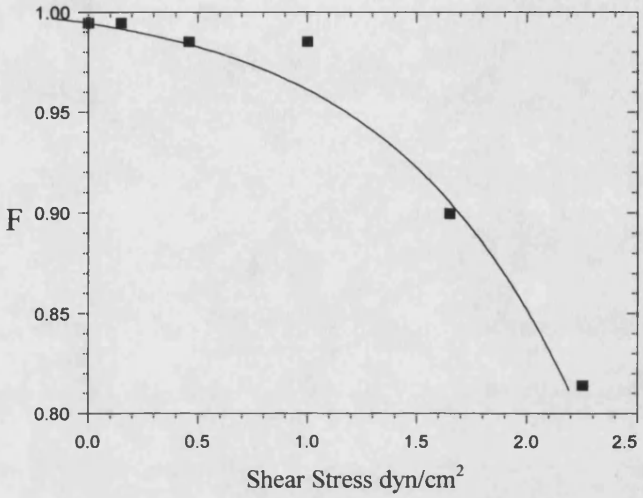

Figure 7.3 (C) R_T 7.06 x 10^6 ovalbumin molecules/bead

S_C=2.25

K_P=1.03

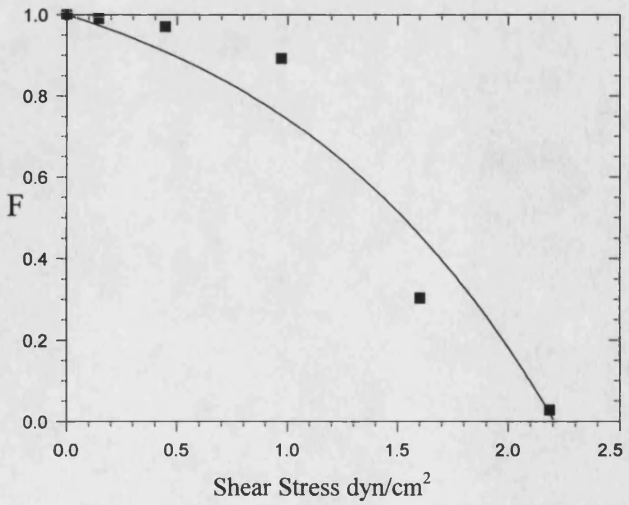

Figure 7.3 (D) R_T 8.30 x 10^6 ovalbumin molecules/bead

S_C=2.89

K_P=1.01

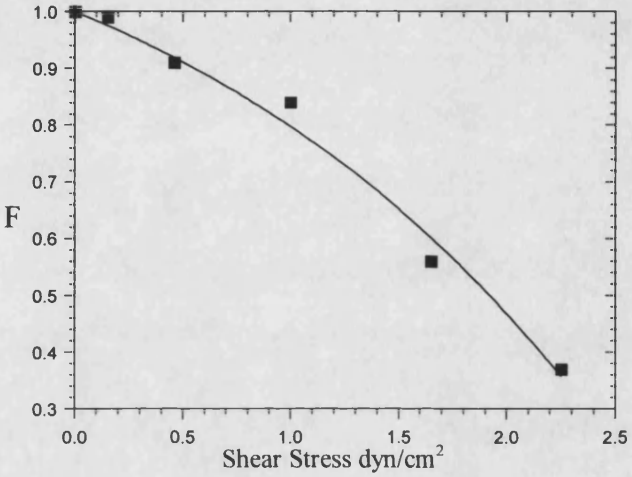

Figure 7.3 (E) R_T 13.90 x 10^6 ovalbumin molecules/bead

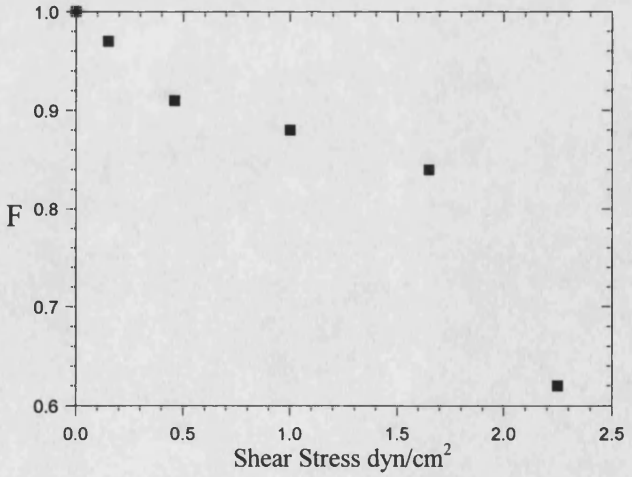

Figure 7.3 (A) shows a detachment profile that does not fit the theoretical model and the highest critical shear stress, of 6.17dyn/cm^2 obtained with the ovalbumin R_T value of 4.79 x 10^6 molecules/bead.

d) Con A Density of 72.5µg/cm^2

Figure 7.4 (A) R_T 4.79 x 10^6 ovalbumin molecules/bead

S_C=1.65

K_P=1.41

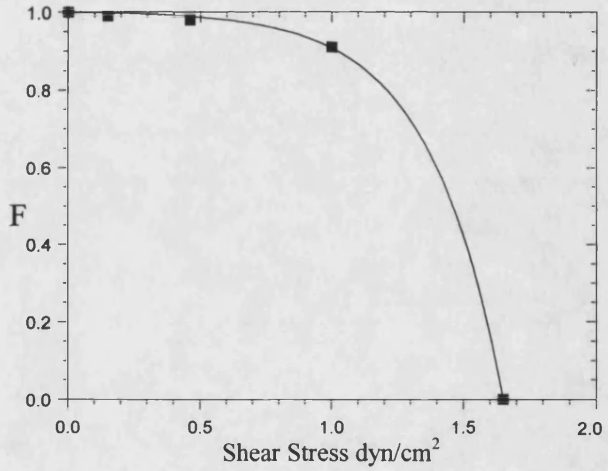

Figure 7.4 (B) R_T 5.21 x 10^6 ovalbumin molecules/bead

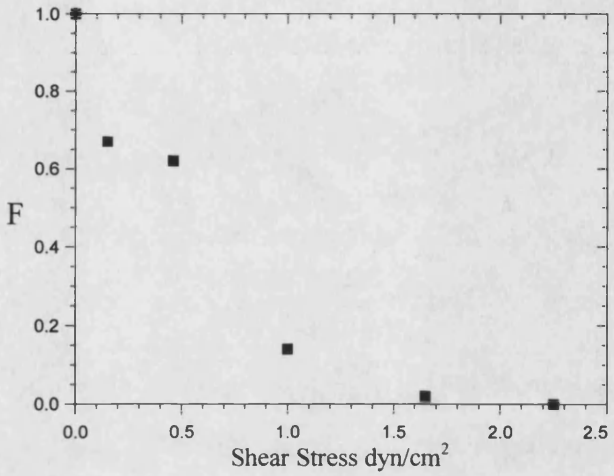

Figure 7.4 (C) R_T 7.06 x 10^6 ovalbumin molecules/bead

S_C=1.65

K_P=1.22

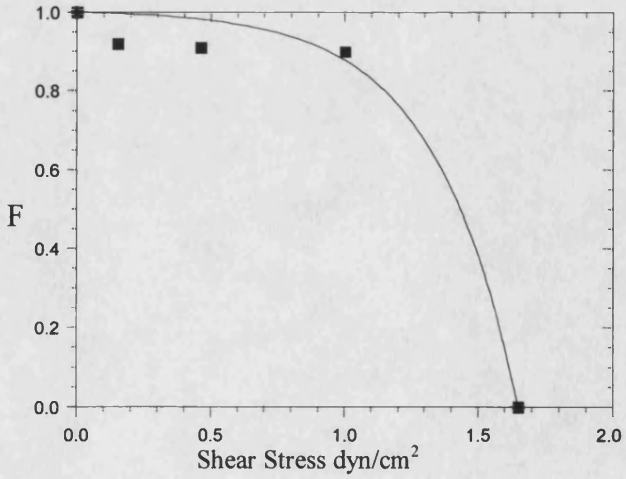

Figure 7.4 (D) R_T 8.30 x 10^6 ovalbumin molecules/bead

S_C=1.65

K_P=1.16

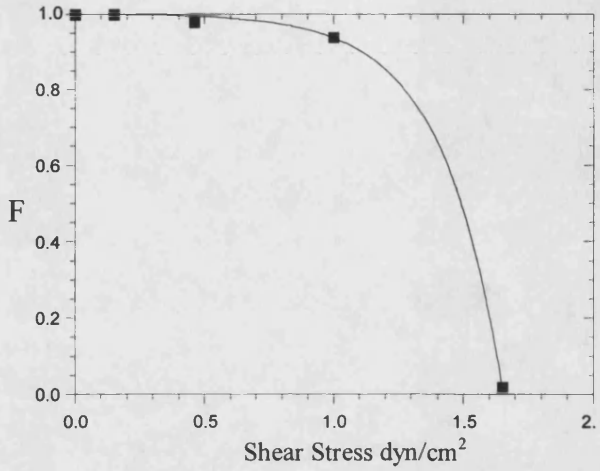

Figure 7.4 (E) R_T 13.90 x 10^6 ovalbumin molecules/bead

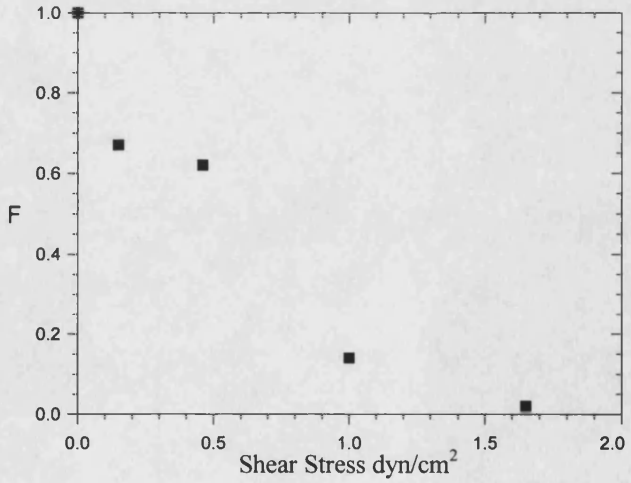

Figures 7.4 A, C and D fit the model whereas figures 7.4 B and E show a different type of binding curve and do not fit the mathematical model. Little variation is seen in the surface association constant.

e) Con A Density of 119.5μg/cm^2

Figure 7.5 (A) R_T 4.79 x 10^6 ovalbumin molecules/bead

S_C=1.00

K_P=1.06

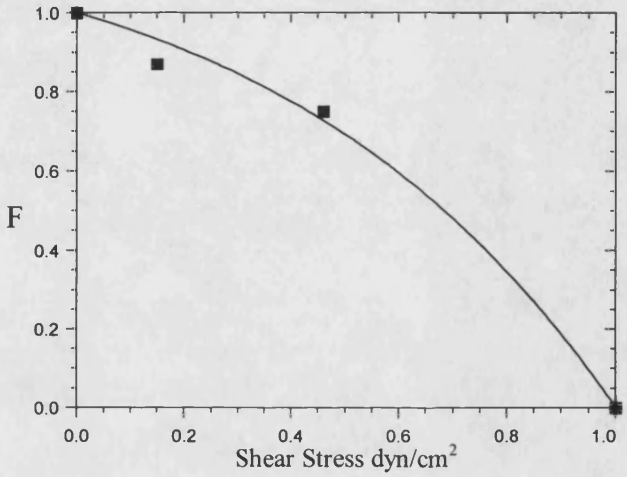

Figure 7.5 (B) R_T 5.21 x 10^6 ovalbumin molecules/bead

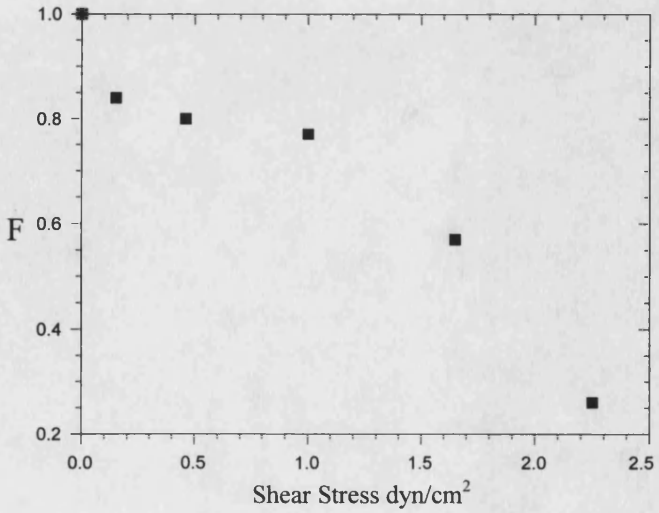

Figure 7.5 (C) R_T 7.06 x 10^6 ovalbumin molecules/bead

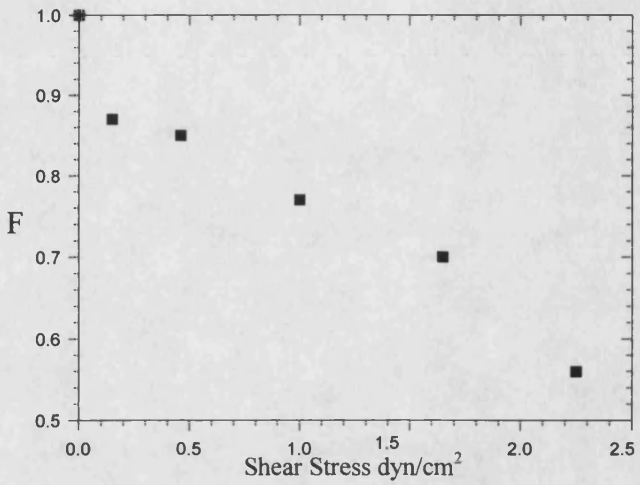

From the data of the simulated curves it can be seen that two types of detachment curves are obtained. One detachment curve is as expected and is found to fit the mathematical model whereas the other detachment curve does not. The effect of Con A and ovalbumin receptor per bead on critical shear stress values are shown in figures 7.6-7 & table 7A-B.

As two distinct types of detachment behavior are observed, type A, that fit the model and type B, that deviate from the model . From these two types of curves it can be suggested that in some cases additional factors are in place effecting the type of detachment behavior obtained. These additional factors may include clustering of receptors on the beads leading to delay in bead detachment (Ward *et al.,* 1994). The extent of clustering found in each sample and effect of receptor clustering on detachment behavior is discussed in detail in chapter 8.

7.2.2 Effect of Ligand/Receptor Densities on Critical Shear Stress

The relationship between the Con A loading and the critical shear stress values obtained from the mathematical fit of the data was assessed (figure 7.6 & table 7A)

Table 7A Relationship Between Con A Loading [L] and the Critical Shear Stress for the five Ovalbumin concentrations where R_T (x 10^6) is number of ovalbumin molecules/bead.

[L] (mg/ml)	Critical Shear Stress (dyn/cm^2)				
	R_T4.76	R_T 5.21	R_T 7.09	R_T 8.30	R_T 13.90
1.0	1.65	-	1.65	1.65	-
2.5	-	-	2.25	2.89	-
5.0	-	1.70	1.84	-	-
10.0	1.00	2.87	-	-	-
25.0	-	4.67	3.30	-	2.80

Figure 7.6 The Effect of Con A Loading on Averaged Critical Shear Stress Value (Sc) and Association Conatant (Kp).

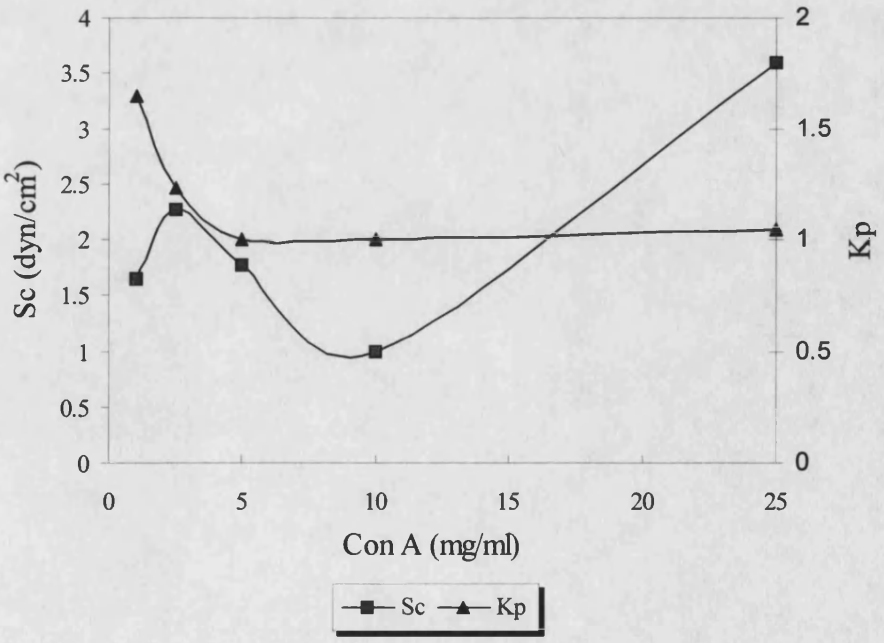

The curves obtained for the effect of Con A loading against critical shear stress and association constant show an overall trend of increase in shear stress at Con A loadings of 2.5mg/ml (68.5μg/cm^2) and of 25mg/ml (41.5μg/cm^2) with a decrease in shear stress at a Con A loading of 10.0mg/ml (119.5μg/cm^2). There does not appear to be an obvious relationship between ligand loading and the critical shear stress. This is discussed further in chapter 8.

The K_P values obtained are all within the range of 1.01-1.60 Little variation is observed in the value of the surface association constant obtained on fitting the data points to the mathematical model.

Table 7B The Relationship Between Ovalbumin Receptors per bead and Critical Shear Stress where R_T is the number of ovalbumin receptors per bead and, C_b is the Con A bound on the membrane (μg/cm^2).

R_T/bead (x 10^6)	Critical Shear Stress (dyn/cm^2)				
	C_b 41.5	C_b 67.0	C_b 68.5	C_b 72.5	C_o 119.5
4.79	-	-	-	1.65	1.00
5.21	4.67	1.07	1.65	-	-
7.06	3.30	1.84	2.25	1.05	-
8.30	-	-	2.89	1.65	-
13.90	2.80	-	-	-	-

The relationship of the number of receptors on the beads (R_T) was plotted against the averaged critical detachment shear stress as there was not a complete data set for the ovalbumin receptor numbers due to crtical shear stress values obtained from the data that did not fit the model and hence the valuse were considered meaningless (figure 7.7).

Figure 7.7 The Effect of Ovalbumin Receptor's on the Average Critical Shear Stress.

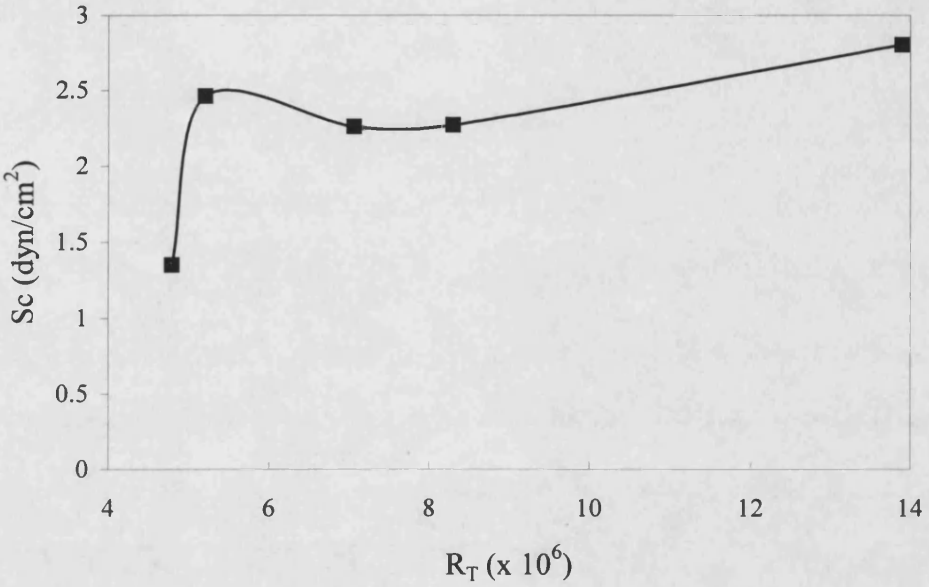

The curve obtained for the effect of ovalbumin receptor number on the averaged critical shear stress for the Con A surface concnetrations show that the lowest shear stress value obtained shown is for the ovalbumin loading of 4.79 x 10^{-6} molecules/bead.

The fact that two different types of binding behavior is observed could explain the relationship between the receptor number and critical shear stress. As can be seen from figures 7.6 & 7.7 not all five sets of data are plotted this is due to the fact that there are not enough data points to plot graphs for each type of detachment curve. Some of the data obtained did not give significant curves when fitted to the model and the values of critical shear stress calculated were meaningless as the data deviated from the model to a great extent. These data was therefore ignored when

plotting graphs to determine the relationship between both the Con A and ovalbumin concentrations against critical shear stress.

The number of bonds formed within the contact region was calculated for each ovalbumin and Con A concentration using the equations of total force applied (F_T) and the force per bond (1 x 10^{-5} dyn) as outlined in sections 6.1.1 & 7.1. (table 7C).

Table 7C The Total Number of Bonds Formed (B_{tot}) in the Contact Region Between Con A and Ovalbumin whereR_T (x 10^6) is number of ovalbumin molecules/bead.

Con A ($\mu g/cm^2$)	B_{tot}				
	R_T4.76	R_T 5.21	R_T 7.09	R_T 8.30	R_T 13.90
41.5	-	26.00	18.37	-	15.59
67.0	-	9.46	10.24	-	-
68.5	-	9.18	12.52	16.09	-
72.5	9.18	-	9.18	9.18	-
119.5	5.56	-	-	-	-

The greatest number of total bonds formed in the contact region are found at a Con A density of 41.5$\mu g/cm^2$ and an ovalbumin R_T value of 5.21 x 10^6. The detachment curve obtained at this Con A and ovalbumin concentrations fits the mathematical model, whereas higher values of number of bonds were obtained with the critical shear stress values for the data that did not fit the model. This deviation from the model has been attributed to receptor cluster formation which delays detachment (Ward *et al.,* 1994) and is discussed further in chapter 8.

7.2.3 Effect of Pre-Incubation Contact Time

To study the effect of pre-incubation time on detachment experiments were set up as outlined in section 4.2.10 (b). The data obtained from these experiments is shown as

the fraction of attached beads against shear stress (chapter 6) and is fitted to the model (figures 7.8A-F& table 7C).

Figure 7.8(A) Contact Time of 4 Hours

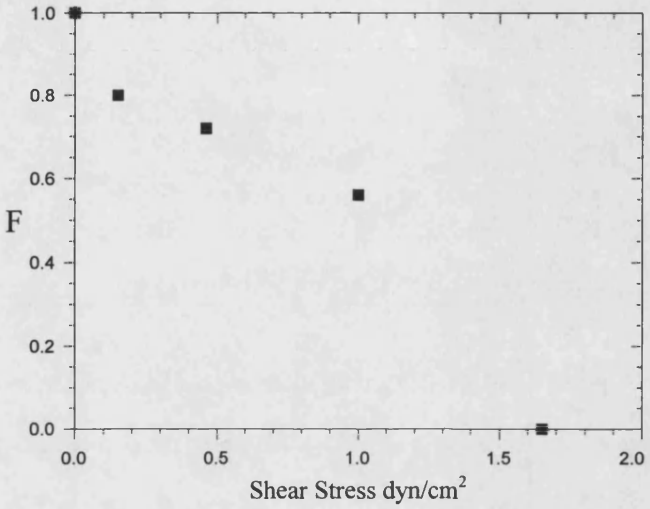

Figure 7.8 (B) Contact Time of 8 Hours

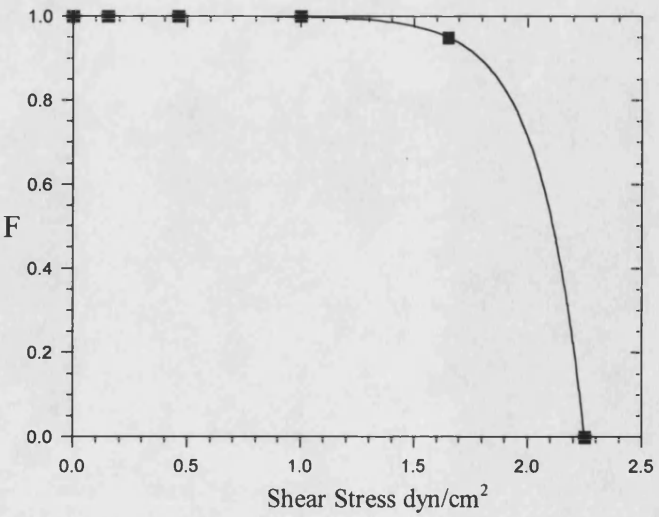

Figure 7.8(C) Contact Time 16 Hours

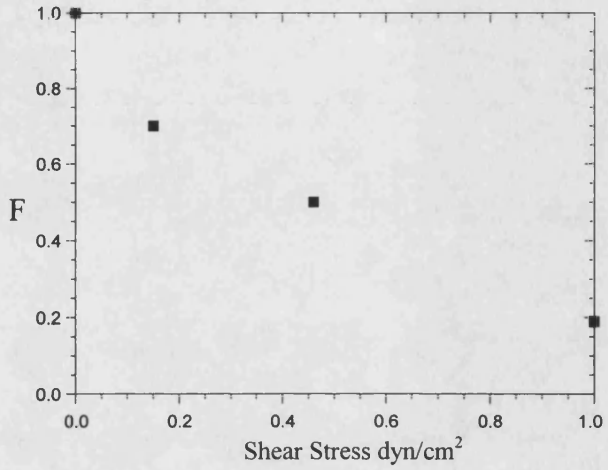

Figure 7.8 (D) Contact Time of 24and 48 Hours.

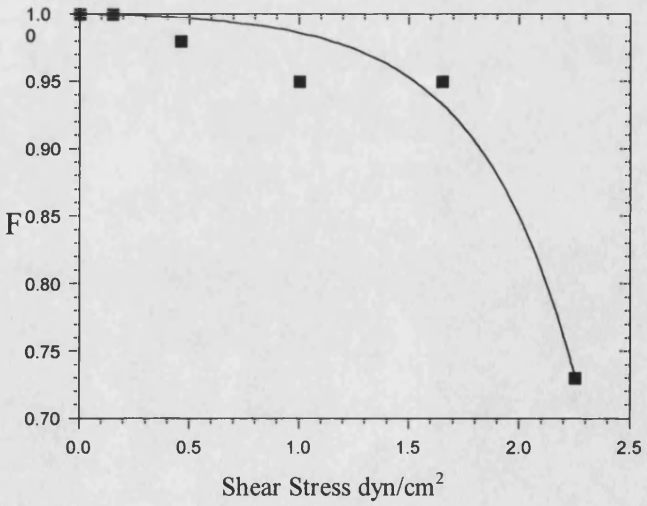

Figure 7.8 (E) Contact Time of 72 Hours

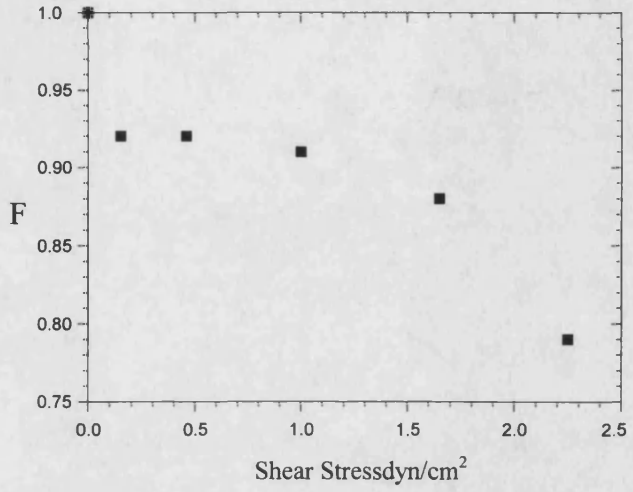

Figure 7.8(F) Contact Time of 96 Hours.

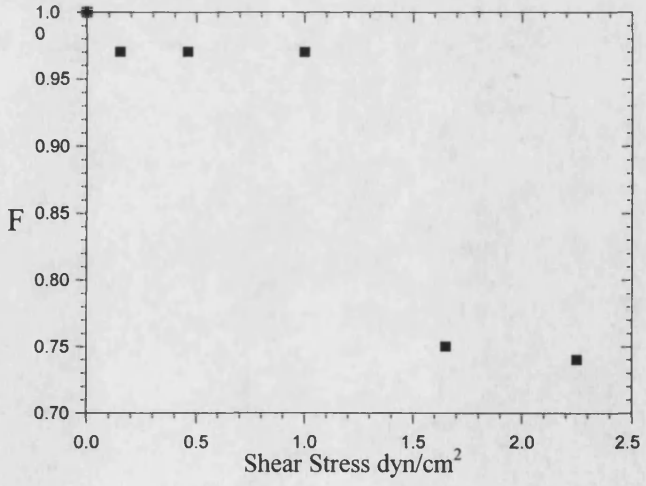

It can be seen from the data on contact time that the four detachment profiles for 4, 16, 72 and 96 hours do not fit the mathematical model and the possibilities are

discussed in chapter 8. The only variation in this set of experiments is the samples of membranes and ovalbumin-coated beads taken from an original batch containing the same Con A surface concentration and ovalbumin receptor number. Therefore the different types of binding profiles obtained suggest that different samples may lead to different populations of receptors and ligands found on the membranes and beads, this is discussed further in chapter 8.

7.2.4 Glucose Competition

The effect of addition of glucose on the detachment behavior of ovalbumin -coated beads off immobilised Con A was investigated (section 4.2.10c). The attached beads in the flow-chamber were subjected to an applied shear force of 1.00dyn/cm^2.

Figure 7.9 Effect of Glucose Addition on Detachment.

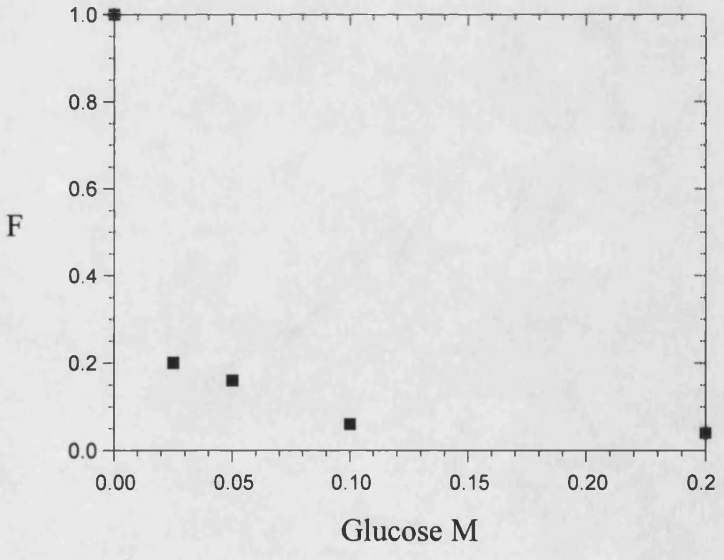

As seen in figure 7.9 a sharp decrease in the fraction of beads attached is observed as glucose concentrations is increased. The step-wise decease in the fraction of beads

bound with increas in glucose concnetration suggests the number of bonds formed require greater glucose concnetration in order to be removed.

CHAPTER 8

Discussion

Receptor-mediated cell adhesion to surfaces, including other cells as well as biomaterials, is an important element of many physiological and biotechnology-related processes. For example, the migration of neutrophils from the bloodstream to an infected tissue area is accomplished by specific receptor interactions with endothelial ligands (Springer *et al.,* 1990). Biotechnological examples that may involve receptor-mediated adhesion include cell/biomaterial interactions (Parekh *et al.,* 1994), and cell separation techniques such as cell affinity chromatography (Norden *et al.,* 1994), which can be used for the depletion of tumor cells from bone marrow for transplantation, and isolation of fetal blood from maternal blood for genetic testing (Sharma *et al.,* 1980).

The use of the lectin Con A in the affinity system studied was chosen on the basis of the similarities between Con A and the lectins found in the inflammatory response (chapter 2). All other detachment studies to date have employed immobilised antibodies onto beads/surfaces to mimic receptors on cells (Cozens-Roberts *et al.,* 1990*b*:*c*; Hammer *et al.,* 1993: Saterbak *et al.,* 1993). The advantage of using antibodies is the ease of quantification of the immobilised antibodies by employing secondary antibodies, but the *in vitro* antibody system does not reflect the true nature of the cell adhesion molecules, selectins, *in vivo*, as does the *in vitro* Con A system. Also one of the advantages of lectin chromatography is the ability to use relatively high salt concentrations, as binding between the sugar residue on the glycoprotein and the lectin is not due to ionic interaction. The advantage of the lectin system over the antibody system can also be discussed in terms of the dissociation constants for both. The dissociation constant found for the lectin-sugar system is usually within the range of 1×10^{-4}-10^{-5} in comparison with that found for antibody-antigen system

of 1 x 10^{-6}-10^{-7}. Therefore the ease of elution of the cell or protein of interest attached onto a lectin immobilised support is much greater then that for an antibody due to the lower affinity found in the lectin system. These weak and almost transient interactions are also found in the inflammatory response as discussed in chapter 2 (Parekh *et al.*, 1994).

Although the use of Con A-ovalbumin *in vitro* system provides a novel model detachment system it introduces problems in terms of protein quantification. The ease with which antibodies can be quantified is not mirrored in lectin based systems due to the lack of non-antibody based sensitive protein determination methods. The techniques employed in the quantification of immobilised Con A and ovalbumin are discussed in section 8.1.

It has been shown that adhesion strength can be measured as a function of affinity, using a parallel-plate flow chamber. Choosing a simple cell model system has allowed the different factors contributing to the adhesion process to be studied. By using polystyrene beads possessing well characterized properties, many complications arising from using real cells have been minimized.

A simple cell adhesion assay has been developed to study the fundamental aspects of receptor-mediated adhesion. The advantages of using a parallel-plate flow chamber include, direct observation of cell detachment and application of a constant shear field to allow reproducible and quantitative measurement of the adhesive force. The study of 4.5μm diameter receptor-coated beads (prototype cells) and a ligand-coated membrane surface is reported. The major advantages of the coated beads are that uniform properties can be produced and can be varied in range typical for cell-surface adhesion. The shear stress range examined was between 0-2.25dyn/cm^2, which is within the range of physiological interest. The shear stress found in venules and veins, where margination of neutrophils occurs is between 0-4dyn/cm^2 (Cozens-Roberts *et al.*, 1990*b*).

An analysis of the parameter effects on cell detachment is given and the experimental results obtained are analyzed with a mathematical model developed for multiple receptor-ligand mediated adhesion in the parallel-plate flow chamber.

8.1 Quantification of Immobilised Con A and Ovalbumin

It is essential to determine the success of a protein immobilisation procedure at the time of the coupling in order to establish the validity of the immobilisation methodology employed. The methods employed in the determination of the proteins immobilised in this system included a colourimetric assay as well as the use of a spectrofluorimetry. The total amount of Con A bound was determined using the BCA assay (section 4.2.4), this method was used because it is generally less affected by the presence of compounds which have been found to interfere with the Lowery procedure. Importantly, immobilised proteins can be easily quantified with the BCA assay, also a more sensitive range of immobilised protein can be detected with a microassay procedure.

Although the BCA assay was employed for the quantification of immobilised Con A on application of this assay for the determination for immobilised ovalbumin the readings obtained were not reproducible. As the ovalbumin concentration range was smaller by a factor of 10^{-3} in comparison to the Con A concentration used the BCA assays was found unable to detect the lower protein range. Therefore several methods were used to quantify the total ovalbumin bound on the beads (section 4.2.8) These methods include enzyme proteolysis and acid hydrolysis as well as the difference method which relied on determining the ovalbumin before and after incubation with the beads. As fluorescamine was used in the quantification assays of ovalbumin spectrofluorimetry was employed in the determination of ovalbumin in all the above mentioned methods (section 4.2.8).

Fluorescamine has been employed in several protein determination assays including the simultaneous measurement of cytochrome P4501A's catalytic activity and the total protein concentration (Kennedy et al., 1994) and the sensitivity and utility of protinase assays employing fluorescamine to form a fluorescent adduct has also been assessed (Evans *et al.,* 1984).

Fluorescence is the phenomenon where a molecule, after absorbing radiation, emits a longer wavelength. Thus a compound may absorb radiation in the ultraviolet region and emit visible light. The major use of fluorimetry in biochemistry for quantitative analysis is where the accuracy, reproducibility and sensitivity of the technique, allows determination of concentrations too low for absorption based spectral analysis. Although fluorescamine is quickly hydrolyzed in aqueous solution, the conjugate it forms with primary amines is not and the excess reagent is concomitantly destroyed with a half-time of several seconds (Udenfriend *et al.,* 1972). While this conjugate is fluorescent, neither the fluorescamine nor its products fluoresce. The comparative rates of the hydrolysis and conjugation reactions are the crucial parameters. These factors make fluorescamine suitable for assaying primary amines including amino acids, peptides and proteins.

Assays involving proteinases may be constructed in two ways, as either the substrate or its degradation products may be fluorescently labeled. In the former case, the substrate is prelabeled with fluorescamine and the proteolytic release of its fluorescent breakdown products is monitored (Evans *et al.,* 1984). There are two disadvantages with this approach. First, as intact proteins usually have relatively few free amine groups, the specific activity of the substrate tends to be low. Second, in common with most other types of protinase assay, this method requires separation from its breakdown products. Greater sensitivity and facility are achieved by fluorescently labeling the breakdown products, rather than the substrate. Each proteolytic reaction produces a free amino group, so that the proteolysis generates a large number of sites at which fluorescamine can react, although the problem arises in that sensitivity will vary with extent of breakdown . As this number usually far

exceeds the number of sites in the original substrate, fluorescamine can be added to the reaction mixture without first removing undigested material. However, the literature suggests that fluorescamine has not found widespread application in the assay of proteolysis.

Initially a difference analysis method was employed in which the amount of ovalbumin was measured before and after the coupling (section 4.2.8a). It was found that the ovalbumin concentrations after coupling had taken place were not high enough for the fluorescamine to detect with confidence and reproducible results were not obtained. An enzyme digest approach was attempted next to cleave the immobilised ovalbumin off the dynabeads (section 4.2.8b). The use of suitable enzymes to hydrolyse immobilised ligands is well established (Harris *et al.,* 1990). However the release of ligands reflects their accessibility to the digestion enzyme and may underestimate ligand concentrations. The enzyme trypsin which hydrolyses polypeptides on the carboxyl side of lysine and arginine was employed to cleave ovalbumin from the beads (section 5.3.3 & figure 5.10). Acid hydrolysis of the immobilised protein was also attempted liberating amino acids from the beads (section 4.2.8c). Both the enzyme digest and the acid hydrolysis assays did not give reproducible results and the factors that may have contributed to this inconsistency are discussed below.

As fluorescence intensity is a relative measure it was necessary to convert the fluorescence obtained to absolute units. This can be achieved via a standard curve constructed by measuring the fluorescence of an appropriate amino acid or peptide or the protein being assayed. For the proteolysis assay ovalbumin was used as a standard (figure 5.9: section 5.3.3) whereas for the acid hydrolysis assay the amino acid glycine was used. Figure 5.9 shows a linear relationship between increase in ovalbumin concentration and the fluorescence intensity. A straight-line plot was also found by Evans *et al.,* (1984), where trypsin was assayed by a fluorometric method, confirming that the fluorescence produced is an accurate measure of proteolysis, also confirming the validity of this assay. Therefore the inconsistencies and lack of

reproducibility of the data throughout the proteolysis and acid hydrolysis assays is not due to the techniques carried out during the assessment of the total ovalbumin concentration.

An important factor that needs to be addressed is that the protein of interest is immobilised and to date the use of both fluorescamine and proteolytic enzymes in conjunction has not been found for the cleavage of an immobilised protein. Therefore the assays employed in this study were attempting the application of assays known to be valid for proteins in solution to a situation were the protein of interest is immobilised.

As the protein is immobilised the accessibility of the sites for the enzyme may be restricted and the length of time the ovalbumin-coated bead samples were incubated with the enzyme needs stringent optimisation. The variation observed in all the assays can also be accounted for by the fact that the orientation of the immobilised ovalbumin onto the beads is likely to vary from bead to bead and sample to sample used. This will no doubt cause a large degree of variation in the assay results. Also, clustering of the ovalbumin receptors on the beads will lead to an additional complication with relation to consistency of results, as increased concentration of the receptors in one area of the bead will again lead to difficulties in accessibility of the enzyme to the cleavage sites, and the clustering effect is likely to occur in a random fashion. This effect is likely to be seen at all ovalbumin concentrations adding to the variation obtained in all the proteolytic experiments.

The decrease of the original incubation concentration of ovalbumin with the beads, for the digest assay, did not lead to any marked improvement on the consistency of the results obtained (section 5.3.3, table 5E). As the amount of ovalbumin immobilised is decreased the availability of the cleavage sites is likely to increase due to less "crowding" of the sites and also the effect of clustering is likely to be reduced. Therefore the increase in the fluorescence intensity observed at these lower initial ovalbumin concentrations can be explained.

Other factors that are in need of further investigation in the ovalbumin quantification assays affecting the amount of fluorescence obtained from the interaction of fluorescamine with primary amines include the following: the amine involved, the pH of the solvent, solvent composition and the amount of fluorescamine added. The last factor is very important in that even though the reaction will be driven to completion by large amount of fluorescamine, the excess reagent will quench the fluorescence of the product. The sequential addition of fluorescamine is more effective than the same amount being added all at once, suggesting that fluorescamine is inactivated by a process whose rate depends on the concentration of fluorescamine.(Chen *et al.,* 1978). These factors were varied and studied to an extent but as the results obtained were giving unreliable data further investigation was suspended.

The acid hydrolysis method is known to be suitable for ligands immobilised onto an agarose matrix where the hydrolysed ligand can be measured in the presence of hydrolysis products of the matrix (Angal *et al.,* 1989). Acid hydrolysis of immobilised ovalbumin was found to give unreliable results that could not be used with confidence. A control experiment of the acid hydrolysis of ovalbumin was carried out and a curve was obtained, therefore the assay itself gives reliable results. The polystyrene beads to which the ovalbumin is immobilised are likely to interfere with the acid hydrolysis assay of the ovalbumin off the beads . This is the most likely explanation for the variation observed in the data obtained. At high temperatures such as 500-1000°C polystyrenes degrade into various products therefore the temperature in the acid hydrolysis assay of 110°C for 24hrs may have had an adverse effect on the decomposition of the polystyrene beads (Doran 1995). Therefore one further experiment to be investigated is the reduction of the temperature at which the acid hyrolysed bead-ovalbumin samples are used in the assays to reduce the degradation of polystyrene and hence the interference of these compounds in the fluorescamine assay. An optimum temperature should be obtained such that the acid hydrolysis of the immobilised protein is still efficient but with a reduced affect on the

polystyrene beads. It may also be advisable to use progressively lower concentrations of hydrochloric acid in order to obtain an optimum hydrochloric acid strength to minimize the effect of the acid on the protein.

The total number of active sites available on the immobilised ovalbumin were determined by the addition of Con A to a sample of immobilised ovalbumin (section 4.2.9 & section 5.4). Therefore the total protein quantification assays were discontinued due to lack of time. The binding of Con A to the ovalbumin allowed easy quantification of the Con A present in solution after binding to the immobilised ovalbumin. This assay gave a direct indication of the activity of the immobilised ovalbumin and the total number of active receptors bound were calculated (section 6.2).

8.2 Comparison with Data on Cell Adhesion

Artificial beads allow easy and systematic manipulation of the type and number of "receptor" on the bead surface (Kuo *et al.,* 1993). Measurement of adhesion strength over a range of receptor numbers is of great importance for elucidating the specific contribution of the receptor/ligand bonds to the overall adhesion strength, relative to non-specific colloidal forces.

The interpretation of cell data is more complicated than that of bead data. For example, on cells, receptors can diffuse into the contact area (Hafeman *et al.,* 1981; Wilkinson *et al.,* 1984), rather than being fixed onto the surface; cells may modulate receptor expression in response to the environment (Eastrabrook *et al.,* 1983), rather than maintaining a fixed receptor number. Cells can also settle on the surface and flatten increasing the contact area between the cells and the surface (Cozens-Roberts *et al.,* 1990*b*). Therefore such complicating features associated with real cells, such as membrane diffusion, receptor/cytoskeletal interactions, cell deformation and

complexities of shape leading to increased heterogenities are absent in the mimic systems.

The covalent binding of ovalbumin "receptors" to the Dynabeads via coupling to tosyl groups present on the beads through amine groups on the proteins, as well as of Con A "ligands" to the cellulose membrane by epoxy activation chemistry prevents alternative modes of disruption of attachment. Though it must be remembered that immobilisation of proteins may lead to random orientations of these proteins on the surface with many orientations precluding productive binding.

Cell adhesion data from different assays have shown behavior that is similar to that observed for beads in the parallel-plate flow chamber as well as the radial-flow detachment assay, RFDA, (Cozens-Roberts *et al.,* 1990*a*:*b*:*c*). These similarities are discussed, while taking into account that modelling of cell data must include physiological effects beyond this basic prototype cell model features.

Ligand and receptor density has been found to effect the adhesive force between cells and surfaces. For example, an increase in the ligand density increases the adhesive force between endothelial cells and fibrinogen-coated coverslips . Also, an increase in the adhesive force between various cell types and lectin-coated fibers has been reported (Rutishauser *et al.,* 1975).

The transport behavior observed for the bead detachment at the lower range of shear stresses is similar to that seen for neutrophils in blood vessels where they may attach and detach several times before either being swept away or remaining attached (Lawrence *et al.,* 1991). This type of behavior is the result of the cells coming to a stop for variable amounts of time. A bead can also serve as a nucleation site for attachment. A bead can detach from a position and "roll" to a position farther out and next to another bead, where it can reattach.

8.3 Analysis of Parameter Effects

8.3.1 Effect of Hydrodynamic Shear

The detachment profiles obtained show a progressive time dependent detachment of beads in a constant shear field (chapter 6). Early theoretical work has presented a deterministic analysis of receptor-mediated cell detachment for a homogenous cell population. However, initial comparison of a deterministic framework with experimental detachment profiles of antibody-coated latex beads did not show qualitative or quantitative agreement (Cozens-Roberts *et al.*, 1990*a*). The contributions of heterogeneity and probabilistic binding to the detachment behavior of this experimental system were investigated (Saterbak *et al.*, 1993).

The basic detachment profile obtained for progressive detachment over time and with increase in shear stress, may be attributed to the possibilities of several heterogeneties. First, the surface concentration of ligand coating (Con A) the membrane may be non-uniform. Second, receptor type heterogeneity may be present and thirdly, the surface concentration of receptors in the bead-surface contact area among individual beads may vary. Finally, the intrinsic forward and reverse rate constants characterizing receptor-ligand binding may vary from receptor-ligand interaction to interaction. Receptors and ligands are covalently bound to the bead and membrane surfaces in such a manner that a range of conformational interactions and a range of intrinsic forward and reverse rate constants, is expected. However these variations average out in a bead-surface contact area and no heterogeneity among beads is expected. As the beads are coated with ovalbumin via tosyl groups on the beads, variation of receptor type is considered negligible. Variation in the surface concentration of receptors in the beads-surface contact area among individual beads is likely to exist. As a result of these heterogeneties, bead-surface interactions among beads may not be the same; these differences may affect the detachment behavior of a population of beads.

The conversion of the critical detachment shear stress to an overall bead/surface adhesion strength is the first step in the interpretation of the detachment data. This is accomplished using the fluid mechanical analysis by Goldman *et al.,* (1967) as applied by Hammer and Lauffenburger (1987). The slopes of the plots of critical detachment stress versus bead receptor number can be multiplied by a conversion factor combining the fluid drag and torque forces that act on the bead due to the fluid shear stress. This factor is defined as the total force (F_T) exerted on the beads (section 6.1.3). The quantity obtained on multiplication of (S_c/R_T) by (F_T) is defined as the bead/surface adhesion strength as outlined in chapter 7 (Kuo *et al.,* 1993).

8.3.2 Intrinsic Properties

(a) Ligand Concentration

The results for the effect of the ligand (Con A) coating concentration (L) on the critical shear stress (S_c) for ovalbumin-coated beads are shown in figure 7.6 & table 7.A. No significant variation in the type of detachment behavior with the different Con A surface densities (41.5-119.0μg/cm^2) was observed. It is very likely however, that even the lowest concentrations of lectin used produced a lectin surface with enough binding groups to interact with all of the available ovalbumin molecules in the binding region. From the lowest receptor number on the beads of 4.21 x 10^6 ovalbumin molecules/bead, the surface concentration can be calculated to be 8.42 x 10^9 ovalbumin molecules/cm^2. This would imply that there may have been more than enough Con A to bind all available ovalbumin molecules even at the lowest Con A coverage of 2.4 x 10^{15} molecules/cm^2. From this it can be concluded that under the conditions investigated, the lectin coverage was a less significant parameter than flow rate and ovalbumin concentration.

The reduced effect of ligand density on cell/bead detachment was also found in the binding of glycophorin covered liposome to a lectin coated surface, where a lower than monolayer coverage of lectin on the surface was necessary to see the effect of the lectin density on adhesion (Wattenbarger *et al.,* 1990). This is further supported by the work of Templeman and Hammer (1994) were the binding of IgE sensitized

rat basophilic leukemia cells to antigen-coated substrate was strongly dependent on the shear rate and on receptor number but weakly on ligand density.

A significant observation was made at the lowest Con A density (41.5μg/cm^2), where the least amount of detachment was found. This would lead to the conclusion that there may be an even Con A coverage allowing the greatest number of Con A binding sites to be available. This would enable the maximum binding to occur between Con A and ovalbumin. At the higher Con A densities it is possible that masking may occur due to the steric hindrance of adjacent ligands such that binding of one ligand leads to the masking of others.

(b) Receptor Concentration

The results for the effect of the ovalbumin receptor number per bead on critical shear stress are shown in figure 7.7 & table 7.B. Two general types of detachment behavior were observed, type A which was shown to fit the mathematical model and type B which did not.

The greatest number of type B curves are seen at the Con A densities of 67.0 and 119.0μg/cm^2, and at the ovalbumin receptor densities of 4.70, 8.30 and 13.90 x 10^6 ovalbumin molecules/bead, where at the highest ovalbumin concentration only one set of data was found to fit the model (figure 7.1E). The highest critical shear values obtained of 6.47 and 9.93dyn/cm^2 show a type B detachment profile, at the lowest Con A density (41.5μg/cm^2). There does not appear to be an obvious pattern for the distribution of the type B curve. This unexplained detachment behavior was attributed to the possibilities of receptor clustering, which is known to delay cell detachment (Ward *et al.,* 1994). Receptor clustering appears to be a random phenomena as it appears to have occurred at both the highest and lowest densities for Con A and ovalbumin. It has been shown that membrane peeling velocity decreases if receptors are clustered within a patch located in the contact region (Ward *et al.,* 1994). As the type B curve is seen at all the five ovalbumin densities, it is possible that receptor clustering is occurring at all the five ovalbumin densities, but is

apparent only in those where the contact area between Con A and ovalbumin contains patches of receptor clusters. Also the close proximity of the receptors in the cluster patches may lead to co-operative multiple binding interactions between the receptors and ligands. Clustering may result from protein aggregation prior to surface attachment.

The number of bonds formed between a bead and the surface at the Con A and ovalbumin concentrations were calculated (table 8A) from the critical shear stress values shown in table 7A (section 7.2.1).

Table 8A The Total Number of Bonds Formed in the Contact Region (B_c) for Con A and Ovalbumin Surface Concentrations, where R_c ($x10^4$) is the receptor number per bead in the contact region and L_c is the number of Con A molecules in the contact region.

L_c ($x10^6$)	B_c				
	R_c 1.78	R_c 1.94	R_c 2.65	R_c 3.11	R_c 5.20
5.70	-	26.00	18.37	-	15.59
9.28	-	9.46	10.24	-	-
9.47	-	-	12.52	16.09	-
10.04	9.18	-	9.18	12.52	-
16.49	5.56	15.98	-	-	-

It was found that the number of bonds formed in the contact region were smaller by a magnitude of 10x in comparison with the estimate of 100-300 bonds formed between thymocytes cross-linked by lectin (Sung *et al.,* 1986). One explanation for the lower estimates of bond density is that the radius of the contact area may be larger than the value used in this study. Alternatively, the contact area between the bead and the surface may be less than the observed interfacial area because contact may be limited to localized regions (Bell 1978). In addition, it is possible that a lower bead density is observed as beads are not deformable and receptor motility into the contact region is not possible.

The number of receptors in contact region (R_c) is 10x greater then that found by Saterbak *et al.,* 1993, for beads 10μm in diameter in comparison to the dynabeads used in this study of 4.5μm diameter, therefore for the same number of total receptors per bead (R_T) the number of receptors in the contact region is higher for the bead with a smaller diameter due to increase in the surface area. The increased number of beads in the contact region will lead to greater proximity of the receptors allowing possible cluster formation.

The R_c values obtained for ovalbumin are much higher then the number of bonds formed in the contact region. The small number of bonds formed may be due to steric hindrance of the immobilised ovalbumin on the beads. Also the figure for the force per bond used to calculate is based on the theory by Bell (1978) and this is used in all the work on cell detachment (Cozens-Roberts *et al.,* 1990*b*:*c*: Kuo *et al.,* 1993) whose work was conducted on antibodies, whereas in this study bonds are formed between the lectin Con A and the sugar groups of ovalbumin. It is possible that the force per bond (*fb*) value may be lower for the interaction between a lectin and a glycoprotein, this may explain the small number of bonds calculated. If the value for (*fb*) is indeed lower for lectin based interactions a greater number of bond will be calculated.

The distance between the receptors on a bead was calculated (table 6B, section 6.1) and it was found that the greater the receptor number per bead the smaller the distance between the receptors on the bead. For the greatest receptor number (13.90 x 10^6 ovalbumin receptors/bead) and therefore the smallest distance between receptors (5.99 x 10^{-4} nm) on the beads, three data sets were found not to fit the model. This suggests that the effect of receptor distance on receptor clustering is a possibility, that is the smaller the receptor distance the greater the likelihood of receptor clustering and hence of the cooperative effect on binding due to the closer proximity of the receptors. The greatest number of detachment sets found to fit the model were at a R_T value of 7.06 x 10^6 ovalbumin receptors/bead, for which the only

deviation from the model was found at the highest Con A density, this deviation from the model was also found at the higher Con A densities for the R_T value of 5.21 x 10^6 receptors/bead. These findings indicate that above a R_T value of 7.06 x 10^6 ovalbumin receptors/bead greater effects of clustering are likely to be observed due to the closer proximity of the receptors. This is in accordance with the observation that only one set of data was found to fit the model at the highest R_T value of 13.90 x 10^6 ovalbumin receptors per bead.

8.3.3 Pre-Incubation Contact Time

Experiments with increasing incubation time suggests that cell-surface contact time affects the strength of adhesion (section 6.2). An increase in critical shear stress with increase in incubation contact time was observed (section 7.2.2). The fraction of beads bound increased at the higher shears with greater contact time, and the critical shear values obtained showed an overall trend of increase in with greater contact time. Mege and co-workers (1986) also showed that the number of cells adhering to the inside walls of capillary tubes, after they had settled and had then been exposed to a particular shear flow, increased with incubation time. The detachment data for the contact times of 16 and 72 hours does not fit the model and this is attributed to the possibilities of receptor clustering.

As expected the total number of bonds formed in the contact region increases with increase in contact time and as the critical shear stress values also increased although some of the experimental data did not fit the model. This would lead to the conclusion that multiple bond formation is occurring and possible cooperative effects may also be taking place. Also unless the ligand and receptor are both uniform over the contact area it is possible that the number of bonds formed will depend on the orientation of the initial contact and the rates at which interactions subsequently occur.

8.3.4 Competitive Glucose Elution

The results obtained from the competitive glucose experiments (sections 6.3 & 7.2.3) show a marked decrease in of the fraction of attached beads in the presence of glucose. This result demonstrates the importance of competitive elution which may be used in conjunction with an applied force for detachment to occur. The addition of a biospecific elutant is the reduction of an external force required for detachment lowering the chances of mechanical damage to the cells in the elution stage of an affinity based system. The concentrations used in this cell mimic system may need to be re-evaluated for use in a cell-based system. Although the highest glucose concentration used in the competitive elution experiments is 0.5M, *in vivo* this concentration of glucose is not found to lyse cells (Suttie 1982).

8.3.5 Steady and Pulsatile Flow

The effect of both steady and pulsatile flow show that a greater fraction of beads detach in the presence of a pulsatile flow. This can be attributed to the additional force exerted on the bead by the pulse weaken the bonds by the continuous backwards and forwards motion. Pulsatile flow resembles the *in vivo* situation more closely than non-pulsatile flow since it parallels the type of flow produced by the heart.

8.4 The Simulated Binding Curves

The simulated binding curves obtained for the model system studied showed two basic forms (chapter 7). One type of detachment curve was as expected (type A), and fitted the mathematical model, whereas the second type of curve obtained (type B) was not explained by the model.

At the Con A density of 41.5μg/cm^2 for four out of the five ovalbumin concentrations studied the simulation curves show an approximate fit to the model. It is at the

lowest ovalbumin concentration (R_T 4.79 x 10^6 molecules/bead) that a deviation is observed from the model fit to the type B curve. This implies that at the lower ovalbumin concentration the availability of the ovalbumin molecules for interaction with the immobilised Con A is limited in comparison with the other four ovalbumin concentrations.

An alternative empirical model has been proposed which does not take into account multivalent interactions and the theory behind it is summarised below (Fang Ming 1995).

Taking N_0 as the initial number of attached beads before fluid force is applied, N_a as the number of attached beads and N_d as the number of detached beads at a given time, the following equations can be formulated:

$$N_a = N_0 - N_d \tag{1}$$

this can be written in fractional terms;

$$f = 1 - \frac{N_d}{N_o} \tag{2}$$

where f, the fraction of cells attached is $f = \frac{N_a}{N_o}$.

The ratio $\frac{N_d}{N_o}$ must relate to the ratio of the applied shear to the minimum shear required to remove the tightest bound cells, (described as the critical shear). It has been shown from published data that this is not a linear relationship and that as the applied shear progressively approaches the critical value, the magnitude of the change in the detached fraction increases for a given incremental shear value and can be described as in equation (3):

$$\frac{N_d}{N_o} = \frac{KS}{KS_c + (S_c - S)} \tag{3}$$

where S is the shear stress applied, S_c the critical shear stress value and K is a dimensionless parameter (the dissociation constant). Using this relationship equation (2) can be re-written as:

$$f = 1 - \frac{K\frac{S}{S_c}}{K + \left(1 - \frac{S}{Sc}\right)} \tag{4}$$

When $S = S_c$ i.e. all the cells have detached , $1 - \frac{S}{S_c} = 0$ and so $f = 0$, and when $\frac{S}{S_c} = 0$, then $f = 1$. These two situations define the experimental system.

Predictions obtained from both the models are very similar but not identical. One advantage of the multivalent model is that it gives some insight into the mechanism of binding, the advantage of the other second model is that it needs no assumptions with respect to the binding mechanisms and therefore is more widely applicable.

Neither the theoretical multivalent model or the empirical model predicts the type B curve.

8.5 Receptor Clustering

The experimental detachment curves obtained gave a variety of types of curves which have been broadly divided into type A and type B curves (chapter 7). Where type A was found to fit the multivalent model and type B did not. There are several curves that were found be a combination of both types of curves. The deviations observed

from the model have been attributed to the possible clustering of receptors. Aggregation is a phenomenon found *in vivo* and several proteins including Con A and ovalbumin are known to aggregate in solution (Mandal et al.,1993).

It was found that all the surface concentrations for both the receptor (ovalbumin) and the ligand (Con A) were too high to observe an effect on binding, lower concentrations were difficult to asses and this area of protein quantification is open to further work. As the concentrations may not have been a parameter effecting the detachment curves obtained it is worth considering in effect whether all the data obtained can be averaged and one curve can show the general trend of fraction of beads bound against shear stress (figure 8.1).

Figure 8.1 The Average Fraction of Beads Attached for both the Receptor and Ligand Surface Concentrations against Shear Stress.

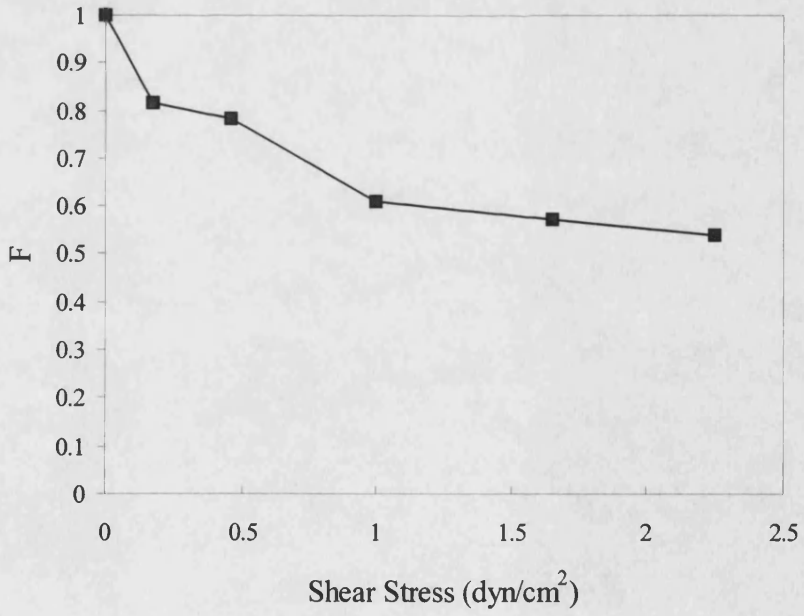

The fraction of beads bound as seen from figure 8.1, decreases and then appear to level off slightly. This suggests that another form of binding is taking place, that is,

possible clustering is occurring requiring a much greater shear stress to detach the beads then used with the flow-cell.

It must be remembered that this curve obtained is a very general trend, from which it can be seen that there is a very sharp drop region of 0-0.25dyn/cm^2, this indicates possible non-specific interactions that are being easily washed off interfering with the shape of the curve obtained. Although a very gentle flow was used to remove unspecifically bound beads before the start of each experiment it is possible from the sharp drop seen in figure 8.1 that the threshold needs to be increased and this can be further investigated.

To obtain an idea of the effect of clustering on the detachment profile curves were simulated to show the profile obtained when two types of receptor populations are present in the same detachment experiment. The ratios of the two types of populations (un-clustered and clustered) have been varied to give an indication of the effect on the types of curves obtained (figure 8.2). These curves were simulated with the data obtained for critical shear stress values and association constant values for both the data that fitted the model and those that deviated from the model.

Figure 8.2 The Simulated Binding Curves of Fraction of Beads Attached (F) against Shear Stress (S) with Varying Ratios of Un-Clustered (Kp 1.05) and Clustered (Kp 1.07) Receptor Populations.

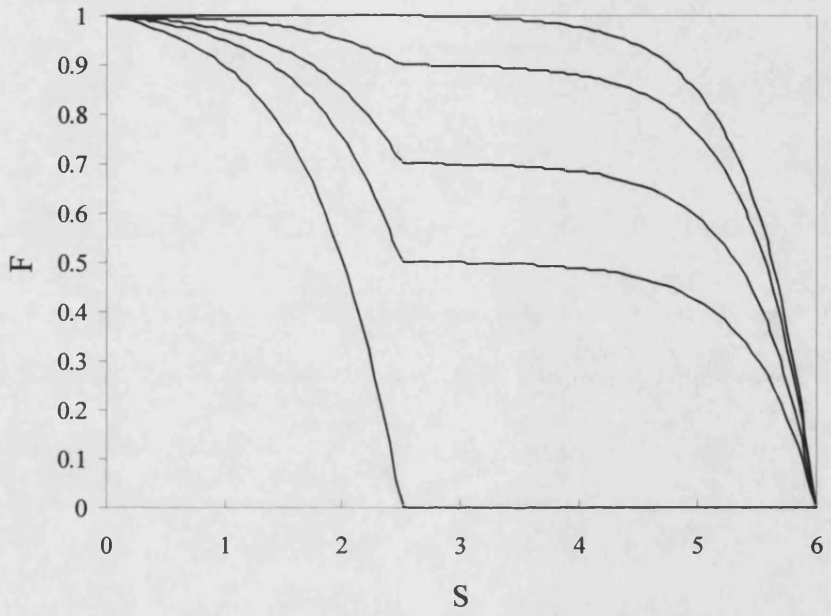

The above figure shows two populations of ovalbumin-coated beads, where the first population is said to contain no clusters and the second contains clusters with a consistent degrees of aggregation. The ratios of clustered to unclustered populations ranged from 100% of clustered population bound to 100% of the unclustred population bound, with a varying fractions of both populations present. As can be seen changing the ratio of the two populations present leads to a change in the type of curve obtained all of which have been observed in the detachment data shown in chapter 7. If the two types of curves obtained with 100% clustered or unclustered populations are observed it will be noted that either will fit the multivalent model, it is a combination of both that deviates from the model and may be responsible for the step-wise detachment curve seen in chapter 7, figures 7.4(B) &7.4(E). The change in the ratios of clustered and un-clustered populations shows a variety of binding curves

that were found on fitting the detachment data to the multivalent model. This suggests that the variation obtained in the types of detachment curves shown in chapter 7 could be due to the two populations of both clustered and unclustered receptors being present in different ratios in one detachment experiment. This would also explain why just two types of curves were not observed on fitting the data. The increase shear stress required to detach the clustered population of bead may also be a result of an increase in the surface association constant (Kp).

The effect of changing the ratios of association constants of the two populations was studied while keeping the ratio of the two populations constant (0.5) for all five simulated curves shown. Therefore the difference in the types of curves obtained is solely due to the change in the association constants (figure 8.3).

Figure 8.3 The Simulated Binding Curves of Fraction of Beads Attached (F) with Varying Ratios of Association Constants for both Un-Clustered and Clustered Receptor Populations.

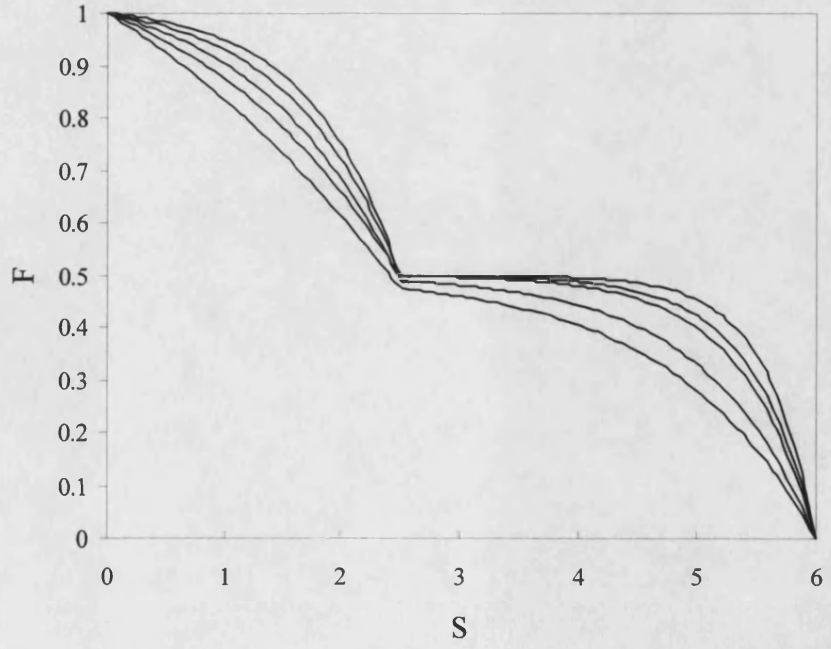

The association values for both populations are very close in value, the value for the clustered population is given a higher value due to the greater association between the receptors and the delayed detachment effect observed at bead samples said to contain clusters. The ratios for the association constants ranged from 1.01-1.09. As can be seen from figure 8.3 the change in the ratios of the association constant does not have as obvious an impact as changing the ratios of the two types of populations present. This is not surprising as the value of K_p was found to show little variation throughout the detachment curves (figure 7.6). Therefore it is very possible that the different detachment profiles obtained are a result of different ratios of clustered and un-clustered receptor populations present on the beads.

The region chosen on the membrane for the detachment assay is arbitrary and assumes uniform distribution of the receptors on the beads as well as uniform distribution of the beads on the membrane. Clustering of ovalbumin-coated beads on the membrane is also a possibility as described in section 5.1.3 as the formation of island-like structures has been known to form on hydrophilic membranes (Uyen *et al.,* 1990). Therefore the detachment profiles obtained may well be expected to differ with different membrane samples. This possibility is highlighted with the variation in the detachment profiles obtained for the pre-incubation contact time data, where the only factor being varied was the membrane sample for each experiment (section 7.2.3).

8.5.1 Effect of Receptor Clustering on Cell Detachment.

Two types of detachment profiles were obtained, as seen from the plots of shear stress against fraction of beads bound (figures 6.1-5B). The simulated binding curves for the detachment assays also showed two types of curves.

In *in vivo* systems clustering of cell adhesion receptors is an essential step in the development of focal contacts, specialized cell-substrate attachment sites where receptors are simultaneously linked to the extracellular ligand and cytoskeletal

proteins. To fully understand cell detachment it is important to have a better understanding of the role of receptor-clustering on cell substrate adhesion and detachment.

Tozern *et al.,* (1992) measured the detachment of T lymphocytes from a planar membrane containing ICAM-1 ligand molecules. Although the LFA-1 receptor for ICAM-1 is constantly expressed on the lymphocyte surface, strong cell attachment ICAM-1 was observed only after pretreatment of the T-cells with phorbol 12-myristate-13-acetate (PMA). Previous studies have demonstrated that LFA-1 associates with cytoskeletal proteins in PMA-treated cells but not with resting cells (Burn *et al.,* 1988). Therefore the enhanced attachment strength of T-lymphocytes upon addition of PMA is a result of cytoskeletal cross-linking and clustering of LFA-1 receptors. A theoretical framework has been presented that examines the influence of receptor-clustering on the dynamics of cell detachment from ligand-coated surfaces (Ward *et al.,* 1994). The framework demonstrated that receptor clusters substantially reduce the rate of cell detachment as does an increase in the extent of receptor clustering, ligand density and receptor-ligand affinity.

8.5.2 The Cluster Model Theory

Previous work on cooperativity has assumed that all the accessible matrix ligands were uniformly distributed and that all sites on the protein (receptor) had access to the same concentration of matrix ligand, that is, it only describes momomeric protein. This theory was adapted to the case of mulitvalency in the cluster co-operative model, it was assumed that matrix ligands were distributed in clusters containing from 1 to N groups within the volume occupied by an N-valent protein, that the distribution of clusters followed a Poisson distribution and that within the ligand cluster the binding of ligands to protein occurred in a highly co-operative manner due to proximity.

There are still assumptions associated with this model. The distribution of the immobilized ligand may not be random, the structure of the cellulose matrix used for Con A immobilisation is non-uniform and this is likely to effect the ligand distribution. The nature of the ligand itself may lead to aggregation or cluster formation as well as the expected clustering due to random distribution. This model also assumes that all ligands within the cluster can bind to the protein, this ignores the fact that restrictive requirements of the spatial distribution of the protein binding site are required, effectively implying that an immobilised protein has a great deal of local flexibility.

The concept of cooperativity to develop a model of a multi-site enzyme binding to an insoluble affinity support where ligand densities permitted multivalent interaction has been extended to describe the interaction of a cell covered with many receptors with a ligand coated surface (Hubble 1996). The deviations from the multivalent binding model have been attributed to receptor clustering and the effects of cooperavtivity on multiple ligand interactions. There is a distinction between local and global surface cooperativity. Where the former type of cooperativity is due to the possibilities of clustering of ligands within the range of a receptor which is predicted by Yons model (1988), and the later form of cooperativity is found with respect to the contact area.

One type of curve was as expected, in that the data obtained fitted the mathematical model and the second form of curve obtained can be explained by the co-operative cluster model theory (Yon 1988) which considers the effects of localised clustering in terms of binding probabilities.

8.6 Experimental Considerations

The measurement of immobilised proteins is still in the early stages. More sophisticated measuring techniques are required for lower densities of immobilised Con A. A surface coated with lower Con A concentrations may have led to a greater

range in the amount immobilised thereby giving more variance in the detachment behavior in regards to Con A density. Due to the limitations in measuring techniques of immobilised protein, lower Con A concentrations were difficult to measure accurately and used with confidence. This was also made difficult due to the wettability of the membrane employed for Con A binding (section 5.1.3) which is extremely hydrophilic and was shown to bind lower amounts of Con A than the opaque cellulose membrane even though the Con A loadings were kept the same (section 5.1.3).

Protein quantification of immobilised protein onto beads or such prototype "cells" is also in need of further development. Although the use of antibodies makes the determination of the number of receptor sites available on immobilised antigens and antibodies, techniques for immobilised proteins other then antibodies as described in section 8.1 are in need of further investigation and extension. This would allow a more accurate account of the total protein concentration immobilised onto beads as beads are employed as prototype cells in the study of cell adhesion *in vitro* for the reasons detailed in section 8.2.

CHAPTER 9

Conclusions and Proposed Work

Analysis of the experimental data with the multivalent binding model demonstrates some of the critical parameters necessary for specific adhesion of "cells" to other cells or surfaces. The effect of applied shear stress on the detachment of ovalbumin-coated beads from a Con A coated surface has shown progressive time dependent detachment behavior which results in the peeling of the bead from the surface. An increase in shear stress was found to lead to further detachment of beads after a steady-state had been reached at a lower shear stress. Therefore as cell detachment is a time dependent phenomena this implies that cells which have formed fewer bonds with the surface will be progressively removed by the applied force.

The effects of ligand and receptor densities on detachment behavior were not as apparent, this was attributed to a receptor clustering effect which is known to delay detachment (Ward *et al* 1994). The effect of ligand density can be further studied by extending the lower range of Con A density as it was found that the Con A density range used was sufficient even at the lowest coverage for all the concentrations of the ovalbumin-coated beads to bind. This would allow a greater insight into the effects of ligand density on detachment and adhesion strength.

The average critical shear stress values obtained for both the Con A and the ovalbumin densities did not show an overall dependence on the surface densities. As the Con A surface density for the range used is a factor of 100x greater then ovalbumin concentration it is likely that the number of bonds formed between Con A and ovalbumin is dependent on the ovalbumin concentration.

The experimental data obtained show a variety of detachment curves and only one type of curve is found to fit the multivalent model. The deviations from the model were attributed to receptor clustering and these variations were investigated by simulating curves with varying ratios of clustered and un-clustered receptor populations. From this graph (figure 8.2) a range of binding curves were obtained which are consistent with those seen in the experimental detachment profiles. This suggests that the variety in the experimental data obtained may be due to sample differences for both Con A and ovalbumin containing different ratios of both clustered and un-clustered populations. Also both curves for 100% clustered and un-clustered were found to fit the model, therefore it is a combination of both populations that leads to the deviation from the model. The surface association constant does not show much difference between the data that fits the model and data that deviates from the model. As shown in figure 8.3 varying the ratios of the surface association constant while keeping the ratios of the clustered and un-clustered ratio constant, does not show a great change in the type of curve obtained. This suggests that the change in the ratios of the clustered and un-clustered populations is of greater significance on the type of detachment curve obtained then varying the ratios of the surface association constant.

This is a factor that needs to be addressed in future work. The induced clustering of receptors on a cell membrane is a known phenomenon which is not present in mimic systems. Therefore the clustering of receptors may be due to over-crowding of the protein on initial contact with the surface and is another factor that would require the lowering of the surface density on the beads as well as to observe a greater dependence of receptor concentration on critical shear stress.

In order to further investigate the effects of shear stress, ligand and receptor densities on adhesion strength, the quantitative aspects of attachment of prototype cells to a protein coated surface should be studied under flow. Therefore allowing an investigation of the requirements for attachment using the carbohydrate-lectin system as the basis for this study as these form the basis of a wide range of naturally occurring interactions. The experiments can be further extended for both attachment

and detachment assays with both mimic (where both ligand and receptor densities can be varied) and prokaryotic and eukaryotic cell types (*E.coli*, *S.cerviseae* and Human neutrophils).

The experiments on pre-incubation contact time for detachment assays have shown that strength of attachment is incubation time dependent. In the prototype system studied there is no possibility of surface migration of either receptor or ligand. Therefore a study to extend the assessment of surface stabilization can add to the data obtained in this investigation.

Also the effects of the hydrophobicity of the surface employed for ligand immobilisation can be further investigated. In this study it was found that increased wettability of the surface led to a decrease in the amount of protein bound. The design of the flow cell allows the use of a semi-permeable membranes which, with some red-design could allow the effects of forces applied normal to the surface to be investigated.

In summary the results show that the experimental system used can be used to effectively study cell-surface interactions. Techniques need to be developed to allow accurate production of systems with lower ligand/receptor densities. The significance of clustering appears worthy of further study, particularly as active clustering occurs in mammalian cell systems. Finally a quantitative model accounting for clustering needs to be developed to provide a more complete description of the interactions observed here

References

Angal S., Harris E.L.V., eds. (1989) Protein Purification Methods: a practical approach. IRL Press.

Axen R., Porath J., Ernback S., (1967) *Nature.*, **214** 1302-1308.

Bhattacharyya L., Khan M.I., Brewer C.F., (1987) *J.Biol.Chem.*, **262** 1294- 1299.

Belford D.A., Rogers M.L., Regester G.O., Francis G.L., Smithers G.W., Liepe I.J., Priebe I.K., Ballard F.J.,(1995) *In Vitro Cell Dev.Biol.Anim.*, **31** 752-760.

Bell G.I., (1978) *Science* **200** 618-627.

Bell G.I., (1981) *Cell.Biophys.*, **3** 289-304.

Bell G.I., Dembo M.m Bongrand P., (1984) *Biophys.J.*, **45** 1051-1064.

Bohlen P., Stein S., Imai K., Udenfriend S., (1974) *Anal. Biochem.*, **58** 559-562.

Boldt D.H., Lyons R.D., (1979) *Cell. Immuno.*, **43** 82-93.

Brewer C.F., Sternlicth H., Marcus D.M., Grollman A.P., (1973) *Proc. Nat. Acad. Sci. USA.*,**70** 1001-1011.

Butcher E., Scollay R., Weissman I., (1980) *Eur.J.Immunol.*, **10** 556-562.

Castell J.V., Cervera M., Marco R., (1979) *Anal. Biochem.*, **99** 379-391.

Castel O., Grollier G., Agius G., Toullat G., de Ratulin de la Roy Y., (1990) *Eur.J.Clin.Microbiol.Infect.Dis.*, **9** 667-671.

Chen R.F., Smith P.D., Maly M., (1978) *Biochem.Biophys.*, **189** 241-250.

Cozens-Roberts C., Quinn J.A., Lauffenburger D.A., (1990*a*) *Biophys.J.*, **58** 107-125.

Cozens-Roberts C., Quinn J.A., Lauffenburger D.A., (1990*b*) *Biophys.J.*, **58** 841-856.

Cozens-Roberts C., Quinn J.A., Lauffenburger D.A., (1990*c*) *Biophys.J.*, **58** 857-872.

Dalton S.L., Marcantonio E.E., Assoian R.K., (1992) *J.Biol.Chem.*, **267** 8186-8191.

Davies J.E., Winotomobach S., Ulrichs K., James R.A., Roberts G.S.M., (1996) *Transplant.*, **62** 1301-1306.

Derewenda Z., Yariv J., Helliwell J., (1989) *EMBO.*, **8** 2189-2193.

Doran P. (1995) "Bioprocess Engineering Principals" ed. Academic Press: London.

Doroszewski J., (1980) "Short-term and incomplete cell-substrate adhesion. *In* Cell Adhesion and Motility. A.S.G. Curtis and J.D. Pitts, eds. Cambridge University press, UK. 171-179.

Dubios M., Gilles K.A., Hamilton,J.K., Rebers P.A., Smith,F., (1956) *J.Chromat.*, **28** 350-356

Duddridge J.E., Kent C.A., Laws J.F., (1982) *Biotech.Bioeng.*, **35** 273-281.

Dulaney J.T., (1979) *Mol.Cell.Biochem.*, **21** 43-63.

Eastrabrook A., Berger C.I., Mittler R., LoGerfo P., Hardy M. (1983) *Transplant. Proc.* **15** 651-656.

Eichner M., Dietz K., (1996) *Amer.J.Epidemiol.*, **143** 816-822.

Egland (1993) *Transplant.Proc.*, 1261-1263.

Evans C.H., Ridella J.D., (1984) *Anal.Biochem.*, **142** 411-420.

Finger L.S., Amioton D.C., Rosenburt A,O., (1996) *J.Biol.Chem.*, **354** 3521-3526.

Foa R., Cignetti A., Guarini A., (1996) *Clin.Immunotherap.*, **6** 238-249.

Forrester J.V Lackie J.M., (1984) *J.Cell.Sci.*, **70** 93-110.

Gee A.P., Mansour V.H., Weiler M.B., (1991) *J.Immuno.Methods*, **142** 127-136.

Gray.,Glew (1973) *J. Biol. Chem.*, **248** 7547-7551.

Goldman A.J., Cox R.G., Brenner H., (1967) *Chem.Eng.Sci.*, **22** 653-660.

Hafeman, D.G., von Tscharner, V., McConnell, H.M., (1981) *Pro. Natl. Acad. Sci.*, **78** 4552-4556.

Hammer D.A., Lauffenburger D.A., (1987) *Biophys.J.*, **52** 475-487.

Hammer D.A., Apte S.M., (1992) *Biophys.J.*, **63** 35-57.

Hammer D.A., Templeman L.A., Apte S.M., (1993) *Blood.Cell.*, **19** 261-277.

Hammer D.A., Tempelman L.A., Park.S., (1994) *Biotech.Progess.*, **10** 97-108.

Hardman K.D., Anisworth C.F., (1976) *Biochem.*, **15** 1120-1128.

Hardman K.A., Agarwal R.C., Freiser M.J., (1982) *J.Mol.Biol.*, **157** 69-86.

Harlan J.M., (1975) *Blood.*, **65** 513-521.

Harris E.L.V., Angal S. eds. (1990) Protein Purification Methods- a practical approach. United States: Oxford University Press.

Hermanson G.T., Mallia A.K., Smith P.K., (1992) Immobilised Affinity Ligand Techniques. London: Academic Press.

Hertz C.M., Graves D.J., Lauffenburger D.A., (1985) *Biotech.Bioeng.*, **27** 603-612.

Heuff G., van de Loosdrecht A.A., Betjes M.G., Beelen R.H., Meijer S., (1995) *Hepatology* **21** 740-745.

Hjerten S. (1964) *Biochem, Biophys. Acta.*, **79** 393-398.

Horowitz P.M., (1984) *Chrom.*, **17** 446-449.

Hubble J., Esienthal R., Whish W.J.D., (1995) *Biochem.J.*, **311** 917-919.

Hubble J., Ming F., Eisenthal R., Whish W., (1996) *J.Theor.Biol.*, **182** 169-171.

Jason J.C., Porath J., (1966) *Meth.Enzym.*, **8** 615-621.

Kemmner W., Holdenhawen P., (1992) *J.Immuno.Meth.*, **147** 197-200.

Kennedy S.W., Jones S.P., (1994) *Anal.Biochem.*, **222** 217-223.

Kimata H., Bernson J., Kagan J., Saxon A., (1990) *Clin.Immunol.Immunopathol.*, **54** 134-147.

Kuo S.C., Lauffenburger D.A., (1993) *Biophys.J.*, **65** 2191-2200.

Lawrence M.B., Springer T.A., (1991) *Cell.,* **65** 859-873.

Lewis S.D., Schafer J.A., Goldstein I.J., (1976) *Arch.Biochem.Biophys.,* **172** 689-695.

Lilly (1994) *Biochem.,* **33** 1189-1195

Liener I.E., Sharon N., Goldstein I..J., eds., (1986) The Lectins:Properties, Functions and Applications in Biology and Medicine. Orlando: Academic Press.

Lorenzen A., Kennedy S.W., (1993) *J. Chrom Meth.*, **205** 88-91.

Lund V., Schmid, R Rickwood,D., Hornes E., (1988) *Nucleic.Acid.Res.,* **16** 10861-10880.

Mandal D.K., Brewer C.F., (1992) *Biochem.,* **31** 12602-12609.

Mandal D.K., Brewer C.F., (1993) *Biochem.,* **32** 5516-5120.

Mandal D.K., Kishore N., Brewer C.F., (1994*a*) *Biochem.,* **33** 1149-1156.

Mandal D.K., Bhattacharaya L., (1994*b*) *Biochem.,* **33** 1157-1162.

Mandrusov E., Houng A., Klien E., Leonard E., (1995) *Biotech.Prog.,* **11** 208-213.

Mege J.L., Capo C., Benoliel A M., Depieds R., (1986) *Cell.Biophys.,* **8** 141-160.

Naismith J.H., Field R.A., (1996) *J.Biol.Chem.,* **271** 972-976.

Norden R.E., Milthrope B.K., Schndeim K., Slowialzer P.R., (1994) *Cytometry* **16** 25-33.

Nrgaard-Pedersen B., Larsen S.O., Ardens J., Svenstrup B., Tabor A., (1990) *Clin.Genet.,* **37** 35-43.

O'Conner J.L., Kellom T.A., (1990) *FEBS Lett.,* **261** 315-318.

Parekh R.B., Edge C.J., (1994) *TIBTECH.,* **12** 339-345.

Pauli B.U., Augustin-Voss H.G., El-Sabban M.E., Johnson R.C., Hammer D.A., (1990) *Cancer.Metastas.Rev.,* **9** 175-182.

Pratt K.J., Jarrell B.E., Williams S.K., Carabasi R.A., Rupnick M.A., Hubbard M.A., (1988) *J.Vasc.Surg.,* **7** 591-599.

Puri K.D., Finger E.B., Springer T.A., (1997) *J. Immuno.,* **158** 405-413.

Reisner Y., Sharon N., (1980) *TIBS* February.

Roit I.M., Brostott J., Male D.K., (1985) Immunology. Edinburgh: Churchill Livingstone

Roesnburg R.F., Goardt F.D., (1986) *Biophys.J.,* **45** 621-629.

Rose J.W., Hjortso M.A., eds: Bioprocess Technology: Cell Adhesion (1988) Marcel Dekker Inc.,

Rottman W.L., Walther B.T., Hillirquist C.G., Umbrett J., Roseman S., (1974) *J.Bio.Chem.,* **249** 373-380.

Rutishauser U., Sachs L., (1974) *P.N.A.S USA* **71** 2456-2460.

Saterbak A., Kuo S.C., Lauffenburger D.A., (1993) *Biophys.J.,* **65** 243-252.

Schmid-Schoenbien G.W., Skalak K., Simon S.I., Engler R.L., (1987) *Ann.NY.Acad.Sci.,* **516** 348-355.

Schwarz F.P., Puri K.D., Bhat R.C., Surolia A., (1993) *J.Biol.Chem.*, **268** 7668-7677.

Sekarudu Y.C., Rao V.S.R., (1984) *Int.J.Biol.Macromol.*, **6** 337-345.

Sharma S.K., Mahendroo P.P., (1980) *J.Chrom.*, **184** 471-499.

Sharpe P.T., (1988). Laboratory Techniques: In Biochemistry and Molecular Biology. Amsterdam: Elsevier.

Sidebotham R.L. (1974) Dextrans: In "Adv. Carbohydr. Chem. Biochem. 30", ed. Tipson R.S and Horton D., Academic Press: New York.

Smith P.K., Krohn R.I., Hermanson G.T., (1985) *Anal.Biochem.*, **150** 76-85.

Smith J.P., Liu G.Z., Soundararjan V., MclaughlinP.J., Zagon, I.S., (1994) *Amer.J.Physiolo.*, **266** R277-R283.

Spaltenstein A., Whitesides G.M., (1991) *J.Amer.Chem.Soc.*, **113** 686-689.

Springer T.A., (1990) *Nature* **346** 425-434.

Sumner J.B., Howell S.F., (1936) *J.Bio.Chem.*, **115** 583-591.

Sunberg L., Porath J., (1974) *J.Chromat.*, **90** 87-98.

Sung K P., Sung L A., Crimmins M., Burkaoff S J., Chien S., (1986) *Science (Wash DC).*, **234** 1405-1408.

Suttie J.W., Introduction to Biochemistry. (1982) eds. Internaltional Holt-Saunders.

Swann I.D., Dealtry G.B., Rickwood D., (1992) *J.Immunno.Methods.*, **152** 245-252.

Symon F.A., Wardlaw A.J., (1996) *J. Thorax.*, **51** 1155-1157.

Templeman L.A., Park s., Hammer D.A., (1994) *Biotech.Prog.*, **10** 97-108.

Tozeren A., Sung K.L., Sung L.A., Dustin M.L., Chan P.Y., Springer T.A., Chien S., (1992) *J.Cell.Biol.*, **116** 997-1006.

Tuner R.T., ed. (1994) *Immunology.* Chichester: Wiley.

Udenfriend S., Stein S., Bohlen P., Dairman W., (1972) *Science* **178** 871-872.

Uhlen M., (1989) *Nature* **340** 733-735.

Uyen H.M., Schakenraad J.M., Sjollema J., Noordmans J., Jonebloed W.L., Stokroos I., Busscher H.J., (1990) *J.Biomed.Mater.Res.*, **24** 1599-1614.

van der Merwe P.A., Barclay A.N., (1994) *Trends.Biochem.Sci.*, **19** 354-358.

Voet D., Voet J., (1990) *Biochemistry* New York: Wiley and Sons.

Ward M.D., Dembo M., Hammer D.A., (1994) *Biophys.J.*, **67** 2522-2534.

Wattenburger m R., Graves D.J., Lauffenburger D.A., (1990) *Biophys.J.*, **57** 765-777.

Wilikinson, P.C., Lackie., J.M.,Forrester, J.V., Dunn, G.A. (1984) *J.Cell.Biol.*, **99** 1761-1768.

Worthen g.S., Smedly L.A., Tonnesen M.G., Ellis D., Voelkel N.F., Reeves J.T., Hensen P.M., (1987) *J.Appl.Physiol.*, **63** 2031-2041.

Yon R.J., (1988) *J.Chrom.*, **457** 13-23.

Zavazava N., Hausmann R., Mullerrcuholtz W., (1991) *Transplantation* **51** 838-842.